A Technical Memorandum ERL ARL-90

THE BARROW, ALASKA AUTOMATIC CONDENSATION NUCLEI COUNTER AND FOUR WAVELENGTH NEPHELOMETER: INSTRUMENT DETAILS AND FOUR YEARS OF OBSERVATIONS

Mark E. Murphy
Barry A. Bodhaine

Air Resources Laboratories
Silver Spring, Maryland
October 1980

noaa NATIONAL OCEANIC AND ATMOSPHERIC ADMINISTRATION / Environmental Research Laboratories

NOAA Technical Memorandum ERL ARL-90

THE BARROW, ALASKA AUTOMATIC CONDENSATION NUCLEI COUNTER AND FOUR WAVELENGTH NEPHELOMETER: INSTRUMENT DETAILS AND FOUR YEARS OF OBSERVATIONS

Mark E. Murphy
Barry A. Bodhaine

Aerosols and Radiation Monitoring
Geophysical Monitoring for Climatic Change, Boulder, Colorado

Air Resources Laboratories
Silver Spring, Maryland
October 1980

UNITED STATES DEPARTMENT OF COMMERCE
Philip M. Klutznick, Secretary

NATIONAL OCEANIC AND ATMOSPHERIC ADMINISTRATION
Richard A. Frank, Administrator

Environmental Research Laboratories
Joseph O. Fletcher, Acting Director

NOTICE

Mention of a commercial company or product does not constitute an endorsement by NOAA Environmental Research Laboratories. Use for publicity or advertising purposes of information from this publication concerning proprietary products or the tests of such products is not authorized.

CONTENTS

THE BARROW, ALASKA AUTOMATIC CONDENSATION NUCLEI COUNTER AND FOUR WAVELENGTH NEPHELOMETER: INSTRUMENT DETAILS AND FOUR YEARS OF OBSERVATIONS

Mark E. Murphy and Barry A. Bodhaine

Abstract. NOAA's Geophysical Monitoring for Climatic Change program operates a background monitoring station at Barrow, Alaska. Aerosol monitoring at Barrow was initiated in May 1976 with an automatic condensation nuclei counter, Pollak nuclei counter, and four wavelength nephelometer. These instruments provide a continuous aerosol climatology and identify periods of contamination.

The G.E. counter data were calibrated from the G.E.-Pollak data-pairs generated from the raw one-minute G.E. counter voltages. A linear least squares analysis was used to determine a best fit regression for 1976 data with the Pollak data as the independent variable and a multiplicative scaling factor for 1977 through 1979 generated from a histogram of G.E.-Pollak data ratios.

Light scattering data show an annual cycle with a maximum above $10^{-5}m^{-1}$ in March and a minimum of about $10^{-6}m^{-1}$ in June. Condensation nuclei data show a semiannual change with monthly mean concentrations ranging between 50 cm^{-3} and 1000 cm^{-3}. Maxima are present in March and August, minima in June and September. The continuously operating four wavelength nephelometer and G.E. condensation nuclei counter in conjunction with a Pollak nuclei counter, have produced an excellent data set over the four year period, 1976-1979.

I. INTRODUCTION

The Geophysical Monitoring for Climatic Change (GMCC) Observatory located at Pt. Barrow, Alaska is operated by the National Oceanic and Atmospheric Administration (NOAA) as part of a network of remote measurement sites. The Pt. Barrow site (71° 19'N, 156° 36'W, 9m msl), established in 1972, was chosen to be representative of the Arctic atmosphere during favorable local wind conditions. Fig. 1 gives the location of Pt. Barrow at the northernmost tip of Alaska while Fig. 2 shows the observatory site in relation to the Naval Arctic Research Laboratory (NARL) and Barrow village. The prevailing winds are normally from the east so that contamination from local activities is minimized. This report presents the condensation nuclei and total light scattering data from the observatory taken by a General Electric condensation nuclei counter and a four wavelength nephelometer from 1976 through 1979. A brief description of the theory and operation of the instruments is included to aid the potential user in data interpretation. A complete set of the hourly means of condensation nuclei and four wavelength light scattering data may be obtained from NOAA/ARL/GMCC, Boulder, Colorado, 80303.

A regular aerosol measurement program was started with a Gardner counter in September 1971 at the Barrow observatory (Turner and Cotton, 1975). In May 1976, a Pollak condensation nuclei counter, a four wavelength nephelometer, and an automatic condensation nuclei counter were installed. Except for a few

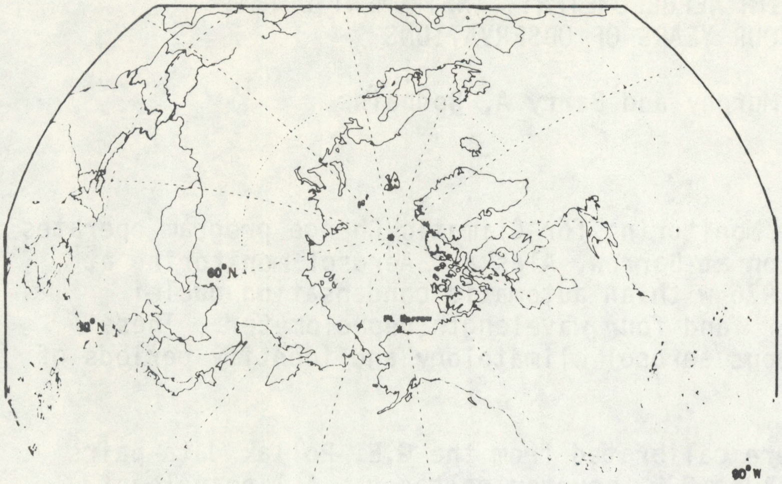

Figure 1. Lambert equal area globe projection about Pt. Barrow, Alaska.

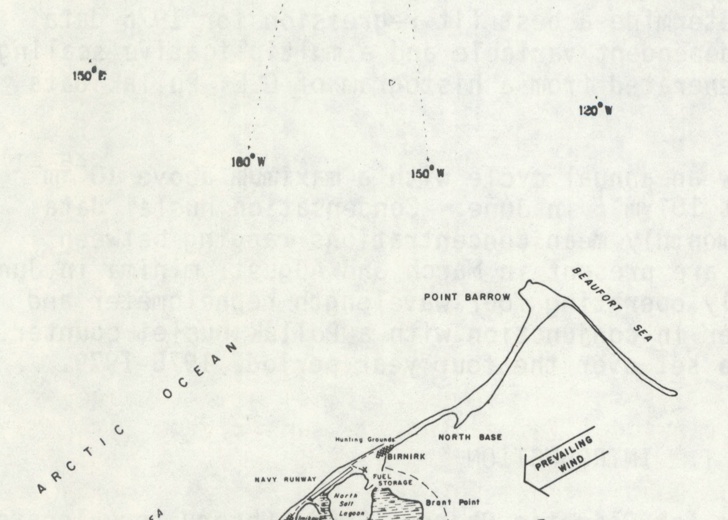

Figure 2. Barrow, Alaska, GMCC Observatory site.

brief periods of downtime, a continuous record of data is available since the instruments were installed.

Since condensation nuclei concentrations at Pt. Barrow range from about 1000 cm^{-3} during the winter months to below 50 cm^{-3} in the summer, an instrument of high sensitivity is necessary and routine calibration is essential. The Pollak counter used is in close agreement with the standard maintained by Austin Hogan at the State University of New York, Albany, and the relative calibration has not changed since its installation. Because of the G.E. counter's inherent sensitivity, regular calibration and maintenance are a necessity for long-term reliability.

The G.E. nuclei counter was calibrated by Liu and Pui (1974) using a differential mobility analyzer technique. They found a linear response over the size range 0.011-0.15 μm and concentrations of up to $6.5 \times 10^{-4} cm^{-3}$. Even though the response was essentially linear for the G.E. counter, a discrepancy of 40% with a previous calibration was found.

In a more recent study by Cooper and Langer (1978), the instrument was tested for calibration and size dependency effects using monodisperse wax, sodium chloride, and silver iodide aerosols generated by Liu and Pui's (1974) technique. They suggest that factory calibration be treated with caution, that frequent calibration checks be made, and that particle losses become significant for particles smaller than 0.03 μm in diameter.

A Liu and Pui (1974) aerosol generator was used by Liu et al. (1975) to calibrate the Pollak photoelectric nuclei counter. This is important because the factory calibration of the G.E. counter was performed with a Pollak-style counter. The difference in the calibrations found by Cooper and Langer (1978) and Liu and Pui (1974) led to a questioning of the accuracy of the Pollak counter, long used as the Aitken nuclei "standard". The Liu et al. (1975) experiments showed agreement between the differential mobility analyzer and the Pollak counter to better than 9% for concentrations less than $10^4 cm^{-3}$.

The nephelometer approach to the measurement of the integrated light scattering of air was first attempted by Beuttell and Brewer (1949) and later by Crosby and Koerber (1963). Ahlquist and Charlson (1967) made improvements in the mechanical and electrical design, increasing the sensitivity such that Rayleigh or molecular scattering coefficients could be measured. A comparison between aerosol light-scattering coefficients and total suspended particulate mass made by Charlson et al. (1967) gave the simple linear relationship $M\ (\mu g\ m^{-3}) = 0.38\ B_{sp} (m^{-1})$ between aerosol mass and the volumetric light scattering. This holds approximately true for a variety of natural and anthropogenic aerosol sources. The standard integrating broadband nephelometer manufactured by Meteorology Research Inc. (Charlson et al., 1969) gained wide use for the measurement of visual range and air quality, and has been increased in sensitivity by the use of photon counting techniques.

Angstrom (1929) found that the aerosol scattering dependence on wavelength could be described by $b_{scat} \simeq \lambda^{-\alpha}$; analagous to Rayleigh scatter by gases, where b_{scat} is the extinction coefficient due to scattering, λ is the wavelength, and α is the Angstrom exponent. A pure Rayleigh or molecular scatter would have α=4 whereas a typical α value for aerosol scatter is about 1.5.

Butcher and Charlson (1972) summarized a simple relationship between the Angstrom exponent and the aerosol size distribution. Whitby (1975) has shown that particle size distributions are probably best described by a multimodal log normal curve fit. However, the power law model of the size distribution of aerosols, $\frac{dN}{d \log r} = Cr^{-\beta}$, developed by Junge (1963) where dN is the number of particles in the radius increment d log r, β is the slope of the size distribution, and C is a constant, is a good approximation over a limited size range. By measuring light scattering at several different wavelengths, the relationship, $\alpha = \beta - 2$, makes it possible to obtain aerosol size distribution information by measuring Angstrom exponents. An instrument to measure light scattering as a function of wavelength was developed by Ahlquist and Charlson (1969).

II. INSTRUMENTATION

Pollak counter SN16 was installed at the Barrow Observatory as a secondary standard to provide routine calibration points for the automatic nuclei counter. The Pollak counter has a 59 cm long and 2.5 cm diameter fog tube with a convergent-beam light source at the top and a photocell at the bottom. The fog tube is pressurized with filtered air to an overpressure ratio of 1.21 after flushing the system with sample air. The subsequent expansion produces a saturation ratio of about 2.81 which activates particles as small as 10^{-7} cm radius. The particles which have grown to cloud droplet size, attenuate the light beam to give a deflection on a microammeter calibrated in terms of nuclei concentration. The minimum sized particle activated is about 1 to 2 x 10^{-7} cm radius, though there is some controversy over the minimum sized particle detected.

The GMCC uses the calibration of the Pollak nuclei counter provided by Pollak and Metnieks (1960). It should be noted that earlier calibrations provided by Metnieks and Pollak (1959) obtained concentrations below 626 cm^{-3} by linear interpolation. Seeing a need for calibration at lower concentrations, Pollak and Metnieks (1960) established nine more fundamental calibration points, the lowest being 23.9 cm^{-3}. In view of the excellent results of Liu et al. (1975), it is reasonable to accept Pollak's calibration for low nuclei concentrations. In any case, this calibration can be verified when a more accurate calibration technique is developed for these extremely low concentrations.

The automatic condensation nuclei counter installed at Barrow is a modified version of the General Electric catalog No. 112642861 instrument. Modifications of the electronics suggested by Norman Ahlquist at the University of Washington have been implemented. The basic "casting", however, containing the cloud chamber, optics, humidifier, and rotating valve is used in its original form. This is important because the method of measuring the light scattered by growing droplets at low forward scattering angles and against a dark field is inherently the most sensitive method of measurement.

The G.E. counter uses a rotating lamp shutter mounted on the valve shaft to provide a bright beam directly through the cloud chamber onto the photomultiplier (PMT) to allow regulation (through the PMT supply) of the effective lamp intensity seen by the PMT. This compensates for any drift in lamp intensity or PMT sensitivity. The direct beam is blocked during the measurement portion of the cycle and only light scattered in the chamber reaches the PMT. After the expansion occurs, a time delay circuit waits 26 ms and then samples the cloud chamber signal to be read out, minus the background level, as nuclei concentration. A logarithmic converter provides instrument output on a logarithmic scale spanning five decades of nuclei concentration. This eliminates the familiar range change problem under conditions of widely varying nuclei concentration.

The linearity of the instrument over the entire range of nuclei concentrations depends primarily on these three factors:

1) the anode current of the PMT must be directly proportional to the light falling on its photocathode;

2) the electronics which process the PMT anode current must be linear;

3) the light scattered by the droplets and incident on the PMT must be directly proportional to the nuclei concentration.

Conditions 1) and 2) are easily achieved with modern electronics and can be checked for the five orders of magnitude of signal over which the instrument operates. Condition 3) has been found to hold true for concentrations below about 100,000 cm^{-3}. That all the droplets grow to the same size in the same time interval, independent of concentration is the important point. At low concentrations, the effects of multiple scattering and vapor depletion are minimized. The logarithmic output of the instrument is adjusted to 1 volt per decade according to the relationship $N = 10^v$ where N is nuclei concentration and v is the instrument output voltage.

In the lower three decades of interest (i.e., 1-1000 cm^{-3}), the G.E. counter has been found to agree well with the Pollak counter. If a zero filter is placed on the intake, the instrument will drift off scale low. Furthermore, at a rate of five samples per second, the instrument has a rapid response time limited only by the intake line length and time of flow through the system.

The four wavelength nephelometer was first described by Ahlquist and Charlson (1969) and its operation by Bodhaine and Mendonca (1974), and Bodhaine (1979). In normal operation, a continuous flow of air through the sample volume is illuminated by a regulated quartz-iodine projection lamp. The scattered light is then detected by a PMT using photon counting techniques. Measurements in four wideband (70 nm) channels centered at 450 nm, 550 nm, 700 nm, and 850 nm, and one narrowband (5 nm) channel centered at 500 nm for use in calibration, are made using a rotating filterwheel with optical interference filters in front of the PMT. To attain an improved signal to noise ratio, the filter wheel can be stopped on any of the filters.

Measurement of aerosol light scatter is accomplished by cycling the nephelometer through three modes: (1) background (BG); (2) normalization (CAL); and (3) ambient (AMB). The BG mode consists of filling the instrument with filtered air and storing the measured scattering signal in memory. This signal contains the phototube dark noise, molecular scattering of the air in the instrument, and light scattered from the interior of the nephelometer. In the CAL mode, clean air remains in the instrument, and a white object (tip of a wire painted with Eastman reflectance coating) is inserted into the field of view of the PMT. The scattering signal due to the white object plus background is measured and stored in memory. During the AMB mode, the instrument is purged with ambient air and the white object removed from the field of view. This scattering signal, consisting of the aerosol scattering signal plus background, is measured and stored in memory.

With signals from each mode stored in memory, the instrument performs the calculation log (AMB - BG) - log (CAL - BG) successively for all four wavelengths and the output of the nephelometer is the volume scattering coefficient of the aerosol particles in units of m^{-1}. The instrument automatically performs all operations and a cycle is repeated once every six minutes, though the time cycle can be set to any desired time interval. Also, an automatic averaging scheme is built into the nephelometer with time constants adjustable from seconds to hours. Sensitivity and noise considerations for this instrument have been discussed by Waggoner et al. (1976).

The calculation performed by the instrument in real time effectively removes the background, including the molecular scattering of air. Furthermore, by taking the ratio of aerosol scatter to white object scatter, the data are normalized for the four wavelengths and compensated for changes in the spectral characteristics of the lamp and the response of the PMT.

III. CALIBRATION

The results of Liu and Pui (1974) and Cooper and Langer (1978) concerning calibration discrepancies of the automatic nuclei counters are not unexpected. These instruments require a fair amount of maintenance and calibration for continuous operation because they exhibit long-term electrical and mechanical drift. Contamination of the cloud chamber (which increases the background signal) or dirty or clogged valve ports, possibly causing false expansions or ther problems, are usually the cause of deterioration of performance in the G.E. counter. A complete recalibration is required after any major breakdown.

The G.E. counter undergoes a daily zero check and a weekly calibration. The daily check is performed by installing a filter on the intake and adjusting the background compensation circuit. The internal voltages are then checked with the filter removed. A comparison of the output reading of the G.E. counter and the average of three Pollak observations is next. An equivalent voltage is found for the average Pollak observation and, if it differs significantly from the G.E. counter, the instrument will be readjusted.

The comparison of a series of five simultaneous Pollak counter observations and G.E. counter voltage reading performed on ambient aerosol constitutes the weekly check. If necessary, the G.E. counter calibration is adjusted to force it to agree with the average Pollak reading. The G.E. counter voltage is recorded at the end of the purge period of each Pollak reading. It is important to emphasize that the instruments are compared on ambient aerosol at the site during periods of typical uncontaminated aerosol concentrations. The instruments are allowed to operate in the regular monitoring configuration, i.e., through the sampling stack (Komhyr, 1979) and intake lines. Installation of an aerosol generator such as the Liu and Pui (1974) instrument at the site for routine calibration purposes is not practical, especially for use at low concentration. Storing either ambient or nichrome aerosol in a mylar bag and performing repeated dilutions is the only practical alternative. However, it is not routinely used because of the uncertainties of aerosol diffusion and coagulation losses in the bag which give changing size distributions and make simultaneous sampling difficult.

The output signal of the G.E. counter spans five decades and will give an error in aerosol concentration of about 2.5% per 10 mV error in voltage over the entire scale. The calibration of the G.E. counter, in practice, is adjusted only if the voltage error exceeds about 100 mV (25% error in concentration).

An accurate bimonthly calibration of the four wavelength nephelometer is performed using the known scattering coefficients of carbon dioxide as the calibration standard (Bodhaine, 1979). The instrument is allowed to collect data in the BG and CAL modes while operating in its normal running mode. Filtered carbon dioxide is then passed through the instrument at a rate of two liters per minute while it is locked in the AMB mode. At this time, the output voltage is proportional to log (AMB - BG) where the AMB signal is the scattering of CO_2. Finally, the instrument output is adjusted to the voltage corresponding to $B_{sp}(CO_2)-B_{sp}(air)$ corrected to the proper pressure and temperature. Analogous to the Pollak-G.E. counter comparison, this procedure establishes the calibration of the nephelometer referenced to the scattering coefficients of air and carbon dioxide.

The weekly check of the nephelometer involves a fourth mode, B_{sp}CAL, which operates in a similar fashion as the AMB mode, but the scattering is from a second white object rotated into view instead of ambient air. Assuming both objects are perfectly "white", the outputs of all four wavelengths would be a constant. Thus, if the weekly check is performed and the outputs are not all nearly equal, then the nephelometer is probably not working properly. Dissimilar outputs are normally caused by one of the two white objects being dirty or a malfunction in the electronics.

The gases usually used for calibrating the nephelometer are air, carbon dioxide, and Freon-12. Because of its low scattering coefficient, helium would be desirable to establish the true zero point of the nephelometers, but since helium can easily diffuse through the glass envelope of the PMT, it has not been used. The nephelometer output has been scaled such that light scattering ranges from $10^{-8}m^{-1}$ to $10^{-3}m^{-1}$ at 2 V/decade according to the relationship: $v = 2 \log (B_{sp}) + 16$.

IV. SCALING OF G.E. COUNTER DATA

Each GMCC observatory is equipped with a computer data acquisition system which digitizes all station data and stores it on magnetic tape in the format of one-minute voltage means. In addition, hourly means in engineering units are calculated for all instrumentation and written in an additional file on the tape at the end of each hour. Therefore, all data are available in both minute and hourly form at the data reduction facility in Boulder. All routine Pollak counter observations are performed manually and recorded by hand on data sheets at the observatory. These data are later punched on computer cards and stored in a disc file in the reduction facility computer.

The determination of the variability of the data from one minute to the next is the first step in the scaling process of the continuous aerosol data. The variability is found from a histogram of successive one-minute voltage differences calculated from the raw one-minute voltage means for approximately the first two weeks of each month (20,000 data points). An example of a histogram using data from 1979 is shown in Fig. 3. The maximum (absolute) allowed voltage difference limit is set at two standard deviations away from the mean since, for any one month, the one-minute voltage differences are fairly constant. The remaining voltage differences above this limit usually correspond to times of large concentration changes. Sampling of contaminated air or change in calibration by the G.E. counter operater are the normal causes of these large concentration changes. These time periods are not to be used for calibration purposes since the G.E. counter is no longer measuring background aerosol concentrations. The maximum of the two standard deviation values of the individual months is used as the final variability criterion for the year. Next, a program is run to select G.E. counter and Pollak counter data pairs to be used as calibration points. The program is designed to read a Pollak counter observation and then test the one-minute G.E. counter data for five minutes on either side of the Pollak observation time to determine if the successive one-minute voltage differences fall within the final variability criterion for the year established from the histograms. If so, then the ten minute mean G.E. counter value and the Pollak observation are accepted as a data-pair calibration point. This continues until a set of data pairs is generated for a time period during which the calibration of the G.E. counter was not changed or the instrument inoperative.

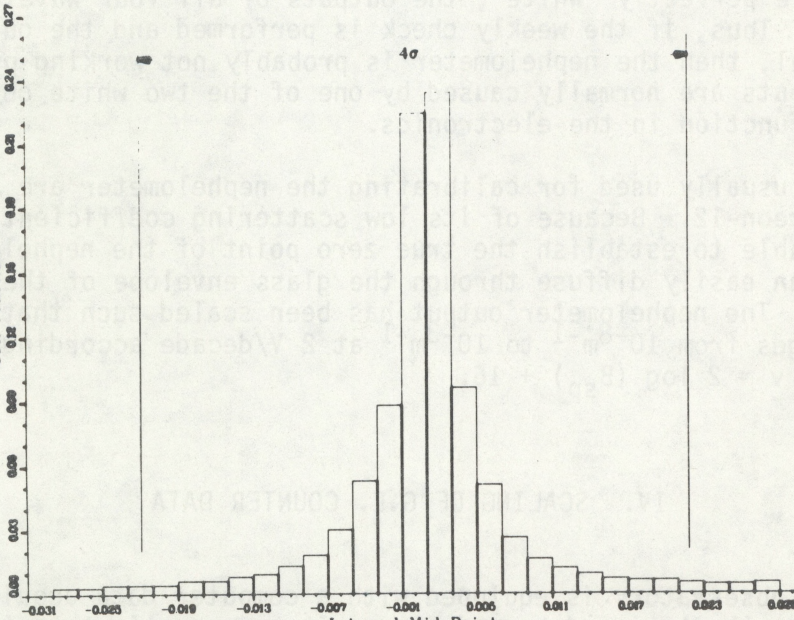

Figure 3. Sample histogram of successive G.E. counter one-minute voltage differences for January 1979.

The scaling of the G.E. counter, initially designed to scale the data from the South Pole (Murphy and Bodhaine, 1980), involves the use of a linear least squares analysis to generate a best-fit regression equation from the data pairs with the Pollak counter observations as the independent variable and the G.E. counter data as the dependent variable. This method was used on the Barrow data for 1976. Some data pairs chosen by the variability criterion as the maximum two-standard deviation value from the months with variability less than this value, may need to be removed. Such points can be removed by checking the standard residuals of the set of data pairs from the regression analysis and eliminating those with absolute value greater than two. This process is repeated to make the ratio of the coefficients of the equation and the standard deviation of the coefficients at least two (to insure at least a ninety percent confidence level in the coefficients), minimize the residual standard deviation, and maximize the multiple correlation coefficient squared. Normally a first degree equation is adequate but occasionally a second degree equation gives a better fit. Equations of degree higher than two are never used. Figure 4 shows an example of the linear least squares analysis run on data from 1976. The ratios of 4.67 and 19.03 in Fig. 4 imply that the confidence level in the values for the slope and intercept of the regression equation is very good. Likewise, the multiple correlation coefficient squared of 0.9628 implies that the data set is quite accurately fit by the equation.

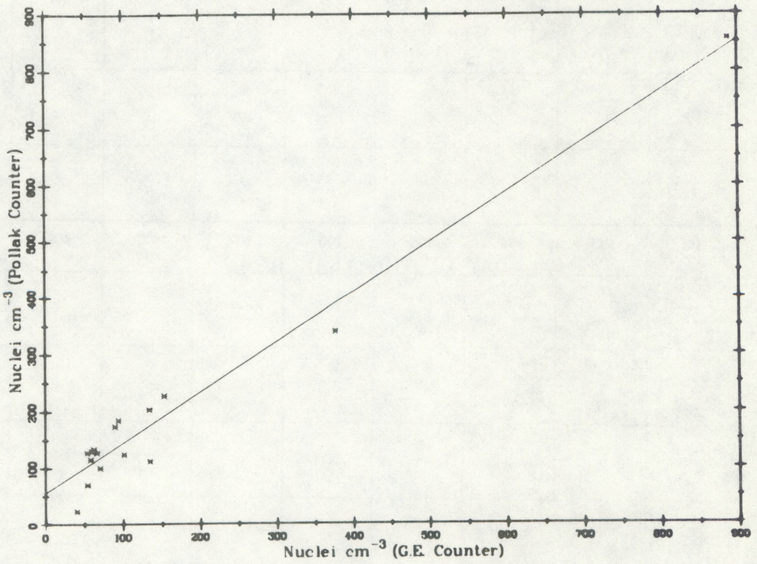

Figure 4. Sample output showing the ratio of the coefficient to the standard deviation of the coefficient for the best-fit regression equation for the time period of May 5 to July 6, 1976:

Residual standard deviation = 38.205

Multiple correlation coefficient squared = 0.9628

Number of points = 14

Indep. Var.	Coefficient	S.D. of Coefficient	Ratio
0	55.512	11.889	4.67
1	0.8855	0.04653	19.03

Though this method is acceptable for the low variability of the South Pole, it is not as accurate for Barrow's higher variability. Since Pollak readings are taken during periods of constant and hence usually low aerosol concentrations (about 100 cm^{-3}), a linear least squares analysis over these time periods is not representative of the actual data which varies greatly (from about 50 cm^{-3} up to 10,000 cm^{-3}). Thus a new method using only a multiplicative scaling factor was developed. Now, instead of running the regression analysis on the data pairs, a histogram is made from the G.E. counter data to Pollak counter observation ratios. Again, by removing the outlying ratios (those outside two-standard deviations from the mean), those data pairs from months with variability less than the maximum two-standard deviation criterion can be removed.

The final step is the application of the regression equation (1976) or the scaling factors (1977 through 1979) to the G.E. counter hourly data so that the results can be presented in the standard hourly format used for archiving all data. Fig. 5 shows a graphical display of both G.E. counter and Pollak counter data before and after scaling was applied to a ten-day interval.

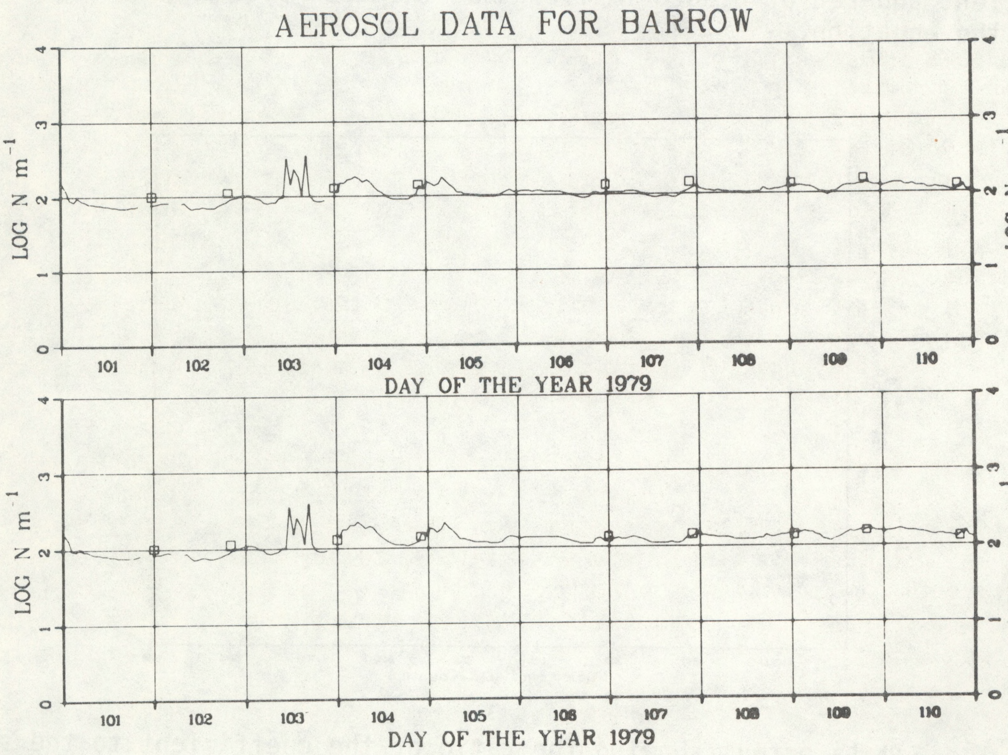

Figure 5. Graphical display of both the G.E. counter (solid line) and Pollak counter (squares) data for the ten-day period, April 11 to April 20, 1979. The upper graph gives data before the scaling procedure was applied, and the lower graph gives the data after the scaling procedure was applied.

V. DISCUSSION

The continuous condensation nuclei data can be used to identify and ultimately exclude periods of contamination due to local pollution sources in other measurement programs. The G.E. counter, with its fast time response, sensitivity over five orders of magnitude of nuclei concentration, and response to small sized particles ($0.001\ \mu m < r < 0.1\ \mu m$) make it particularly useful for detecting local combustion products due to burning of fuel.

The four wavelength nephelometer data can be used in a manner analogous to the G.E. counter data because of its response to aerosol particles in the size range ($r > 0.1\ \mu m$). However, the nephelometer has a response time on the order of one hour so that it does not respond to short pollution episodes. Also, the two instruments are complementary with respect to the size of the aerosol particles detectable.

Considerable effort is required to maintain and calibrate an automatic nuclei counter and four wavelength nephelometer over the long term. Calibration problems become much more critical at extremely low concentrations because the background signal from the instruments becomes large compared with the signal measured. Modifications to the electronics of the G.E. counter have reduced this problem, but the only adequate way to maintain calibration over long periods is to provide frequent comparisons with the on-site Pollak counter on ambient aerosol. Actual calibration adjustments can be made to the G.E. counter in cases of excessive discrepancies but a final adjustment of the data must be made using the scaling process to produce the most accurate data set. In the case of the nephelometer, once a calibration point has been chosen, the amount of error in the measurement is constant over the entire range of the instrument. This is due to the nephelometer's linearity and its logarithmic output scale, the accuracy of which can be checked independently of the light scattering measurements. Thus, as more accurate values for the scattering coefficients of air and CO_2 become available, all nephelometer data can easily be scaled to more correct values.

At the Pt. Barrow station, the Pollak nuclei counter has been accepted as the on-site standard. This instrument's calibration has traceability to the instrument maintained by Austin Hogan in Albany, New York. In view of the results of Liu et al. (1975), the most recent calibration of the Pollak counter provided by Pollak and Metnieks (1960) is currently the best available calibration standard for condensation nuclei measurements at low concentrations.

The seasonal variation in aerosol properties at Pt. Barrow (Bodhaine et al. 1980) can be seen by calculating monthly geometric means using all aerosol light scattering (550 nm) and condensation nuclei data available. The overall mean for light scattering for the years 1976-1979 was found to be $5.79 \times 10^{-6} m^{-1}$ and 172 cm^{-3} for nuclei concentration. Departures from the mean, by month, are presented in Fig. 6. Departures from the mean are expressed in orders of magnitude since the geometric means were calculated using logarithms to the base ten. A clear annual cycle of aerosol light scattering data (solid line) which reaches a maximum in March and a minimum in June with a peak-to-peak change of about one order of magnitude can be seen. Also, a clear semiannual cycle of the condensation nuclei data (dashed line)

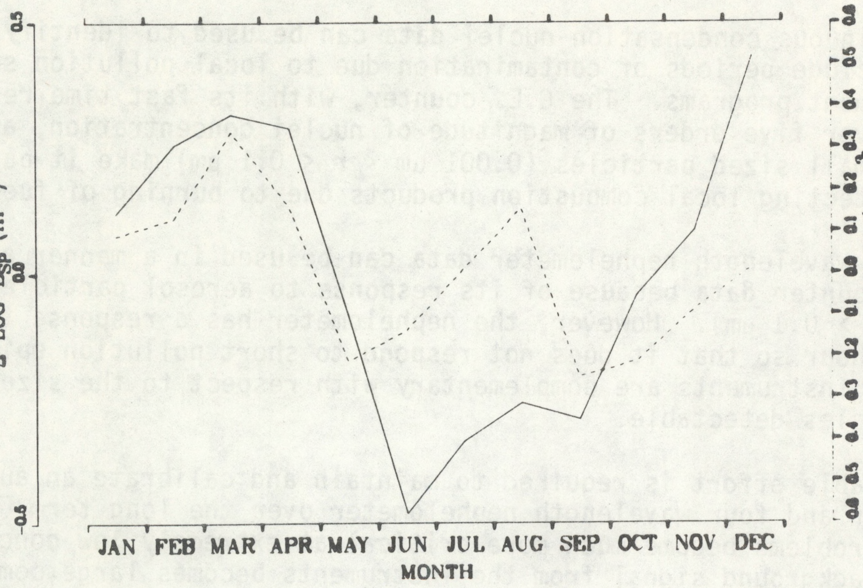

Figure 6. Departures from the geometric mean by month of aerosol light scattering (solid) and condensation nuclei (dashed) for 1976 through 1979 at the Barrow GMCC Observatory. The four-year geometric mean for light scattering is 5.79×10^{-6} m^{-1} and for condensation nuclei is 172 cm^{-3}.

with a maximum in March and a secondary maximum in August can be seen. Note, that this secondary maximum is produced primarily by small aerosols although the light scattering curve does show a very small peak in August. The peak-to-peak variation in condensation nuclei concentration is about 0.6 order of magnitude or about a factor of four. Using the relationship $m = 0.38\, B_{sp}$ (gm m^{-3}) suggested by Charlson et al. (1967), the average March light scattering value of 1.39×10^{-5} m^{-1} predicts an aerosol mass concentration of about 5 μ gm^{-3}, while the June value is about 0.6 μ gm^{-3}. The highest mean monthly value of light scattering, 1.91×10^{-5}m^{-1}, occurred in December, corresponding to a mass concentration of about 7 μ gm^{-3}.

The use of a continuously operating instrument such as the G.E. counter in conjunction with a manually operated standard can provide an excellent data set. Appendices A through D give the Pollak counter data, condensation nuclei data, light scattering data for the four wavelengths, and the Angstrom exponents plotted on a logarithmic scale for the years 1976 to 1979. All times are in Greenwich Mean Time (GMT). The Angstrom exponents are calculated by the following equation:

$$\text{Alpha}\ (i,\ i+1) = -\ \frac{\log B_{sp}(\lambda_{i+1}) - \log B_{sp}(\lambda_i)}{\log \lambda_{i+1} - \log \lambda_i}$$

where $i = 1,2,3$

Each frame shows a ten day period of G.E. counter data (solid line, lower graph) and Pollak counter data (squares, lower graph). Aerosol light scattering data are shown in the center graph of each frame for the wavelengths 450 nm (dashed line), 550 nm (solid line), 700 nm (long dashed line), and 850 nm (short dashed line). The wind speed and direction are also plotted in the middle graph. The angle of the wind arrow indicates the direction from which the wind is blowing; the length of the arrow indicates the speed. The length of the barb is equivalent to 2.5 knots or about 1.25 m sec^{-1} and may be used for scale. In the top graph of each frame are plotted the Angstrom exponents Alpha (1,2) (dashed), Alpha (2,3) (solid), and Alpha (3,4) (long dash). Appendix F shows the Pollak, G.E. counter, light scattering, and Alpha (2,3) yearly data in a single plot of daily means for each year of data at Barrow. The Pollak observations (squares) follow the G.E. counter closely with the exception of time periods where the Pollak observation value is less than or equal to one (Pollak no longer accurate and data not used) and times when contaminated G.E. counter data have been removed. Also, in Appendix F, the semiannual cycle of the condensation nuclei data with maxima in March and August and the minimum in June can be seen. Monthly averages for each year were calculated and are presented in Tables 1 through 4. The annual and semiannual cycles can be seen for the light scattering and condensation nuclei data. The minimum monthly value of condensation nuclei for all four years is 60 cm^{-3} for June 1977 and the maximum is 808 cm^{-3} for August 1976.

Table 1. Monthly mean values of Aitken nuclei concentration (cm^{-3}) and light scattering (m^{-1}) at Barrow, Alaska in 1976.

	Jan	Feb	Mar	April	May	June	July	Aug	Sept	Oct	Nov	Dec
Aitken	--	--	--	--	147	272	710	808	120	174	244	197
455 nm	--	--	--	--	5.7×10^{-6}	2.2×10^{-6}	7.1×10^{-7}	--	--	--	--	--
550 nm	--	--	--	--	4.2×10^{-6}	1.5×10^{-6}	4.7×10^{-7}	--	--	--	--	--
700 nm	--	--	--	--	3.1×10^{-6}	1.1×10^{-6}	3.6×10^{-7}	--	--	--	--	--
835 nm	--	--	--	--	2.1×10^{-6}	7.1×10^{-7}	2.4×10^{-7}	--	--	--	--	--

Table 2. Monthly mean values of Aitken nuclei concentration (cm^{-3}) and light scattering (m^{-1}) at Barrow, Alaska in 1977.

	Jan	Feb	Mar	April	May	June	July	Aug	Sept	Oct	Nov	Dec
Aitken	177	160	518	365	77	60	61	156	86	61	65	147
455 nm	--	3.0×10^{-5}	1.7×10^{-5}	1.9×10^{-5}	1.5×10^{-5}	--	--	4.3×10^{-6}	3.8×10^{-6}	6.7×10^{-6}	1.1×10^{-5}	9.6×10^{-5}
550 nm	--	2.8×10^{-5}	1.5×10^{-5}	1.7×10^{-5}	1.2×10^{-5}	--	--	3.1×10^{-6}	3.0×10^{-6}	4.9×10^{-6}	7.6×10^{-6}	7.2×10^{-5}
700 nm	--	2.1×10^{-5}	1.0×10^{-5}	1.1×10^{-5}	6.7×10^{-6}	--	--	2.8×10^{-6}	2.8×10^{-6}	4.7×10^{-6}	6.6×10^{-6}	6.6×10^{-5}
835 nm	--	1.7×10^{-5}	7.5×10^{-6}	7.9×10^{-6}	4.5×10^{-6}	--	--	2.7×10^{-6}	2.8×10^{-6}	4.6×10^{-6}	6.1×10^{-6}	6.3×10^{-5}

Table 3. Monthly mean values of Aitken nuclei concentration (cm^{-3}) and light scattering (m^{-1}) at Barrow, Alaska in 1978.

	Jan	Feb	Mar	April	May	June	July	Aug	Sept	Oct	Nov	Dec
Aitken	181	152	254	138		76	147	366	122	113	167	101
455 nm	1.3×10^{-5}	1.2×10^{-5}	1.6×10^{-5}	1.5×10^{-5}	6.6×10^{-6}	3.7×10^{-6}	--	2.4×10^{-6}	3.0×10^{-6}	5.0×10^{-6}	8.0×10^{-6}	6.6×10^{-6}
550 nm	9.8×10^{-6}	1.1×10^{-5}	1.3×10^{-5}	1.2×10^{-5}	5.2×10^{-6}	2.7×10^{-6}	--	2.3×10^{-6}	2.9×10^{-6}	4.3×10^{-6}	7.4×10^{-6}	6.2×10^{-6}
700 nm	9.1×10^{-6}	7.1×10^{-6}	8.7×10^{-6}	7.7×10^{-6}	3.2×10^{-6}	1.4×10^{-6}	--	1.9×10^{-6}	2.3×10^{-6}	2.8×10^{-6}	5.4×10^{-6}	4.5×10^{-6}
835 nm	8.9×10^{-6}	5.3×10^{-6}	6.2×10^{-6}	5.4×10^{-6}	2.2×10^{-6}	8.4×10^{-6}	--	1.7×10^{-6}	1.9×10^{-6}	2.0×10^{-6}	4.1×10^{-6}	3.4×10^{-6}

Table 4. Monthly mean values of Aitken nuclei concentration (cm^{-3}) and light scattering (m^{-1}) at Barrow, Alaska in 1979.

	Jan	Feb	Mar	April	May	June	July	Aug	Sept	Oct	Nov	Dec
Aitken	337	521	388	272	111	182	585	199	87	94	125	229
455 nm	6.7×10^{-6}	9.6×10^{-6}	2.2×10^{-5}	1.2×10^{-5}	5.1×10^{-6}	1.4×10^{-6}	3.7×10^{-6}	3.3×10^{-6}	2.2×10^{-6}	6.4×10^{-6}	7.3×10^{-6}	1.5×10^{-5}
550 nm	6.2×10^{-6}	8.8×10^{-6}	2.0×10^{-5}	1.1×10^{-5}	4.3×10^{-6}	1.1×10^{-6}	3.1×10^{-6}	3.0×10^{-6}	2.1×10^{-6}	6.3×10^{-6}	7.2×10^{-6}	1.4×10^{-5}
700 nm	4.4×10^{-6}	6.2×10^{-6}	1.4×10^{-5}	7.5×10^{-6}	2.7×10^{-6}	6.8×10^{-7}	2.1×10^{-6}	2.2×10^{-6}	1.7×10^{-6}	5.0×10^{-6}	5.6×10^{-6}	1.1×10^{-5}
835 nm	3.4×10^{-6}	4.6×10^{-6}	7.9×10^{-6}	4.4×10^{-6}	1.7×10^{-6}	4.8×10^{-7}	1.5×10^{-6}	1.7×10^{-6}	1.3×10^{-6}	4.0×10^{-6}	4.5×10^{-6}	8.1×10^{-6}

VI. REFERENCES

Ahlquist, N. C. and R. J. Charlson, 1967. A new instrument for measuring the visual quality of air. J. Air Pollut. Control Assoc., 17, 467-469.

Ahlquist, N. C. and R. J. Charlson, 1969. Measurement of the wavelength dependence of atmospheric extinction due to scatter. Atmos. Environ., 3, 551-569.

Angstrom, A., 1929. On the atmospheric transmission of sun radiation and on dust in the air. Georg. Ann., 11, 156.

Beuttell, R. G. and A. W. Brewer, 1949. Instruments for the measurement of the visual range. J. Sci. Instrum., 26, 357-359.

Bodhaine, B. A., 1979. Measurement of the Rayleigh scattering properties of some gases with a nephelometer. Appl. Opt., 18, 121.

Bodhaine, B. A. and B. G. Mendonca, 1974. Preliminary four wavelength nephelometer measurements at Mauna Loa Observatory. Geophys. Res. Lett., 1, 119.

Bodhaine, B. A., J. M. Harris and G. A. Herbert, 1980. Aerosol light scattering and condensation nuclei measurements, presented at the Second Symposium on Arctic Air Chemistry, Kingston, RI May 6-8, 1980.

Butcher, S. S. and R. J. Charlson, 1972. An Introduction to Air Chemistry, Academic, New York.

Charlson, R. J., H. Horvath, and R. F. Pueschel, 1967. The direct measurement of atmospheric light scattering coefficient of visibility and pollution. Atmos. Environ., 1, 469-478.

Charlson, R. J., N. C. Ahlquist, H. Selvidge, and P. B. MacCready, 1969. Monitoring of atmospheric aerosol parameters with the integrating nephelometer. J. Air Pollut. Control Assoc., 19, 937-942.

Cooper, G. and G. Langer, 1978. Limitations of commercial condensation nucleus counters as absolute counters. J. Aerosol Sci., 9, 65-75.

Crosby, P. and B. W. Koerber, 1963. Scattering of light in the lower atmosphere. J. Opt. Soc. Am., 53, 358-361.

Junge, C. E., 1963. Air Chemistry and Radioactivity, Academic, New York.

Komhyr, W., 1979. Aerosol and gas sampling apparatus in use at NOAA GMCC baseline stations. Proceedings WMO Technical Conference on Regional and Global Observation of Atmospheric Pollution Relative to Climate, August 20-24, 1979, Boulder, Colorado.

Liu, B. Y. H. and D. Y. H. Pui, 1974. A submicron aerosol standard and the primary absolute calibration of the condensation nuclei counter. J. Colloid Interface Sci., 47, 155.

Liu, B. Y. H., D. Y. H. Pui, A. W. Hogan, and T. A. Rich, 1975. Calibration of the Pollak counter with monodisperse aerosols. J. Appl. Meteorol., 14, 46-51.

Metnieks, A. L. and L. W. Pollak, 1959. Instruction for use of photoelectric condensation nucleus counters. Geophysical Bulletin No. 16, School of Cosmic Physics, Dublin Institute for Advanced Studies.

Murphy, M. E. and B. A. Bodhaine, 1980. The South Pole automatic condensation nuclei counter: instrument details and five years of observations. NOAA Tech. Memo. ERL ARL-82.

Pollak, L. W. and A. L. Metnieks, 1960. Intrinsic calibration of photoelectric nucleus counter. Tech Note 9, School of Cosmic Physics, Dublin Institute for Advanced Studies.

Turner, C. and G. Cotton, 1975. Summaries of Aitken concentrations and associated surface wind data at Barrow, Alaska, from September 1971 to February 1975. NOAA Tech. Rept. ERL 349-ARL 2.

Waggoner, A. P., N. C. Ahlquist, and R. J. Charlson, 1976. Atmospheric aerosols: Their optical properties and effects. Paper TUA4, NASA CP-2004.

Whitby, K. T., 1975. Modeling of atmospheric aerosol particle size distributions. Progress report on EPA Grant No. R800971, Univ. of Minn., Minneapolis, Minnesota.

APPENDIX A

Appendix A contains the hourly mean nuclei concentrations, Pollak counter observations, light scattering data, and Angstrom exponents plotted on a logarithmic scale for 1976. A histogram of successive one minute voltage differences for each month was generated and the variability criterion was determined to be ±0.0446 volts.

The data pairs were obtained from the minute data and grouped into periods where the G.E. counter was operating. The equations generated are:

Day	Equation	Multiple Correlation Coefficient Squared
0-1811	y = (0.885546965 * G.E.) + 55.511712	0.9628
27723-36623	y = (0.837228591 * G.E.) + 42.8456518	0.8441

During days 18812-27222, the G.E. counter was not operative.

Scaled graphical display of aerosol data for 1976.
for each plot;

the top graph contains: Angstrom exponents
- Alpha (1-2): dashed line
- Alpha (2-3): solid line
- Alpha (3-4): long dashed line

the center graph contains: light scattering and wind data
- wavelength 450 nm: dashed line
- wavelength 550 nm: solid line
- wavelength 700 nm: long dashed line
- wavelength 850 nm: short dashed line

the lower graph contains: nuclei concentrations
- G.E. counter: solid line
- Pollak counter: squares

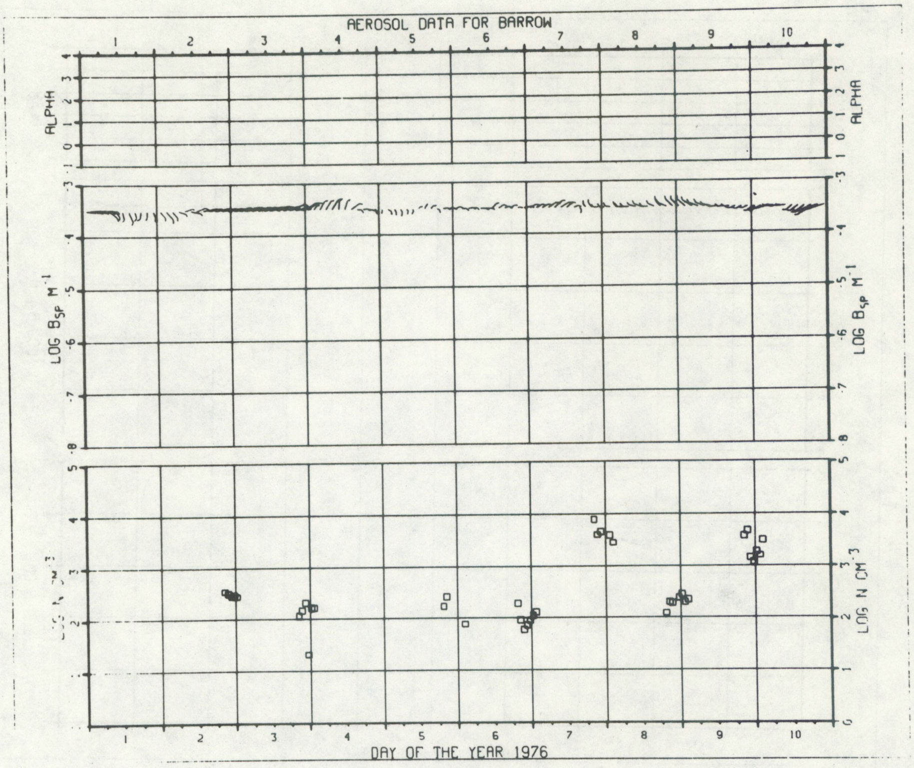
AEROSOL DATA FOR BARROW
ALPHA
LOG B_{SP} M^{-1}
LOG N CM^{-3}
DAY OF THE YEAR 1976

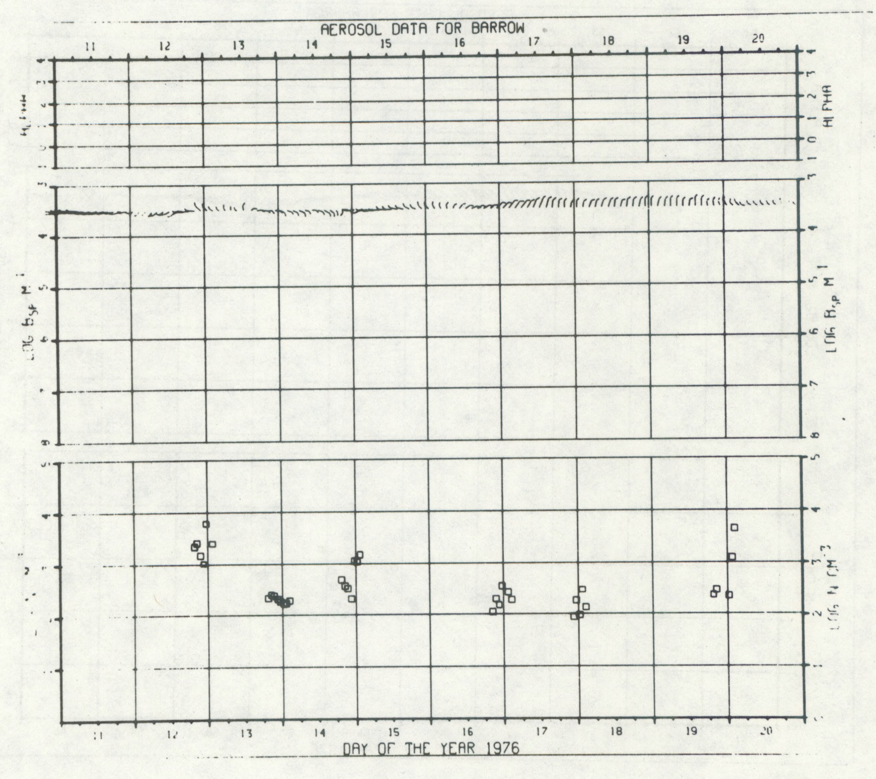
AEROSOL DATA FOR BARROW
ALPHA
LOG B_{SP} M^{-1}
LOG N CM^{-3}
DAY OF THE YEAR 1976

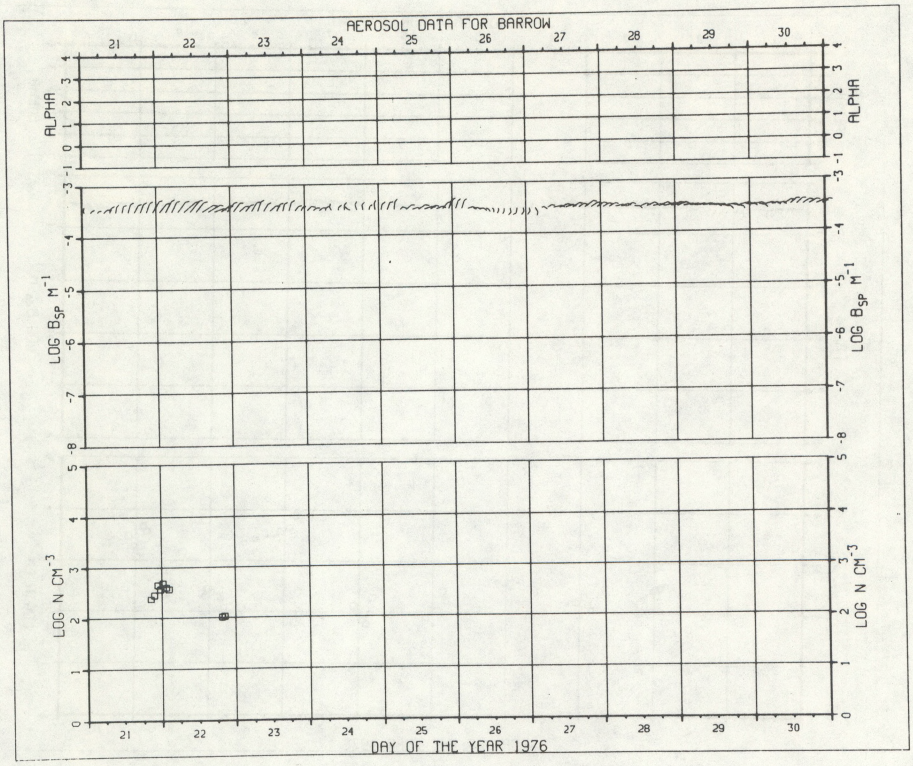
AEROSOL DATA FOR BARROW
ALPHA
LOG BSP M-1
LOG N CM-3
DAY OF THE YEAR 1976

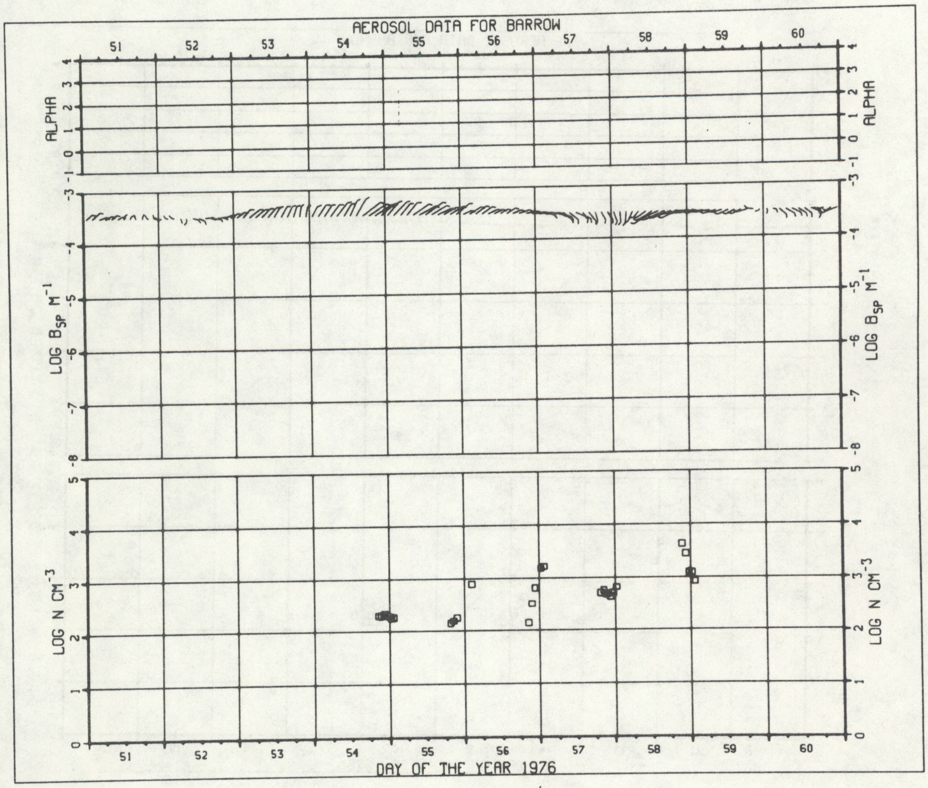
AEROSOL DATA FOR BARROW
ALPHA
LOG BSP M-1
LOG N CM-3
DAY OF THE YEAR 1976

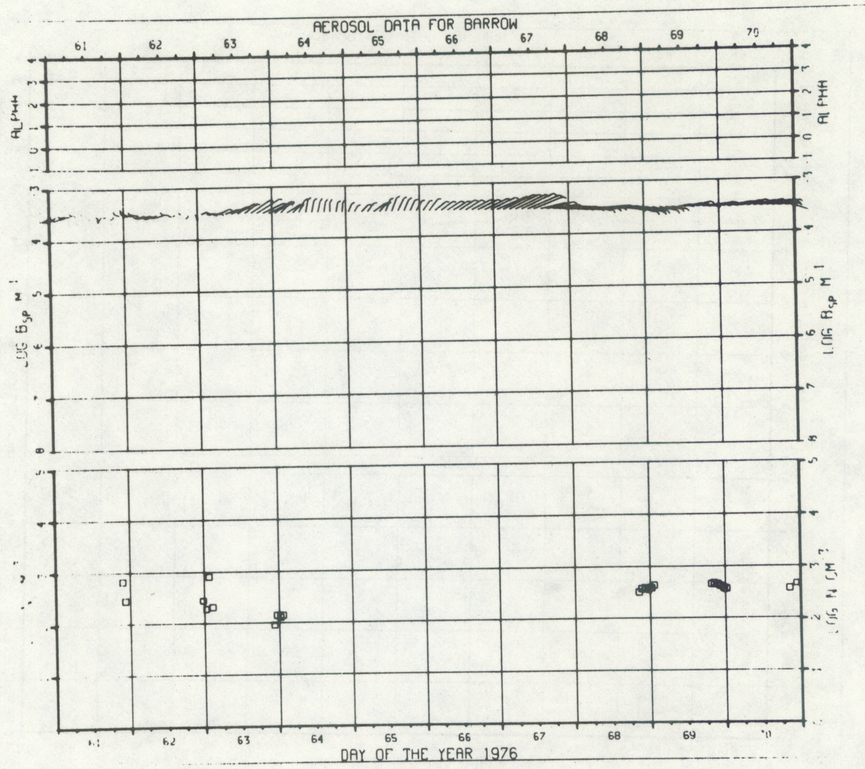
AEROSOL DATA FOR BARROW
ALPHA
LOG BSP M-1
LOG N CM-3
DAY OF THE YEAR 1976

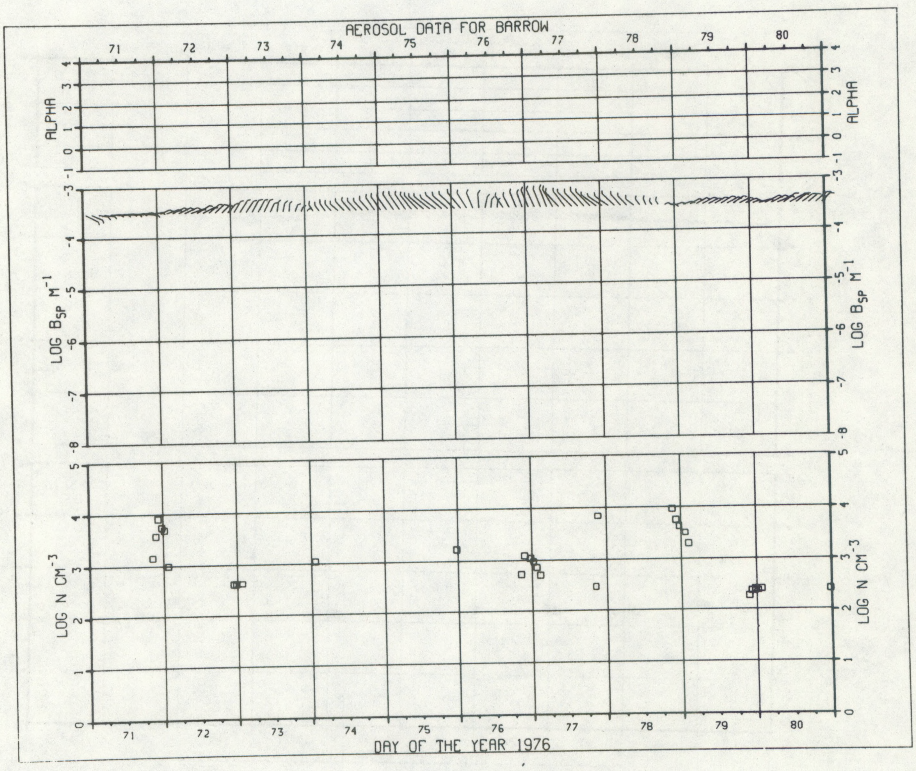
AEROSOL DATA FOR BARROW
ALPHA
LOG BSP M-1
LOG N CM-3
DAY OF THE YEAR 1976

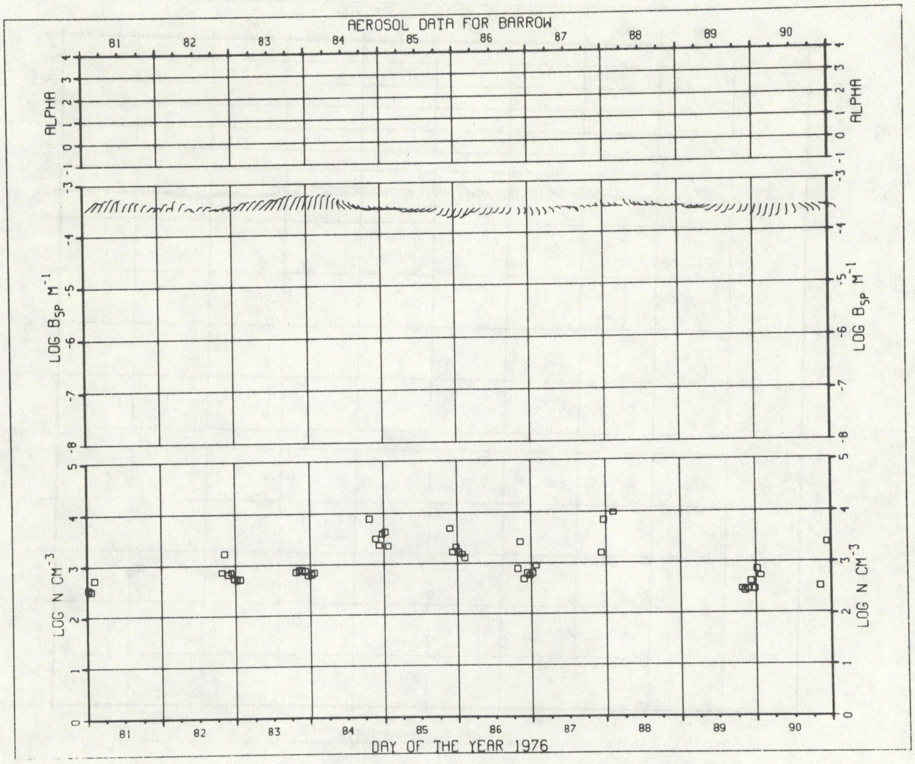
AEROSOL DATA FOR BARROW
81
82
83
84
85
86
87
88
89
90
ALPHA
LOG B_{SP} M^{-1}
LOG N CM^{-3}
DAY OF THE YEAR 1976

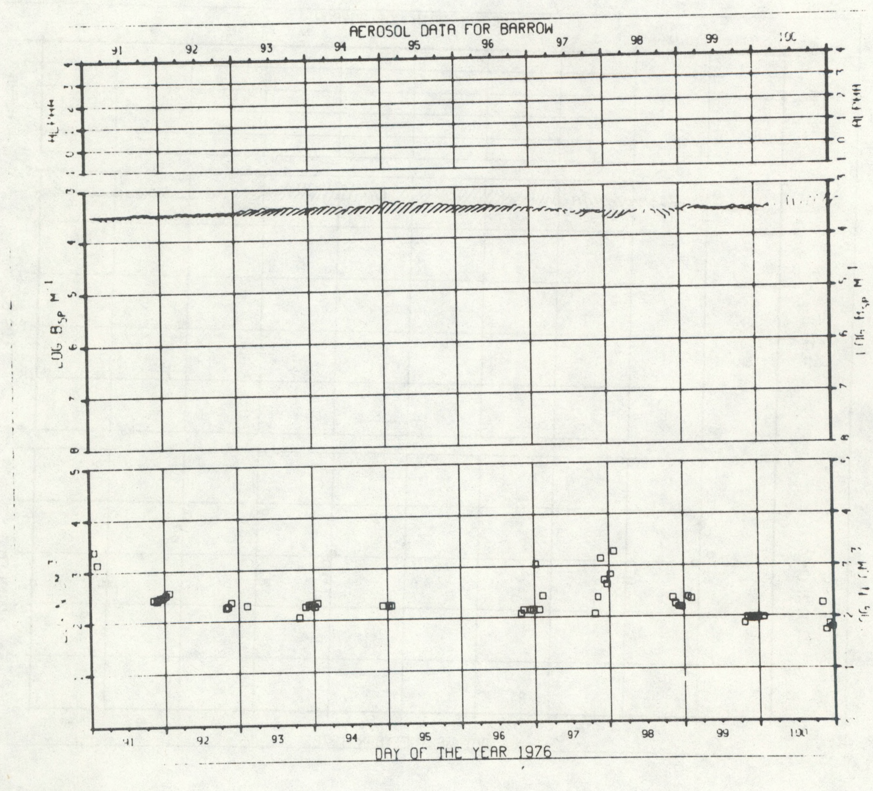
AEROSOL DATA FOR BARROW
91
92
93
94
95
96
97
98
99
LOG B_{SP} M^{-1}
DAY OF THE YEAR 1976

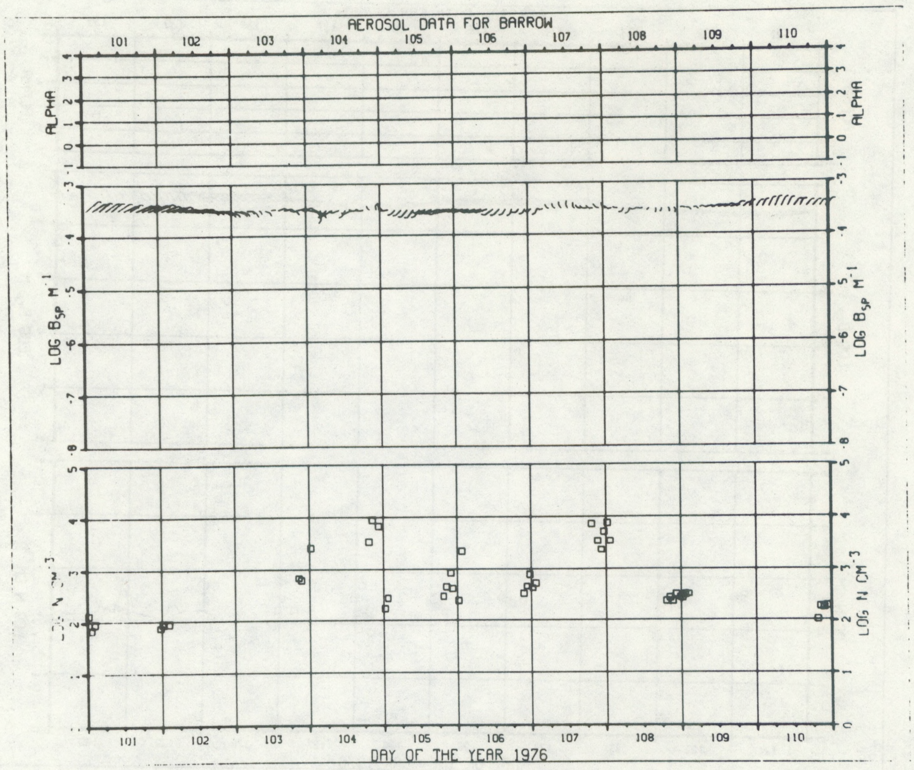
AEROSOL DATA FOR BARROW
ALPHA
LOG B_{SP} M^{-1}
LOG N CM^{-3}
101 102 103 104 105 106 107 108 109 110
DAY OF THE YEAR 1976

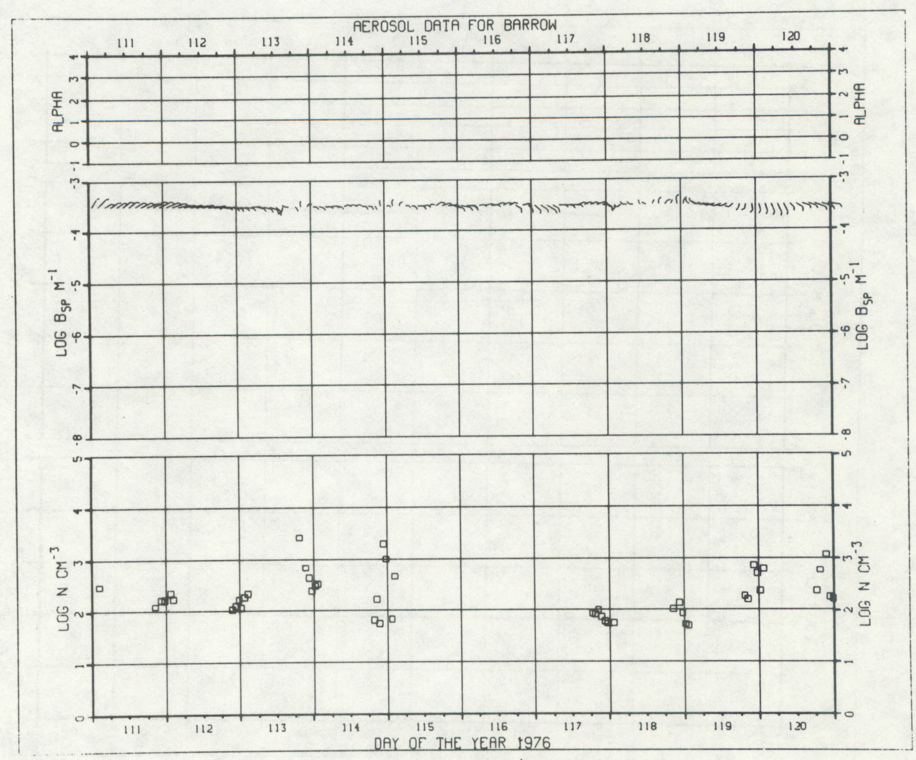
AEROSOL DATA FOR BARROW
ALPHA
LOG B_{SP} M^{-1}
LOG N CM^{-3}
111 112 113 114 115 116 117 118 119 120
DAY OF THE YEAR 1976

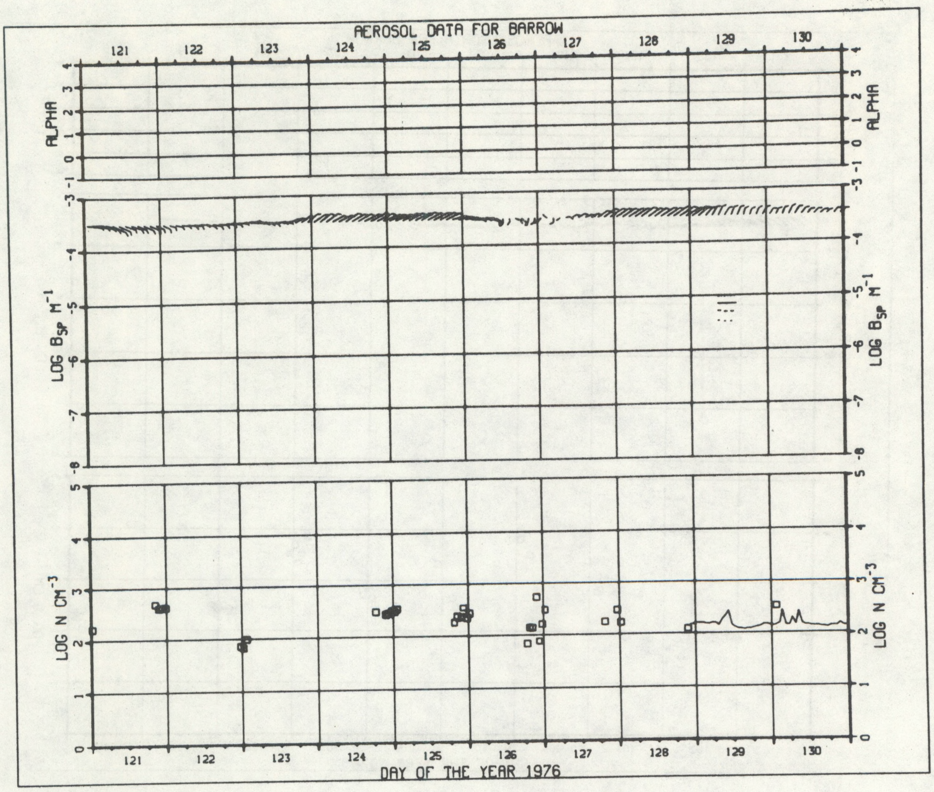
AEROSOL DATA FOR BARROW
ALPHA
LOG B$_{SP}$ M^{-1}
LOG N CM^{-3}
DAY OF THE YEAR 1976

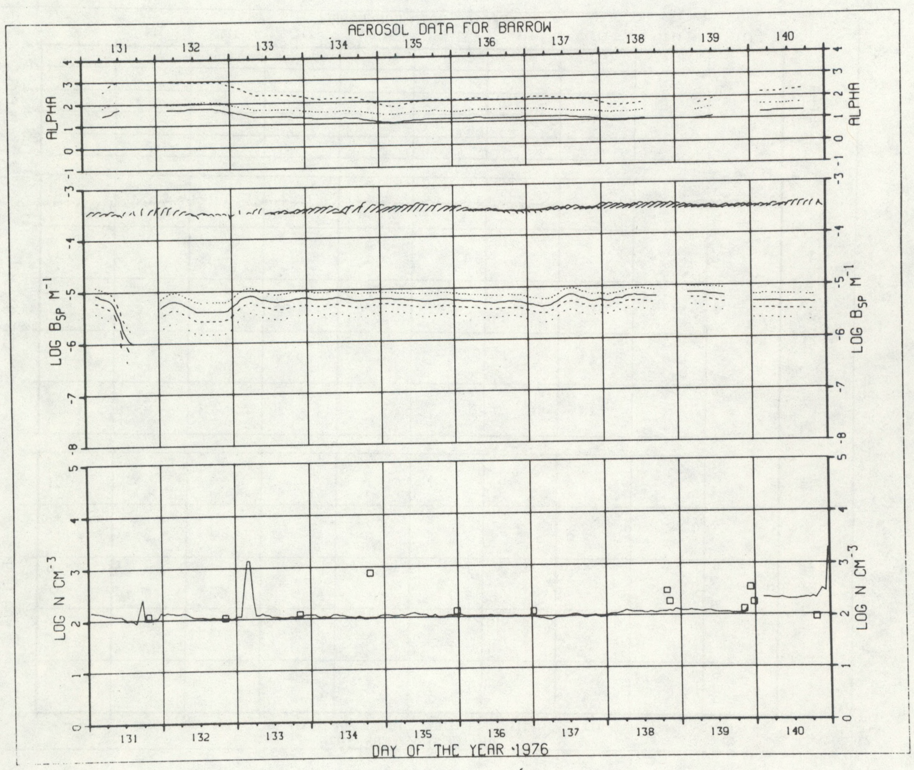
AEROSOL DATA FOR BARROW
ALPHA
LOG B$_{SP}$ M^{-1}
LOG N CM^{-3}
DAY OF THE YEAR 1976

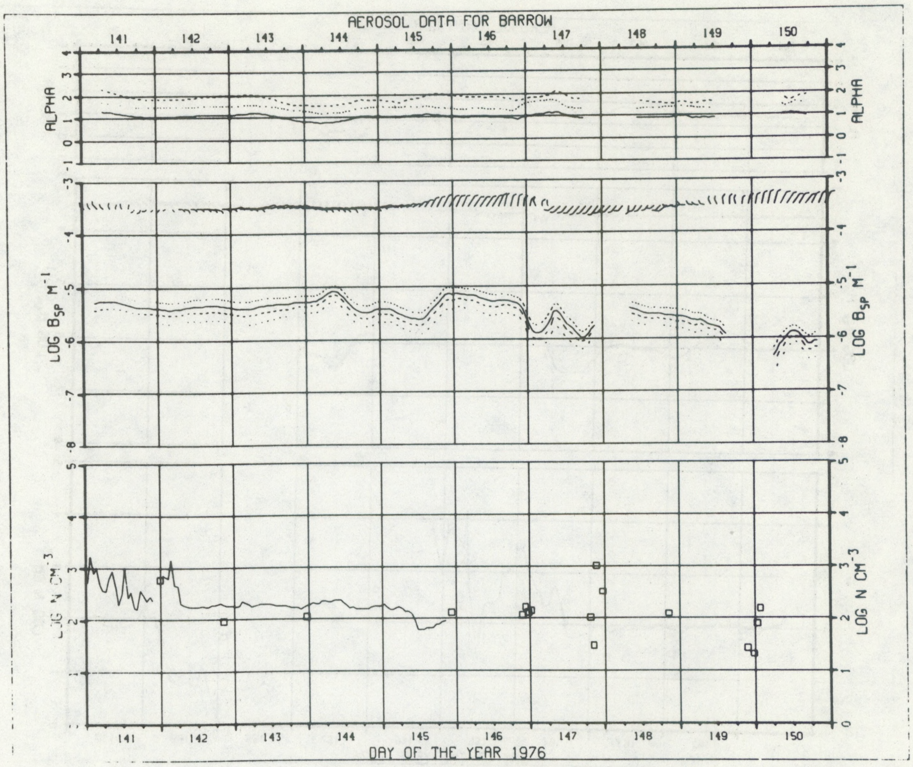
AEROSOL DATA FOR BARROW
ALPHA
LOG B_{SP} M^{-1}
LOG N CM^{-3}
DAY OF THE YEAR 1976

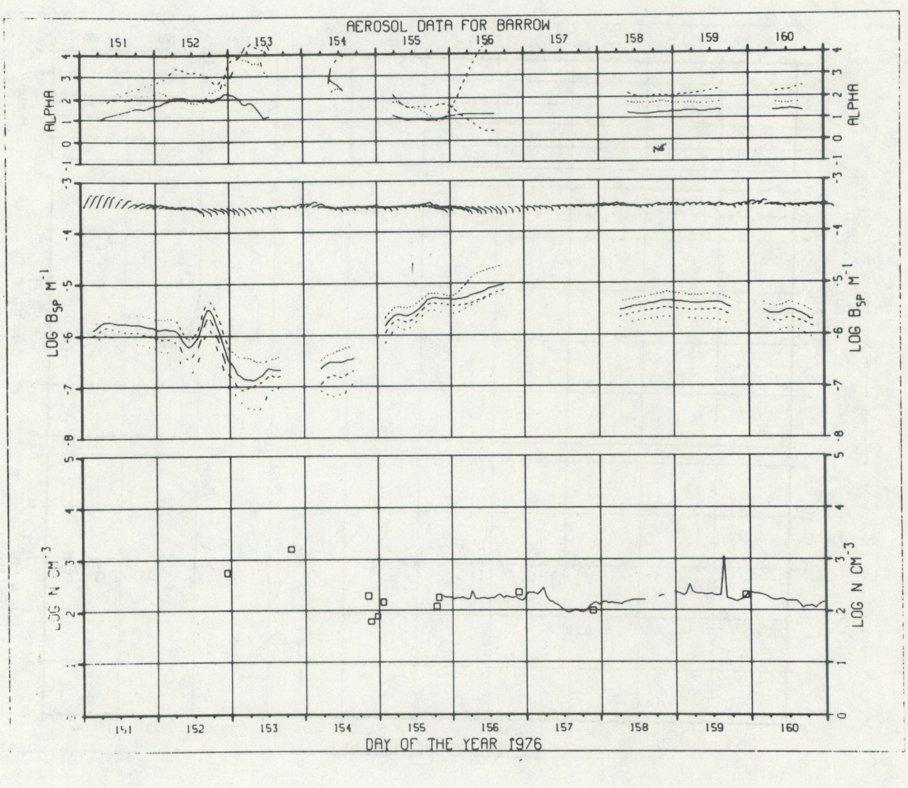
AEROSOL DATA FOR BARROW
ALPHA
LOG B_{SP} M^{-1}
LOG N CM^{-3}
DAY OF THE YEAR 1976

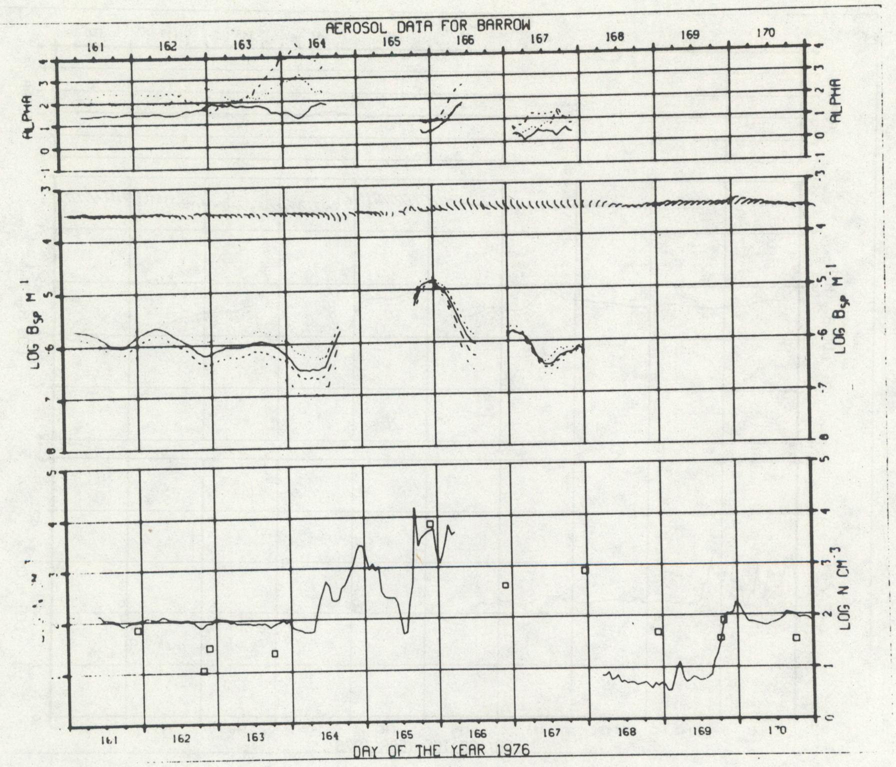
AEROSOL DATA FOR BARROW
ALPHA
LOG B_{SP} M^{-1}
LOG N CM^{-3}
DAY OF THE YEAR 1976

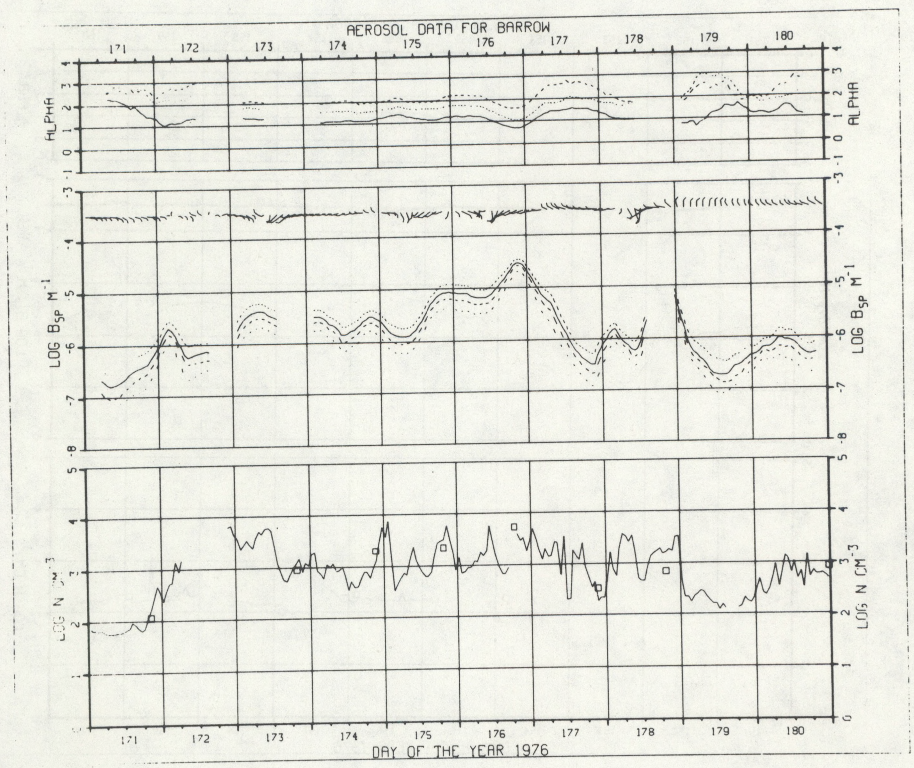
AEROSOL DATA FOR BARROW
ALPHA
LOG B_{SP} M^{-1}
LOG N CM^{-3}
DAY OF THE YEAR 1976

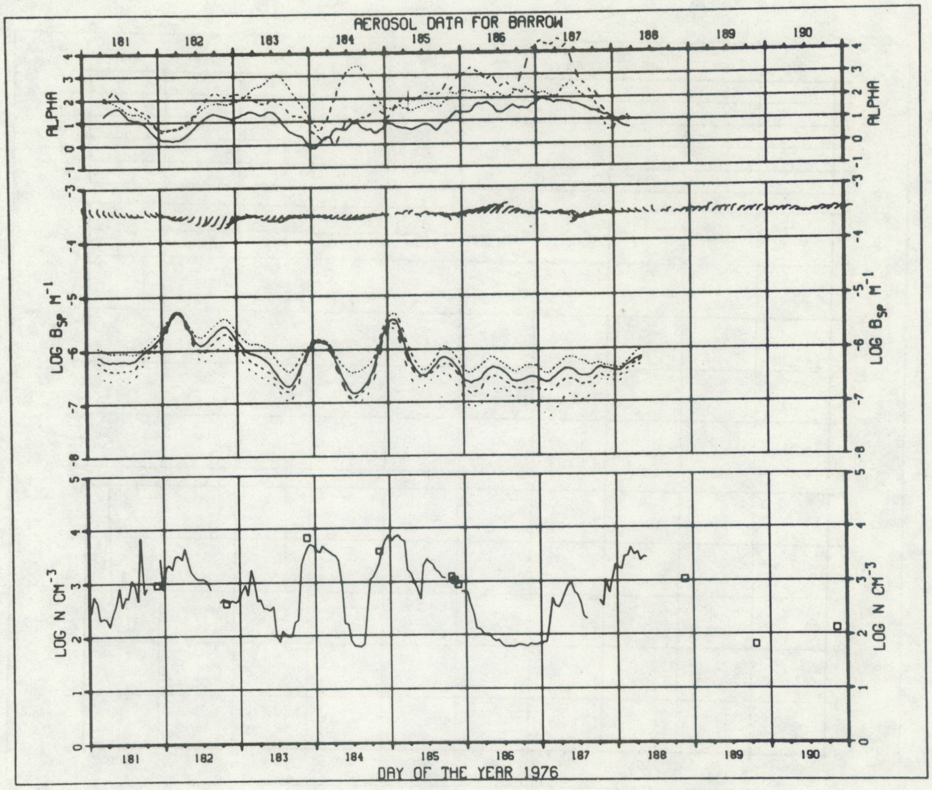
AEROSOL DATA FOR BARROW
ALPHA
LOG B_{SP} M^{-1}
LOG N CM^{-3}
DAY OF THE YEAR 1976

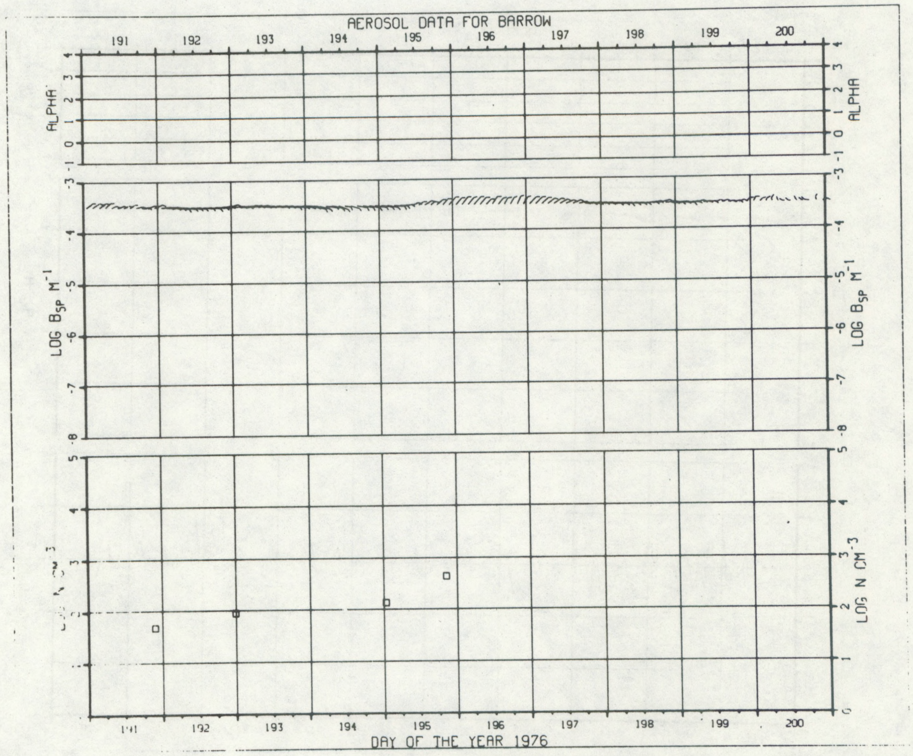
AEROSOL DATA FOR BARROW
ALPHA
LOG B_{SP} M^{-1}
LOG N CM^{-3}
DAY OF THE YEAR 1976

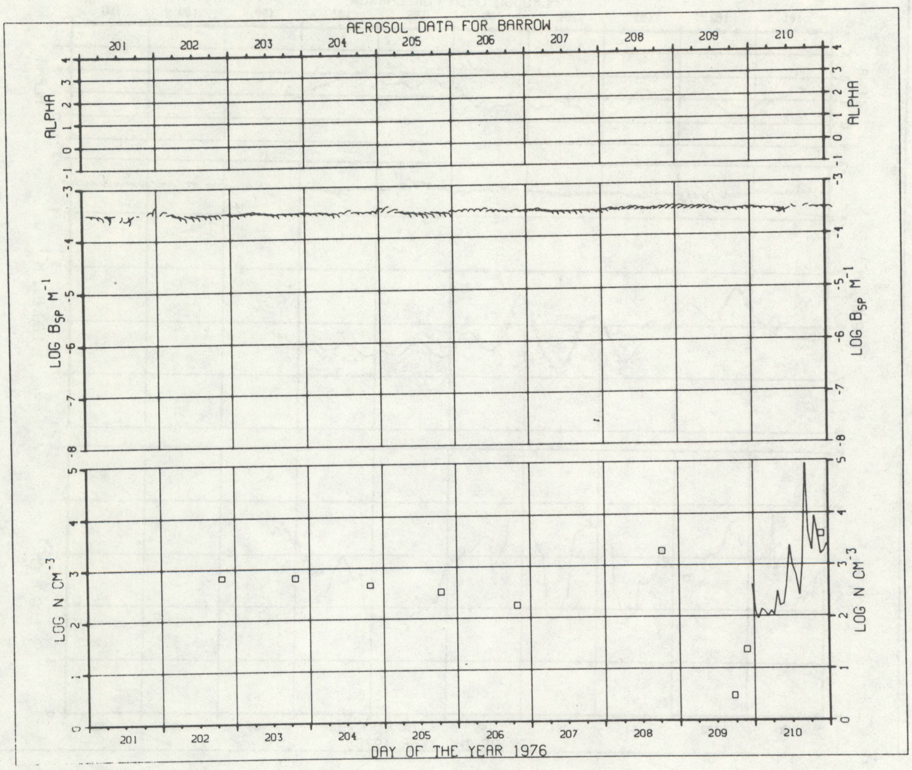
AEROSOL DATA FOR BARROW
ALPHA
LOG Bsp M-1
LOG N CM-3
DAY OF THE YEAR 1976

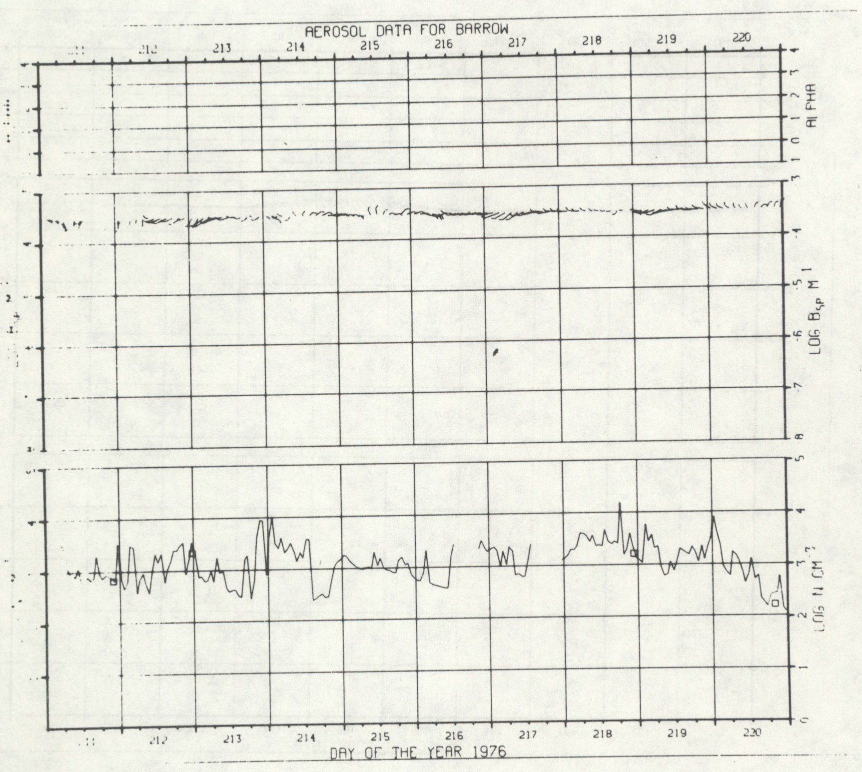
AEROSOL DATA FOR BARROW
ALPHA
LOG Bsp M-1
DAY OF THE YEAR 1976

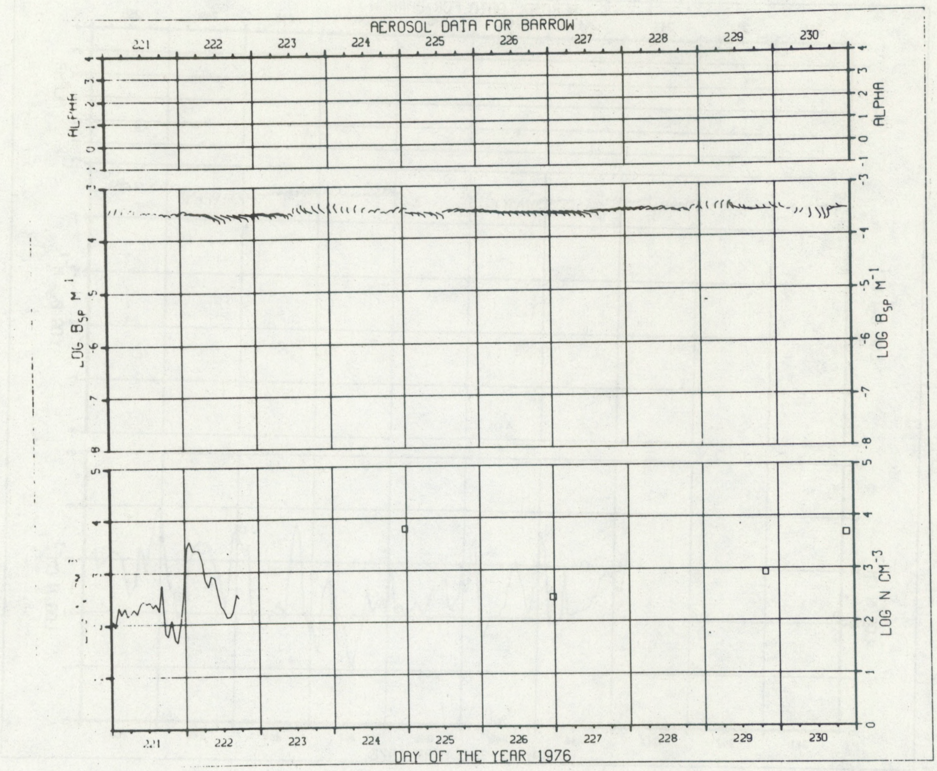
AEROSOL DATA FOR BARROW
ALPHA
LOG B$_{SP}$ M^{-1}
LOG N CM^{-3}
DAY OF THE YEAR 1976

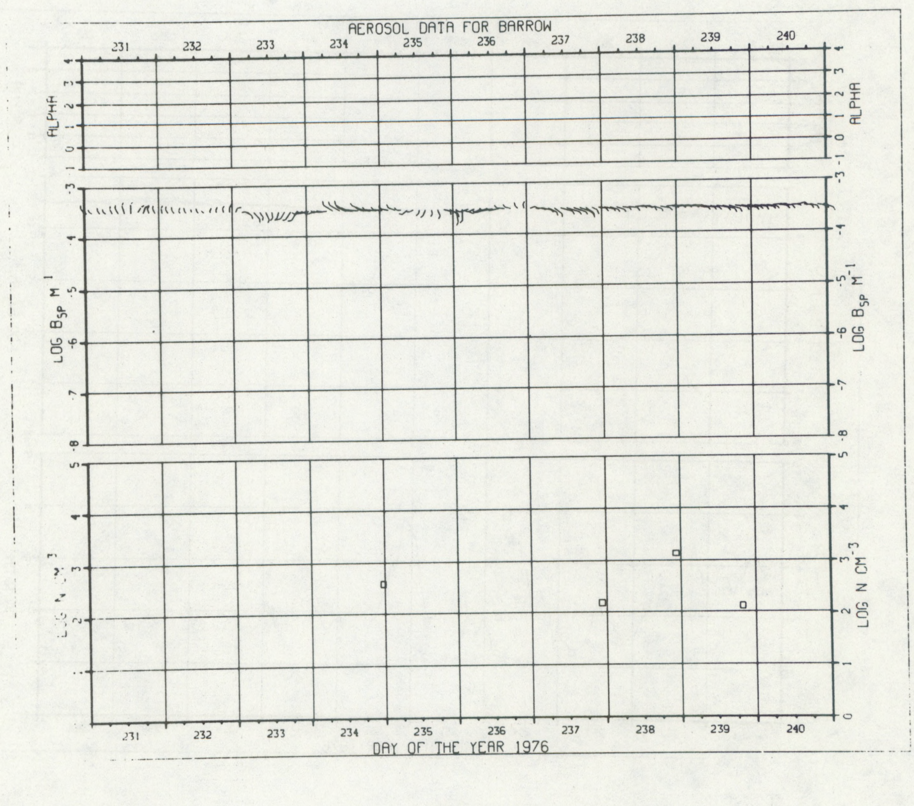
AEROSOL DATA FOR BARROW
ALPHA
LOG B$_{SP}$ M^{-1}
LOG N CM^{-3}
DAY OF THE YEAR 1976

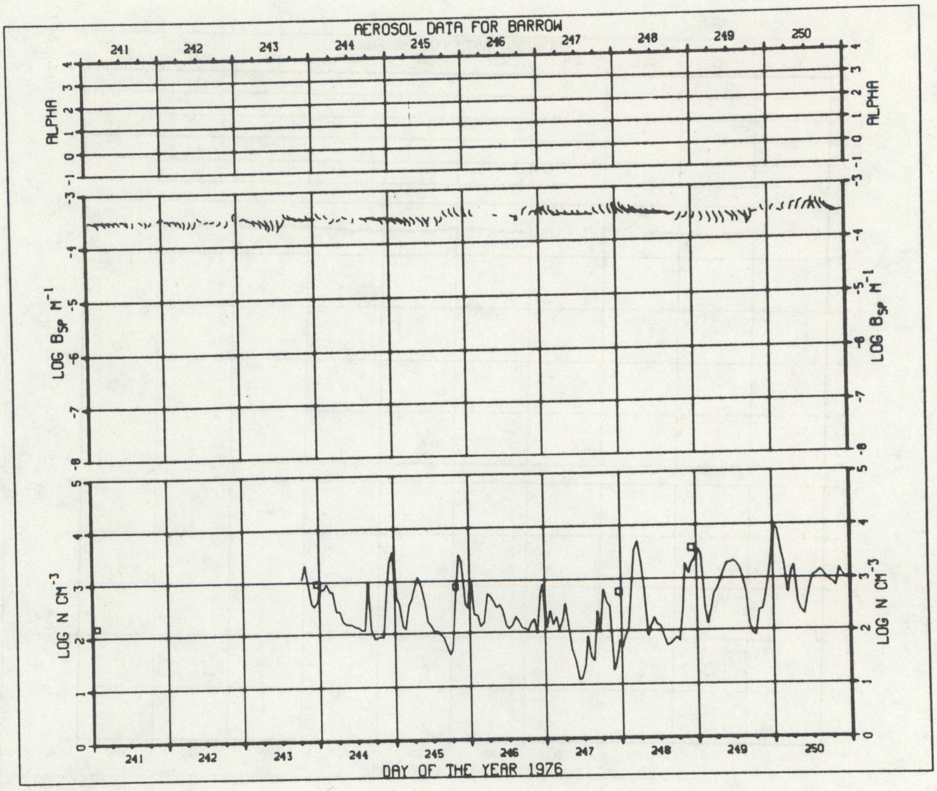
AEROSOL DATA FOR BARROW
ALPHA
LOG B_{SP} M^{-1}
LOG N CM^{-3}
DAY OF THE YEAR 1976

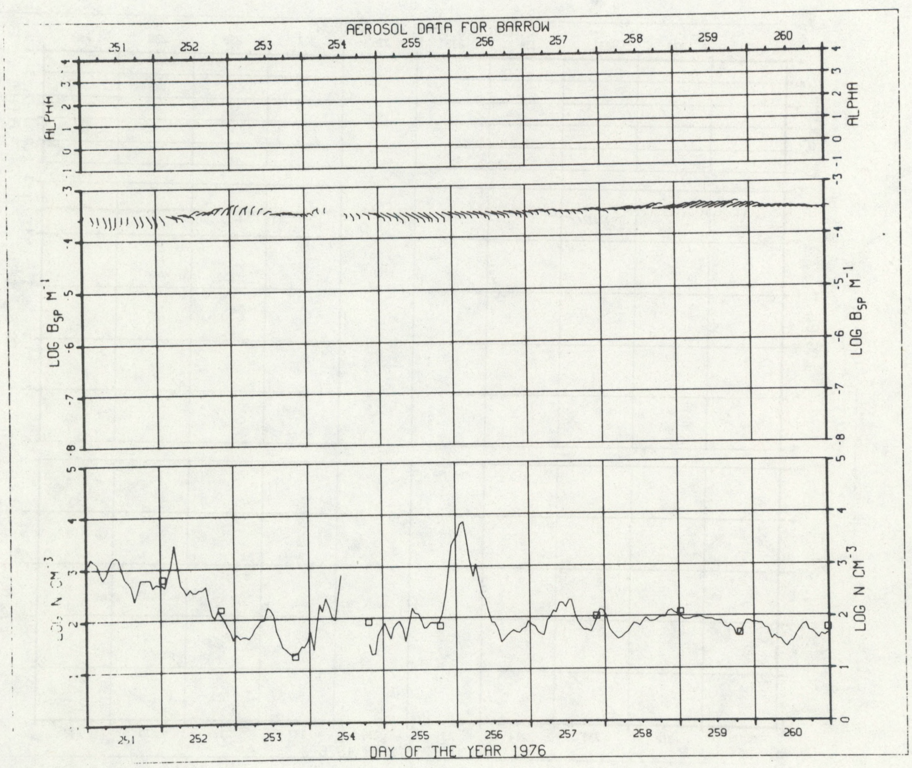
AEROSOL DATA FOR BARROW
ALPHA
LOG B_{SP} M^{-1}
LOG N CM^{-3}
DAY OF THE YEAR 1976

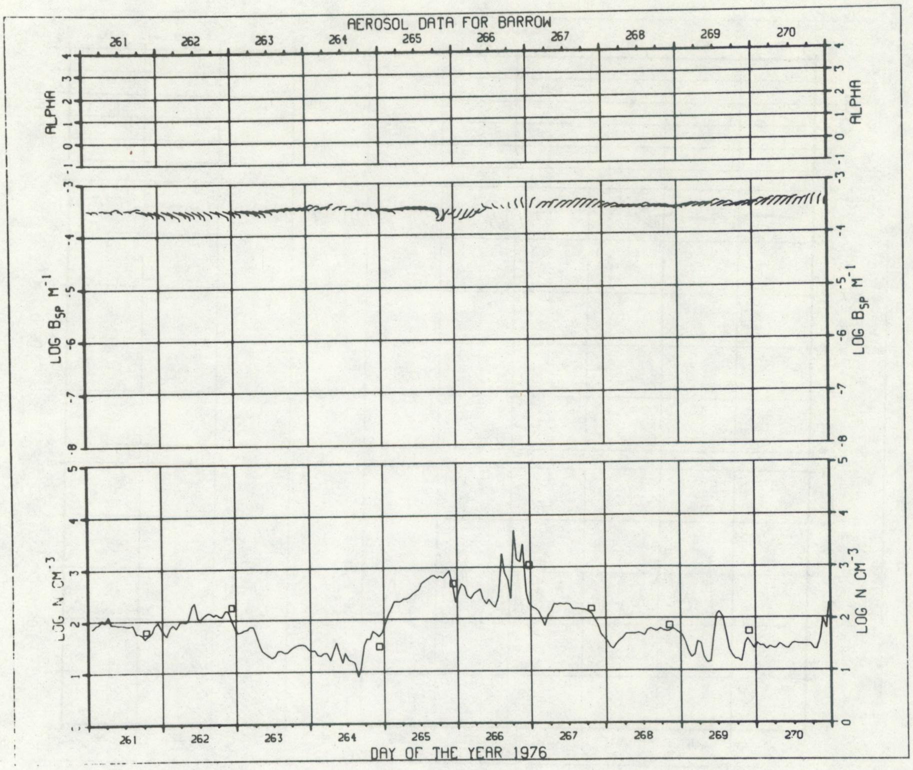
AEROSOL DATA FOR BARROW
261
262
263
264
265
266
267
268
269
270
ALPHA
LOG B$_{SP}$ M^{-1}
LOG N CM^{-3}
DAY OF THE YEAR 1976

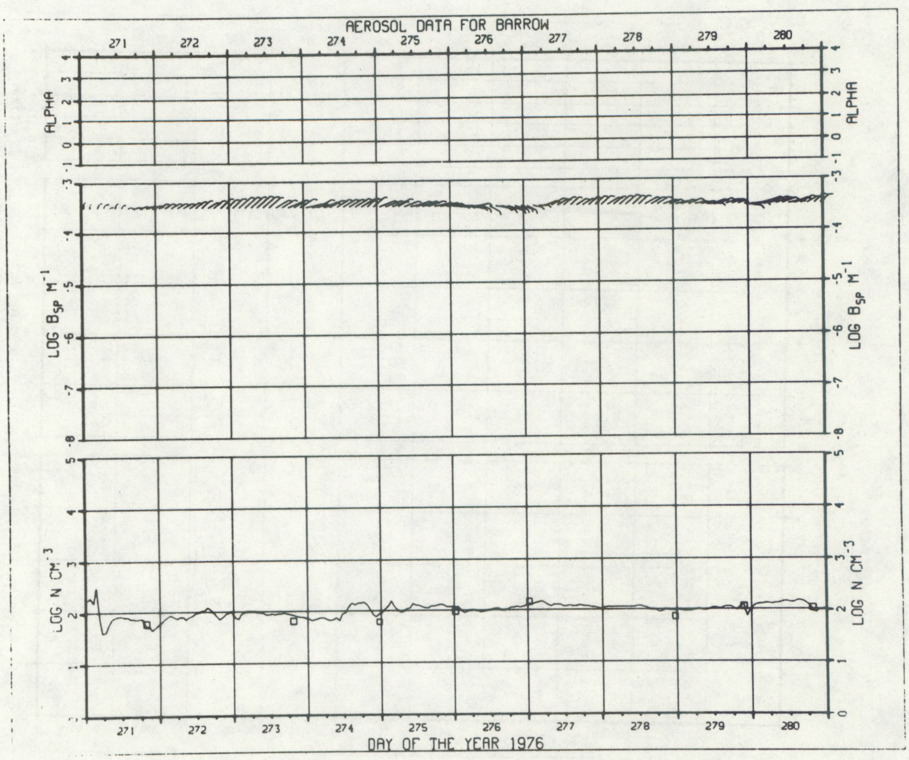
AEROSOL DATA FOR BARROW
271
272
273
274
275
276
277
278
279
280
ALPHA
LOG B$_{SP}$ M^{-1}
LOG N CM^{-3}
DAY OF THE YEAR 1976

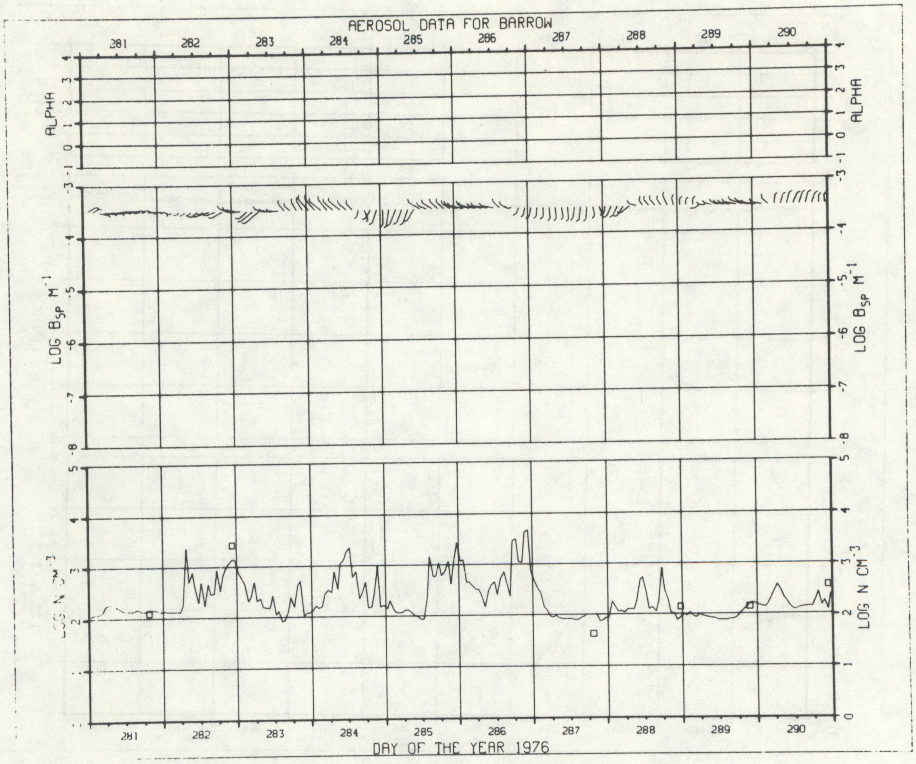

AEROSOL DATA FOR BARROW
ALPHA
LOG B_{SP} M^{-1}
LOG N CM^{-3}
DAY OF THE YEAR 1976

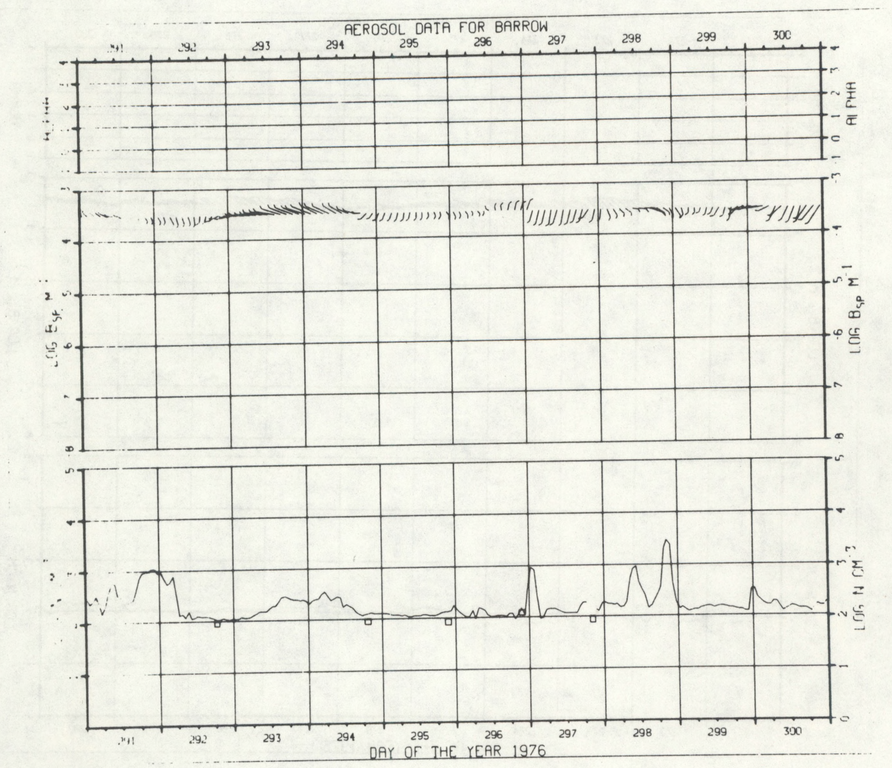

AEROSOL DATA FOR BARROW
ALPHA
LOG B_{SP} M^{-1}
LOG N CM^{-3}
DAY OF THE YEAR 1976

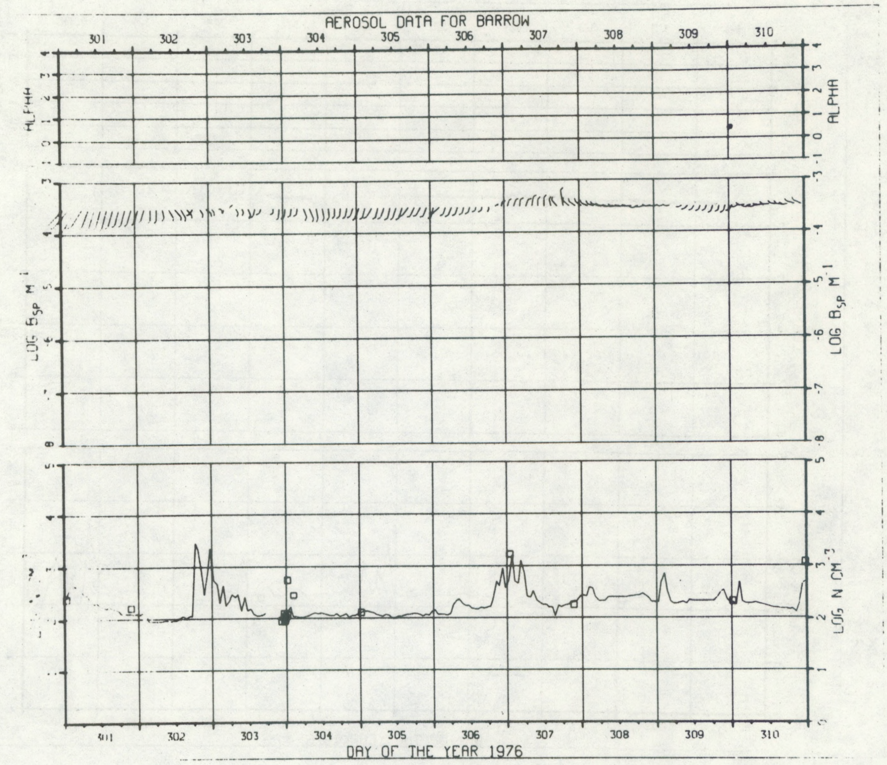

AEROSOL DATA FOR BARROW
ALPHA
LOG B_SP M^-1
LOG N CM^-3
DAY OF THE YEAR 1976

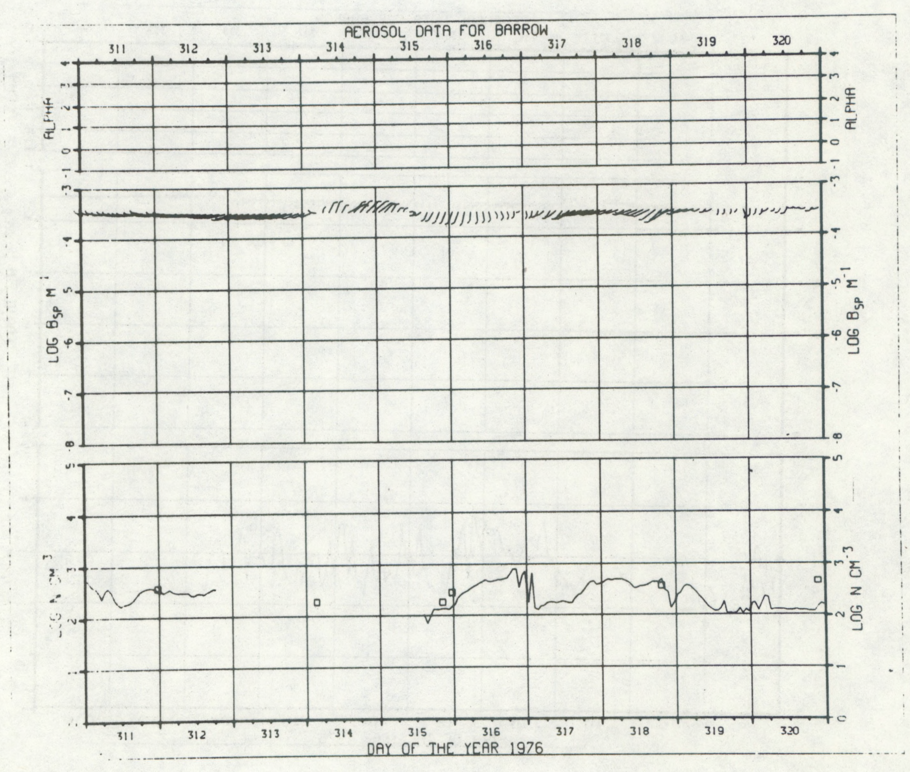

AEROSOL DATA FOR BARROW
ALPHA
LOG B_SP M^-1
LOG N CM^-3
DAY OF THE YEAR 1976

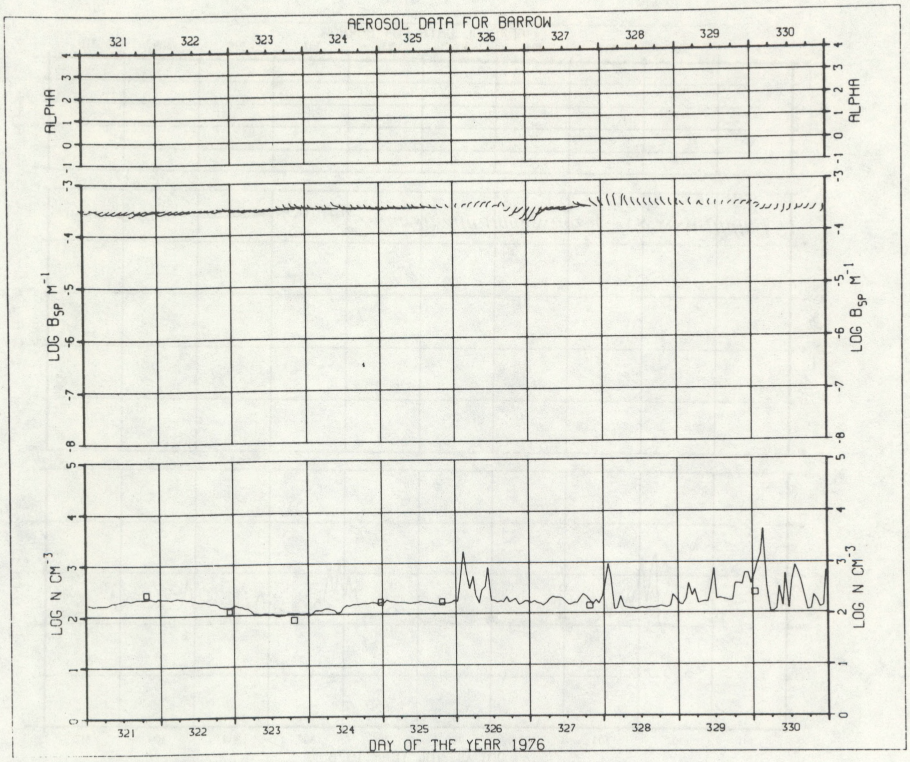
AEROSOL DATA FOR BARROW
ALPHA
LOG B_SP M^-1
LOG N CM^-3
DAY OF THE YEAR 1976

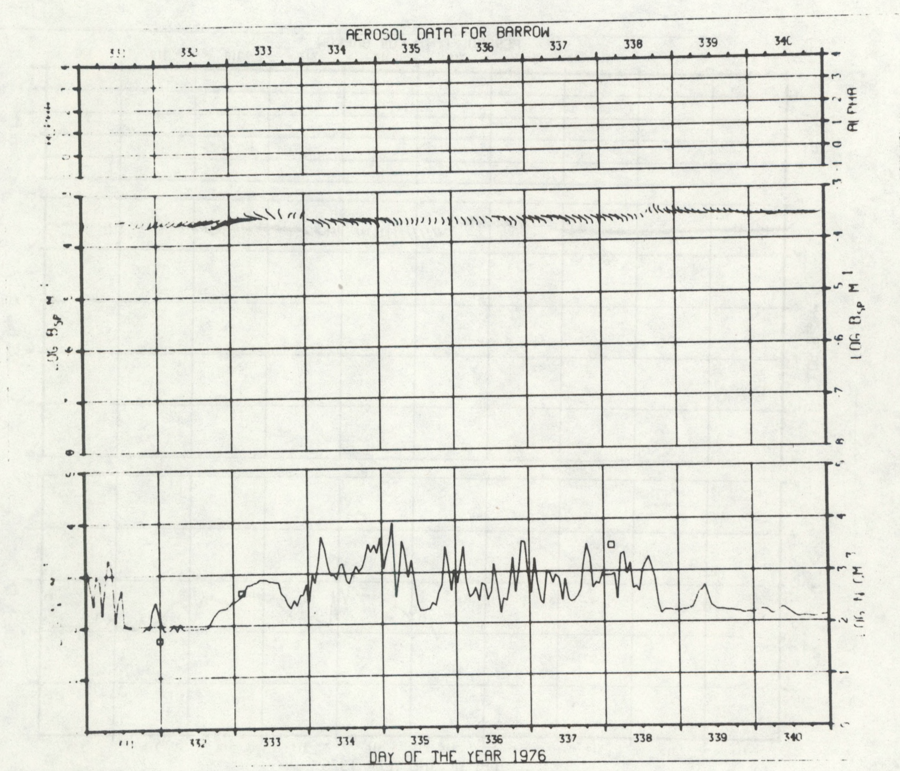
AEROSOL DATA FOR BARROW
ALPHA
DAY OF THE YEAR 1976

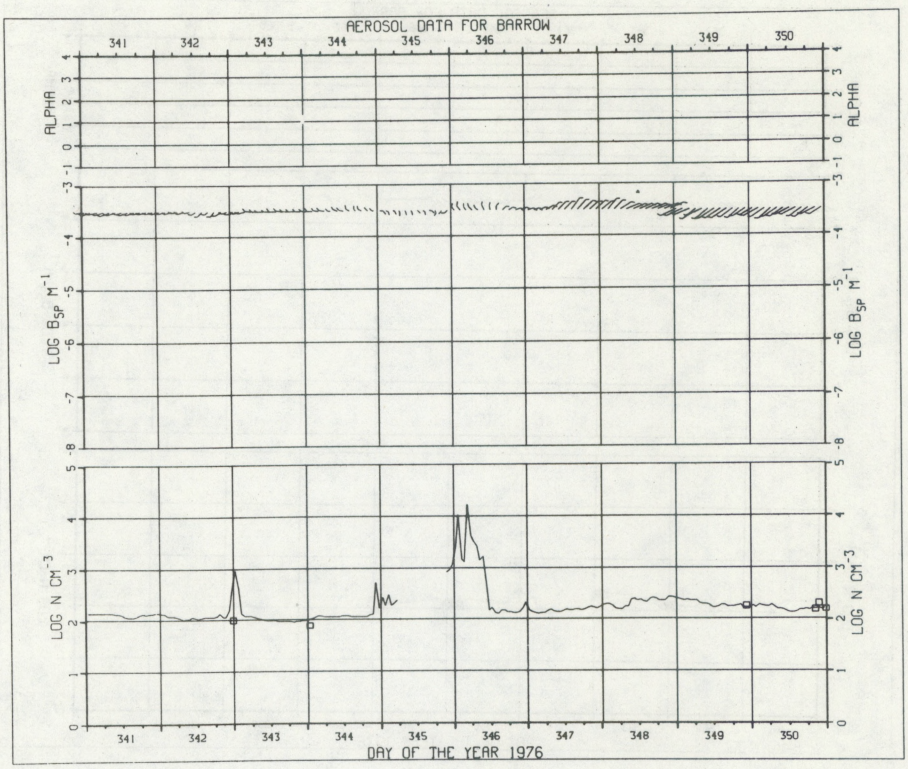
AEROSOL DATA FOR BARROW
ALPHA
LOG BSP M-1
LOG N CM-3
DAY OF THE YEAR 1976

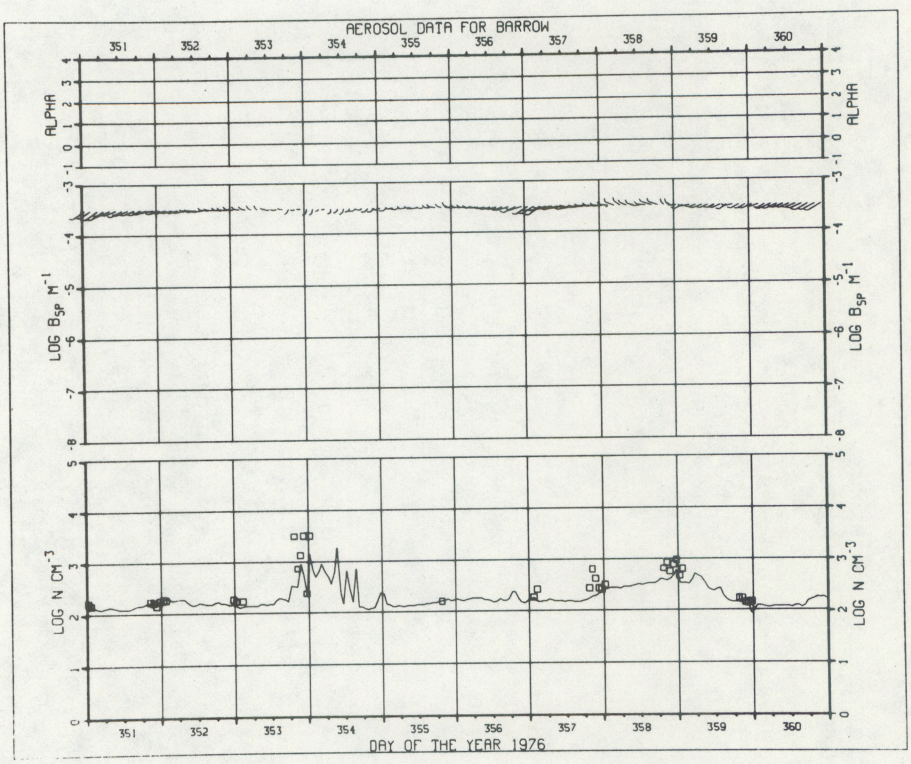
AEROSOL DATA FOR BARROW
ALPHA
LOG BSP M-1
LOG N CM-3
DAY OF THE YEAR 1976

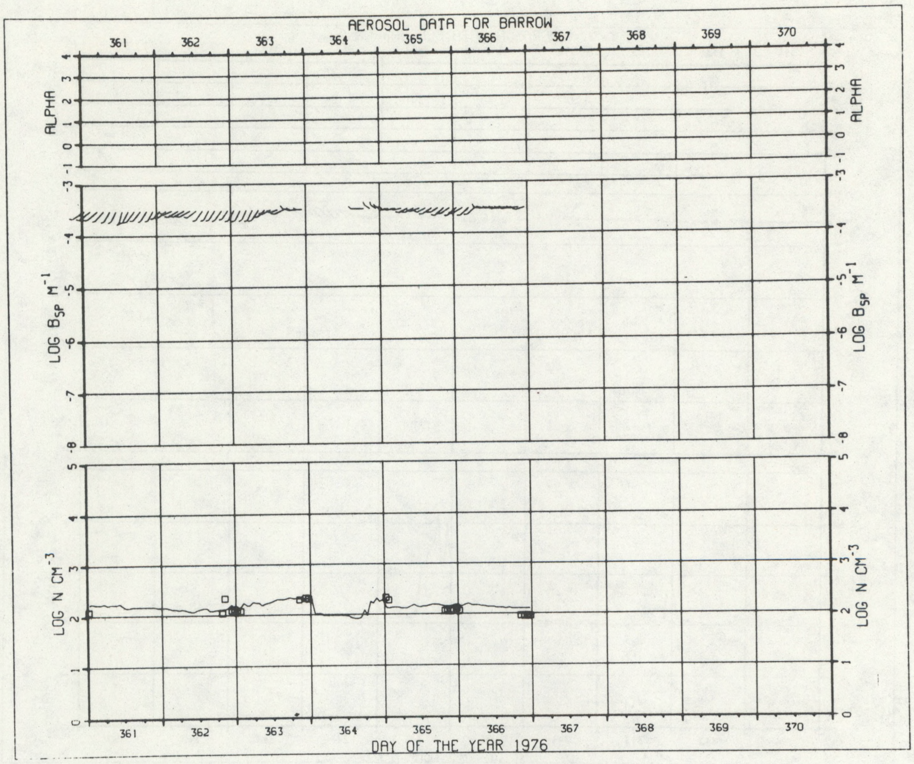
AEROSOL DATA FOR BARROW
ALPHA
LOG B$_{SP}$ M^{-1}
LOG N CM^{-3}
DAY OF THE YEAR 1976

APPENDIX B

Appendix B contains the hourly mean nuclei concentrations, Pollak counter observations, light scattering data, and Angstrom exponents plotted on a logarithmic scale for 1977. A histogram of successive one minute voltage differences for each month was generated and the variability criterion was determined to be ±0.0399 volts.

The data pairs were obtained from the minute data and grouped into periods where the G.E. counter was operating. The scaling factors generated are:

Day	Scaling Factor
00-3201	0.924833351
3202-6320	0.700590126
6321-16817	0.980521376
16818-21718	0.526476861
21719-26523	0.577492344
26620-36523	0.738563736

The G.E. counter was down during days 26600-26619.

Scaled graphical display of aerosol data for 1977.
for each plot;

the top graph contains: Angstrom exponents
Alpha (1-2): dashed line
Alpha (2-3): solid line
Alpha (3-4): long dashed line

the center graph contains: light scattering and wind data
wavelength 450 nm: dashed line
wavelength 550 nm: solid line
wavelength 700 nm: long dashed line
wavelength 850 nm: short dashed line

the lower graph contains: nuclei concentrations
G.E. Counter: solid line
Pollak counter: squares

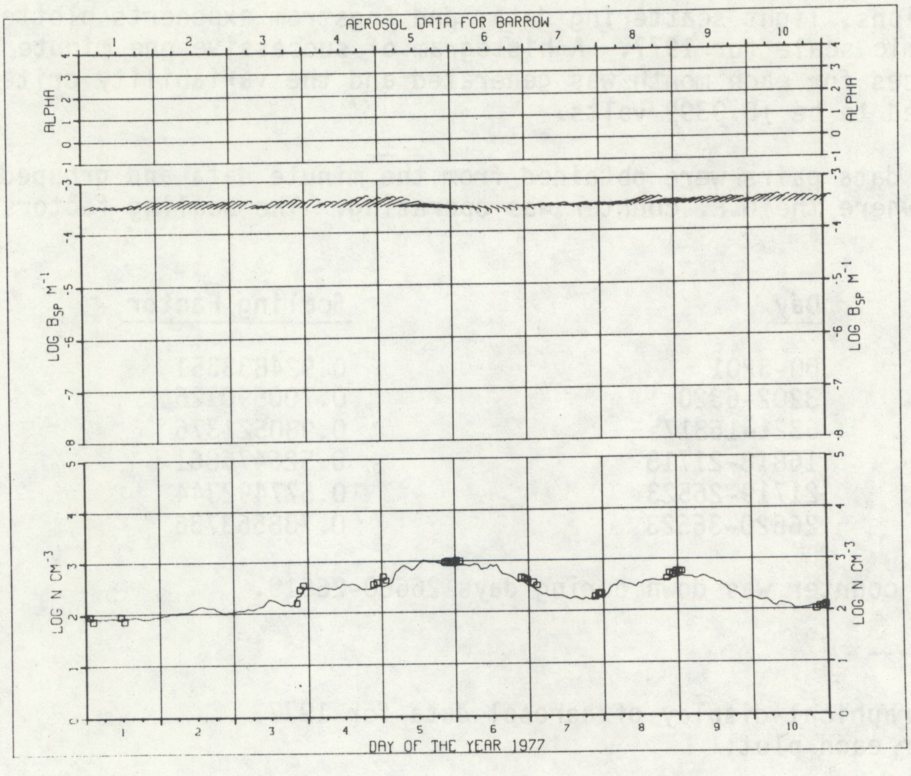
AEROSOL DATA FOR BARROW
ALPHA
LOG B_{SP} M^{-1}
LOG N CM^{-3}
DAY OF THE YEAR 1977

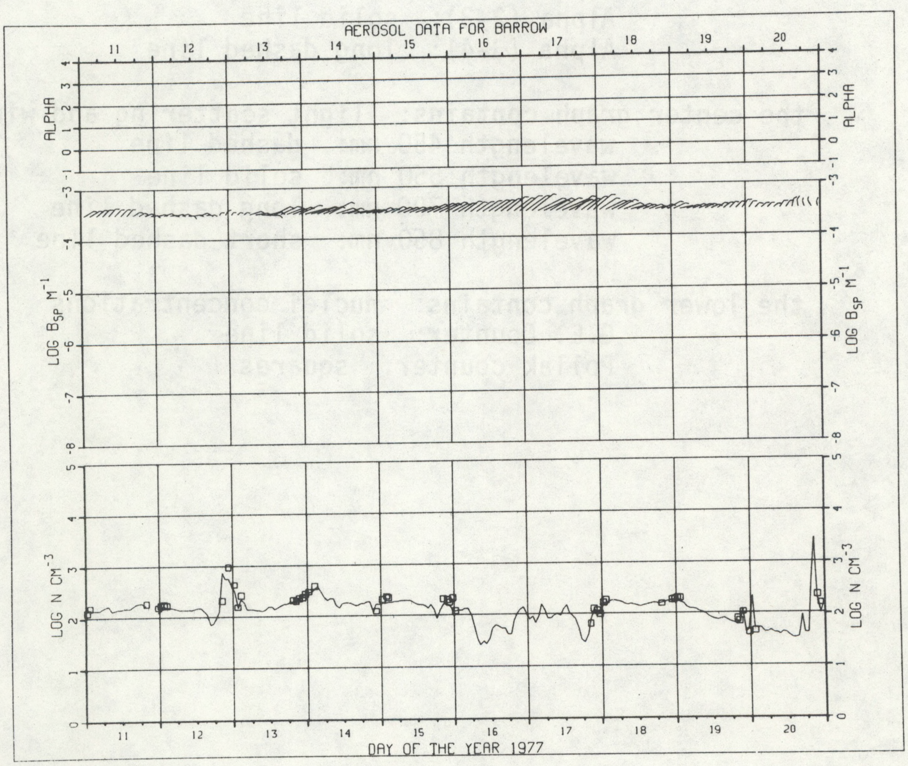
AEROSOL DATA FOR BARROW
ALPHA
LOG B_{SP} M^{-1}
LOG N CM^{-3}
DAY OF THE YEAR 1977

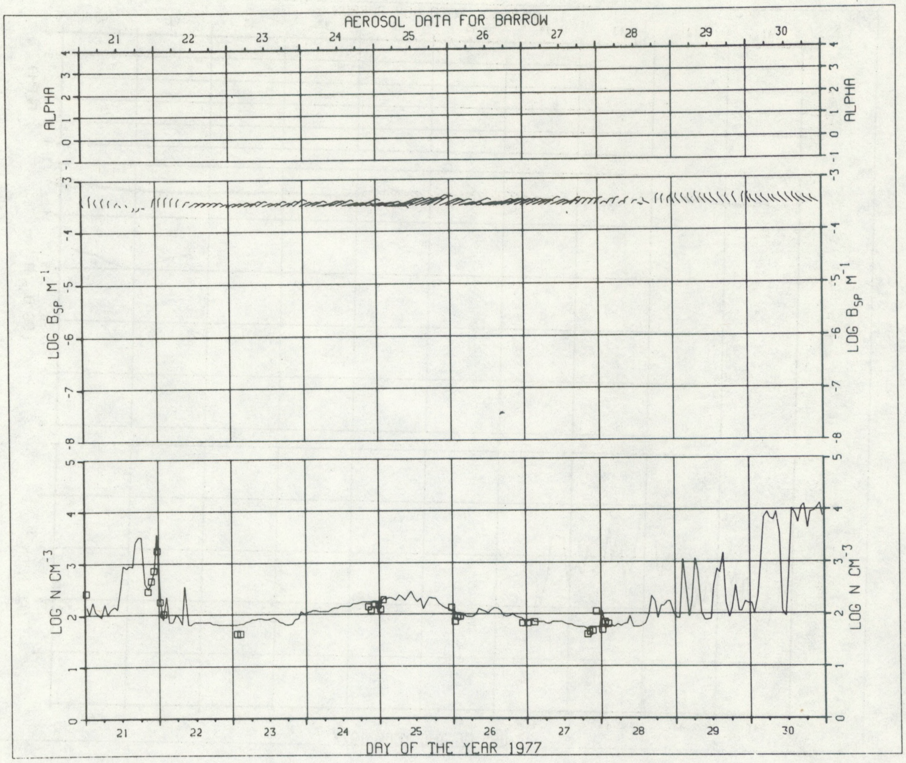
AEROSOL DATA FOR BARROW
ALPHA
LOG B$_{SP}$ M^{-1}
LOG N CM^{-3}
DAY OF THE YEAR 1977

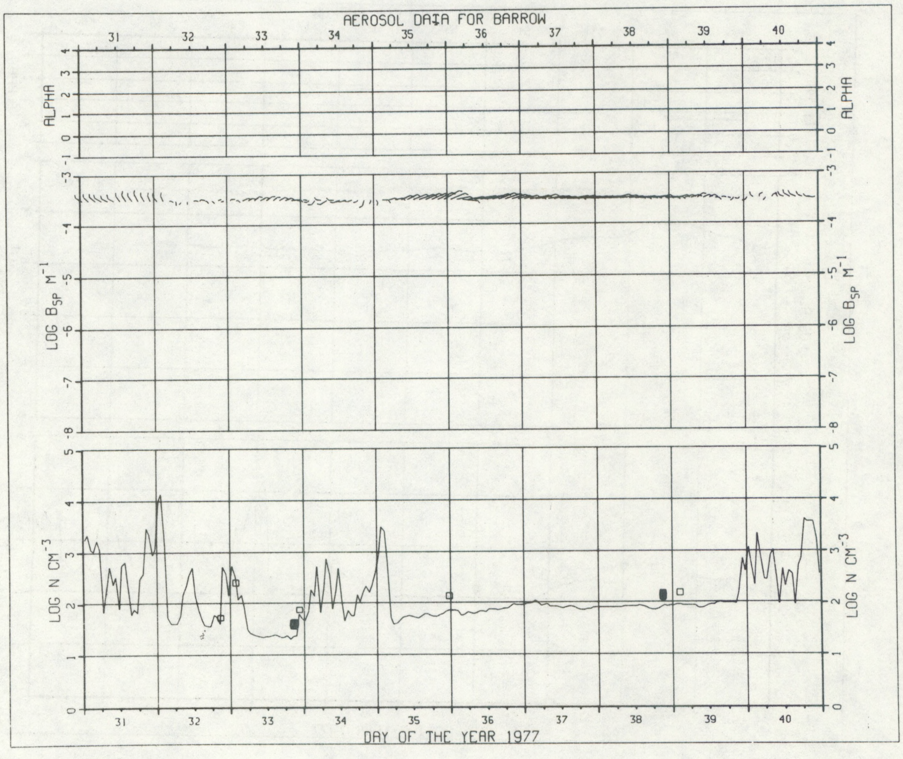
AEROSOL DATA FOR BARROW
ALPHA
LOG B$_{SP}$ M^{-1}
LOG N CM^{-3}
DAY OF THE YEAR 1977

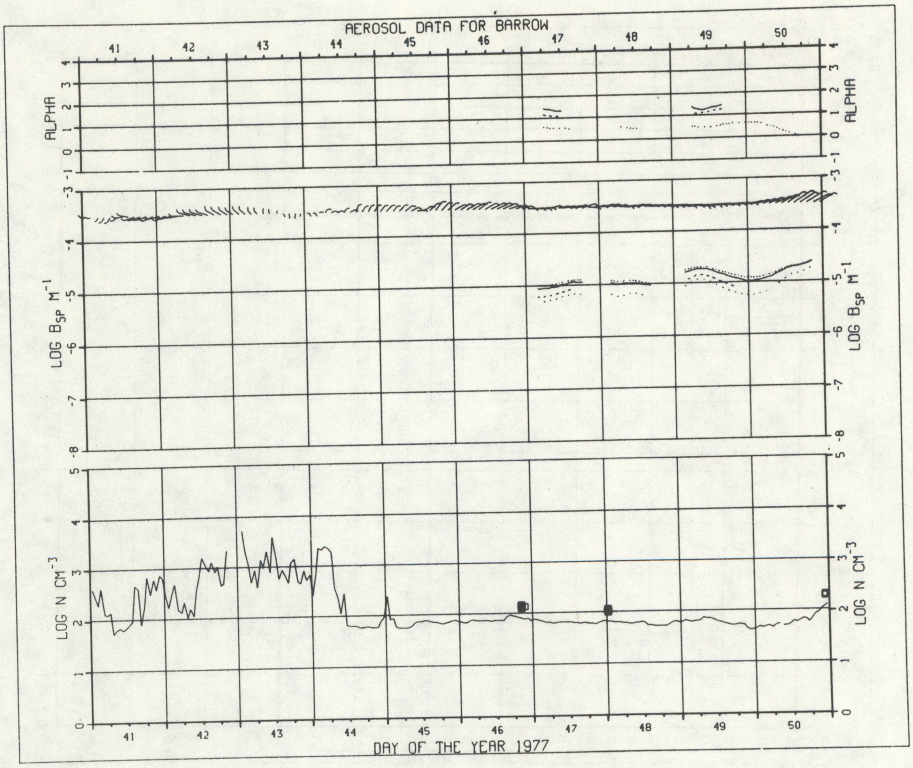
AEROSOL DATA FOR BARROW
ALPHA
LOG B$_{SP}$ M^{-1}
LOG N CM^{-3}
DAY OF THE YEAR 1977

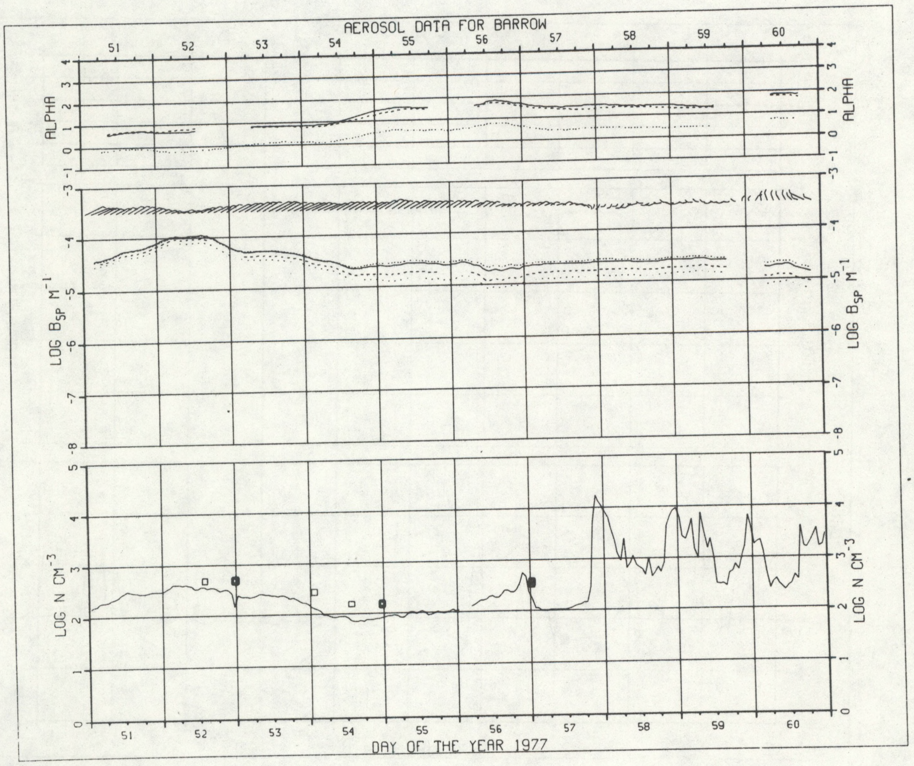
AEROSOL DATA FOR BARROW
ALPHA
LOG B$_{SP}$ M^{-1}
LOG N CM^{-3}
DAY OF THE YEAR 1977

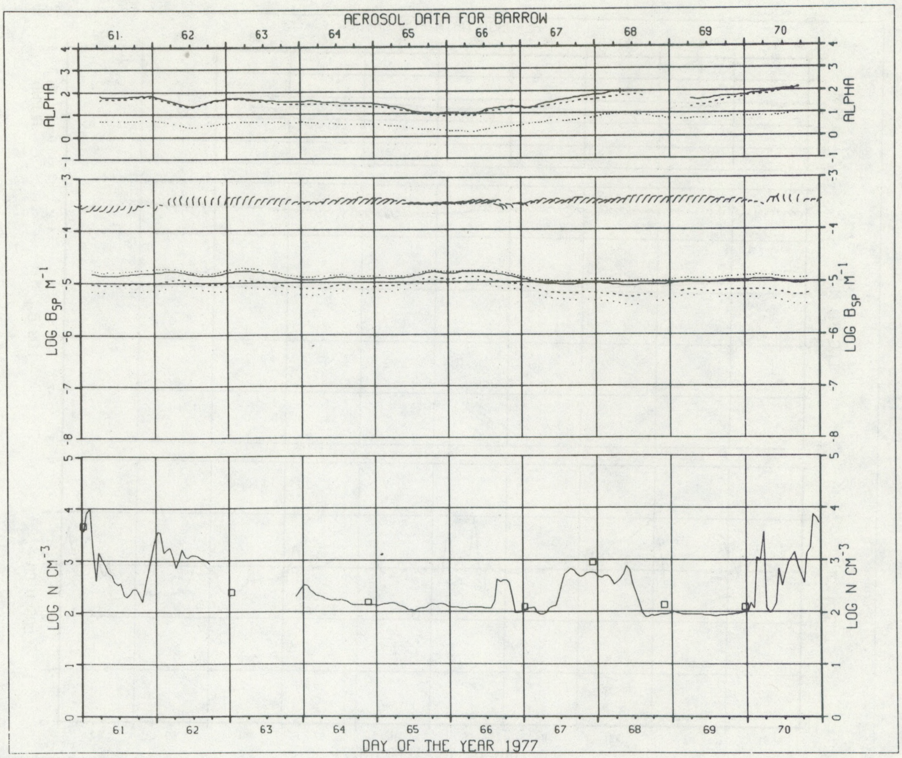
AEROSOL DATA FOR BARROW
ALPHA
LOG B_{SP} M^{-1}
LOG N CM^{-3}
DAY OF THE YEAR 1977

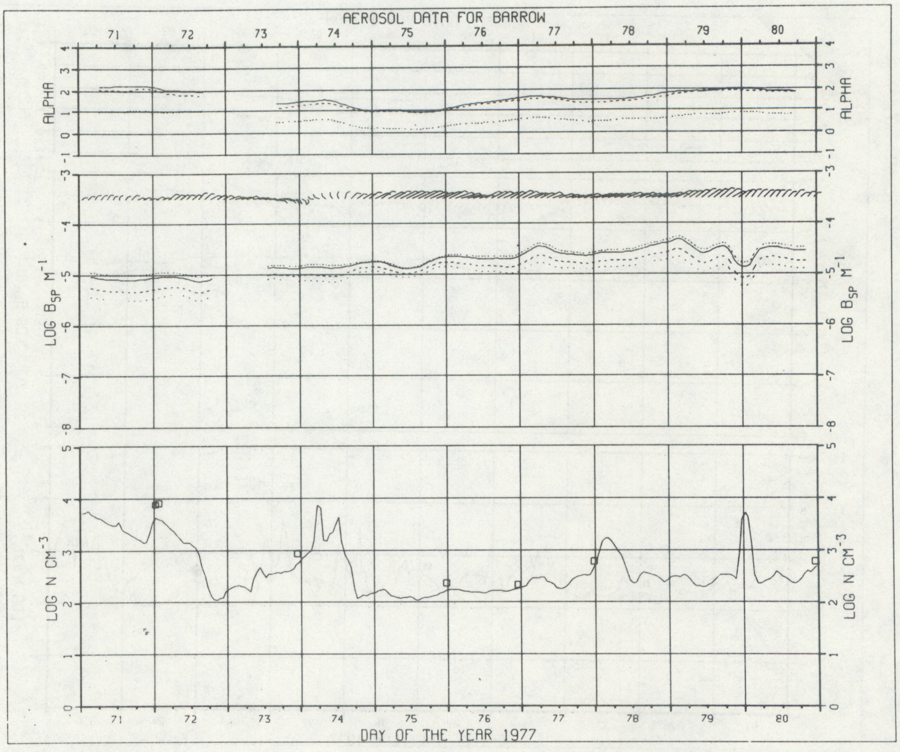
AEROSOL DATA FOR BARROW
ALPHA
LOG B_{SP} M^{-1}
LOG N CM^{-3}
DAY OF THE YEAR 1977

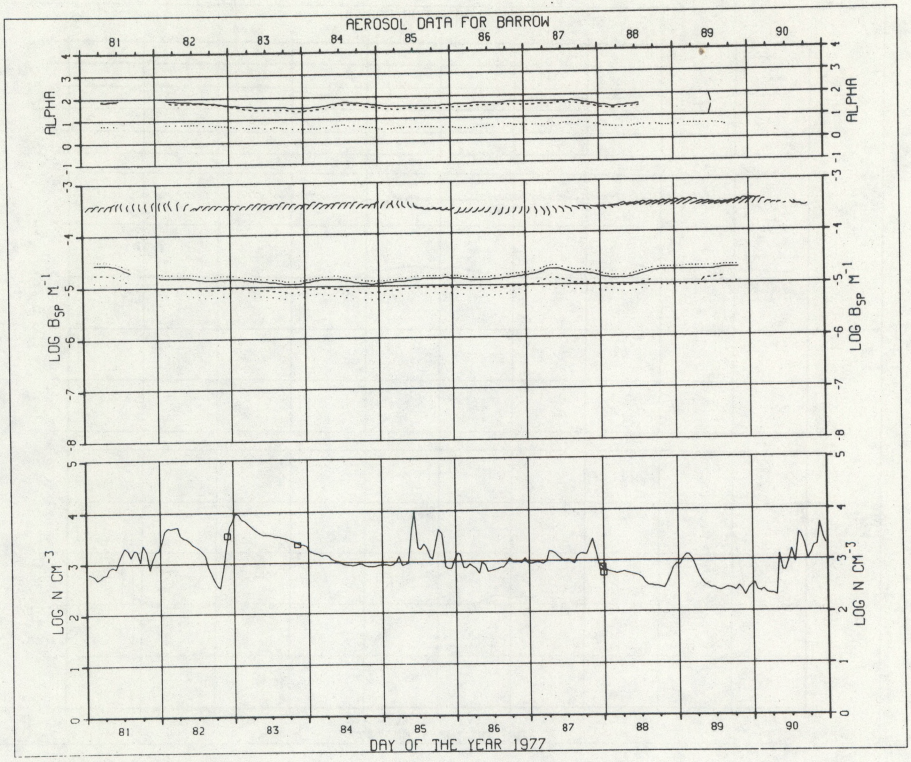
AEROSOL DATA FOR BARROW
ALPHA
LOG B_{SP} M^{-1}
LOG N CM^{-3}
DAY OF THE YEAR 1977

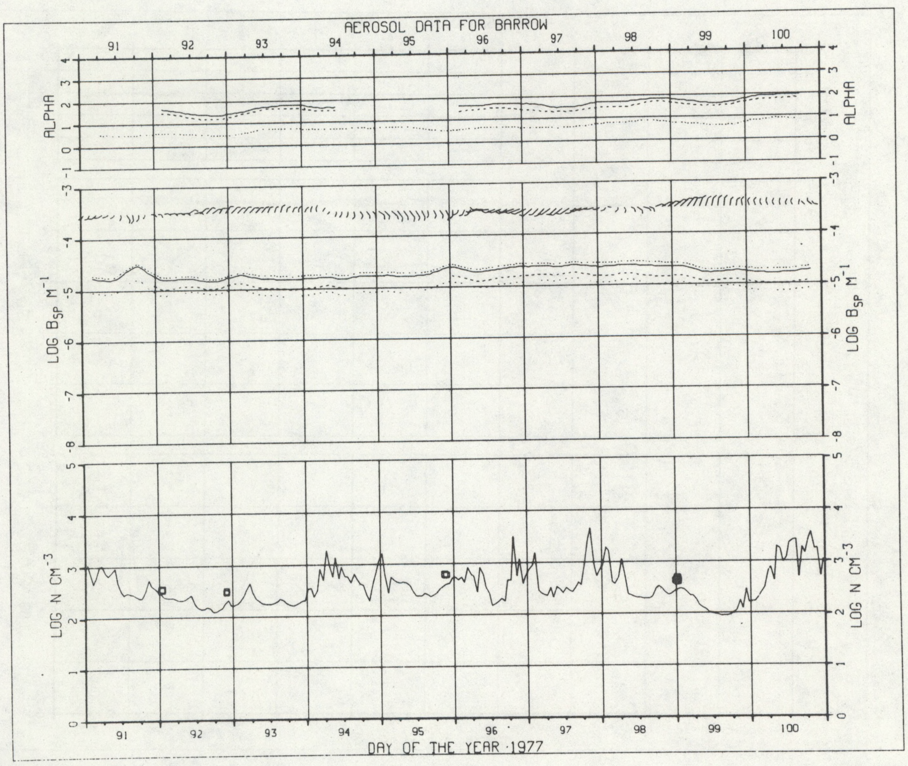
AEROSOL DATA FOR BARROW
ALPHA
LOG B_{SP} M^{-1}
LOG N CM^{-3}
DAY OF THE YEAR 1977

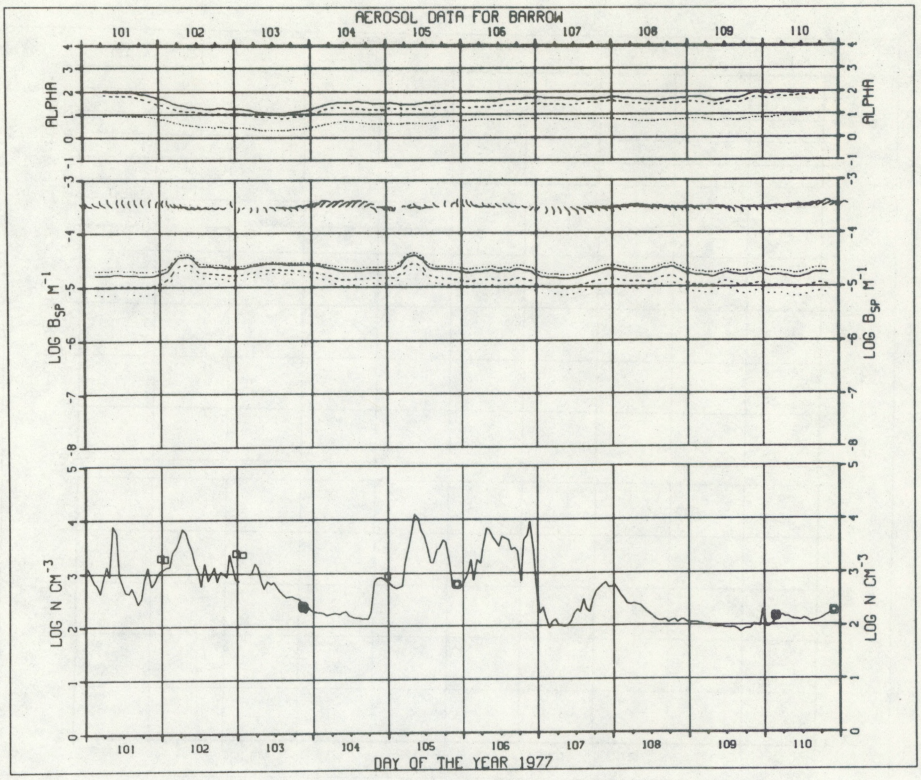
AEROSOL DATA FOR BARROW
101 102 103 104 105 106 107 108 109 110
ALPHA
LOG B_SP M^-1
LOG N CM^-3
DAY OF THE YEAR 1977

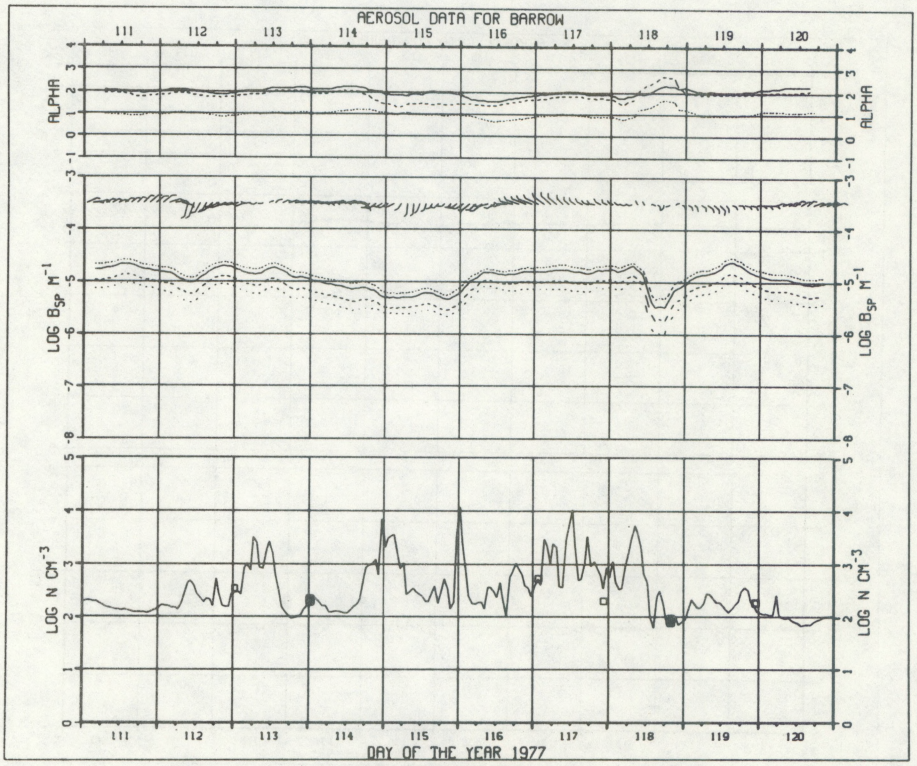
AEROSOL DATA FOR BARROW
111 112 113 114 115 116 117 118 119 120
ALPHA
LOG B_SP M^-1
LOG N CM^-3
DAY OF THE YEAR 1977

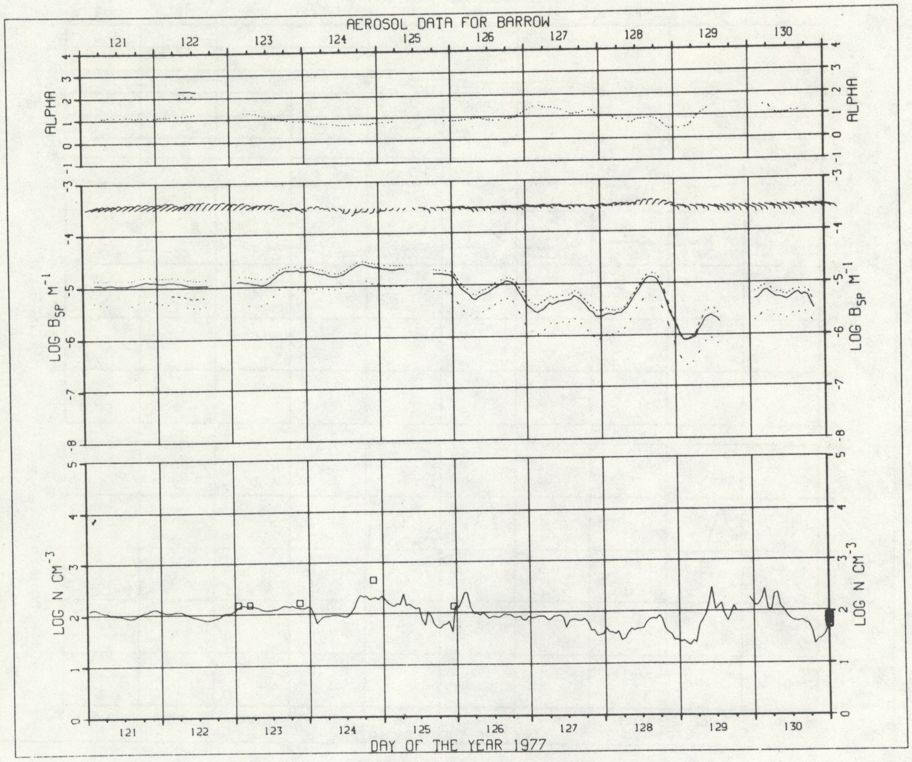

AEROSOL DATA FOR BARROW
ALPHA
LOG B_{SP} M^{-1}
LOG N CM^{-3}
DAY OF THE YEAR 1977

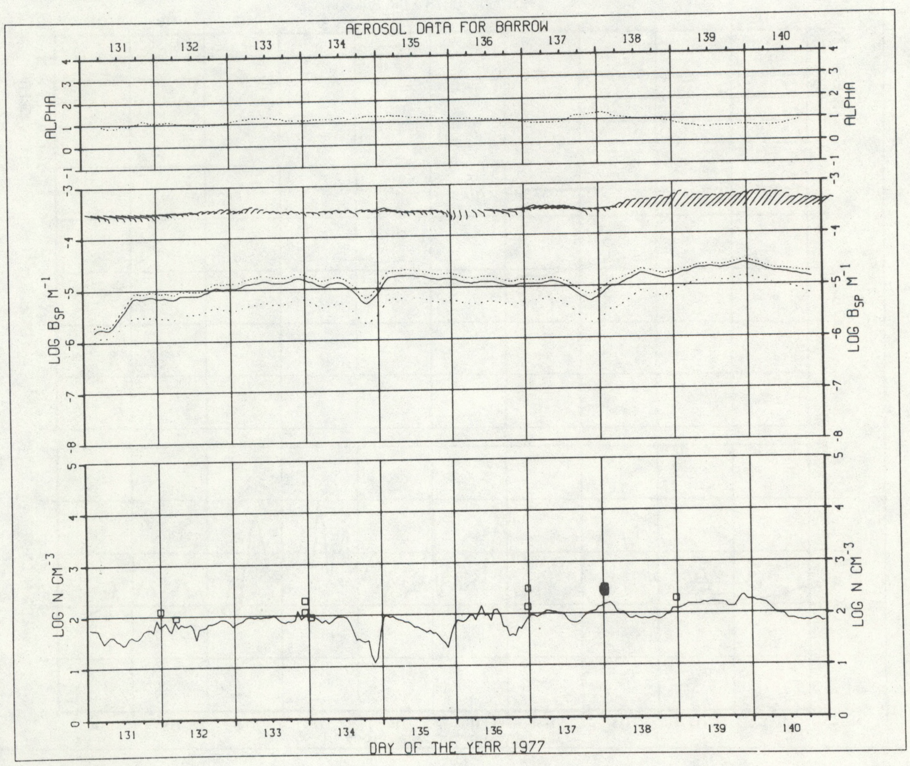

AEROSOL DATA FOR BARROW
ALPHA
LOG B_{SP} M^{-1}
LOG N CM^{-3}
DAY OF THE YEAR 1977

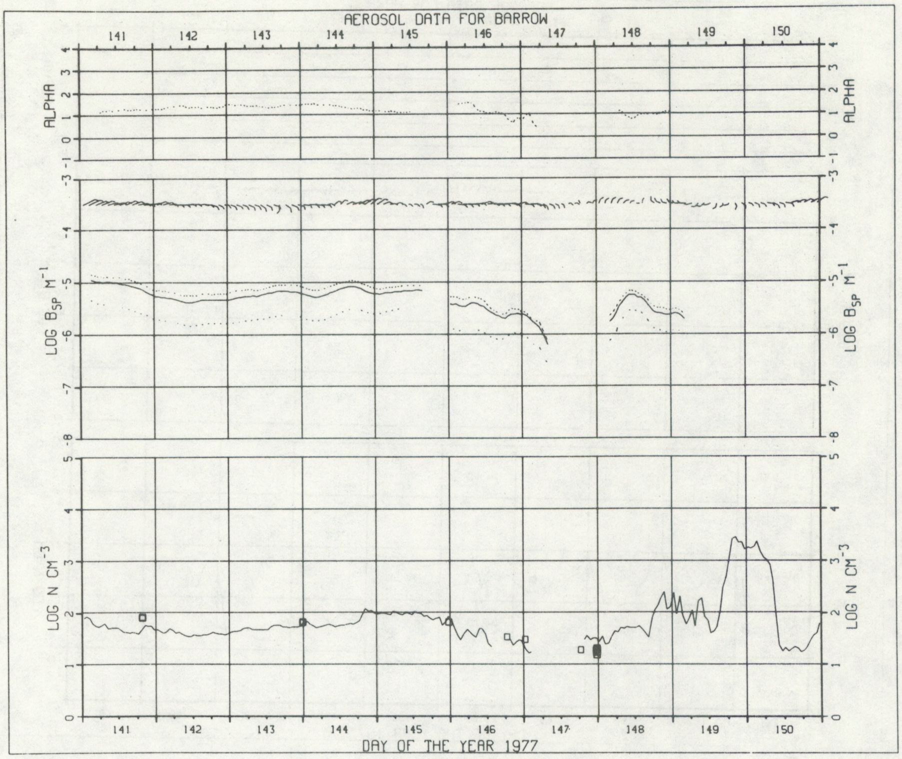
AEROSOL DATA FOR BARROW
ALPHA
LOG B$_{SP}$ M^{-1}
LOG N CM^{-3}
DAY OF THE YEAR 1977

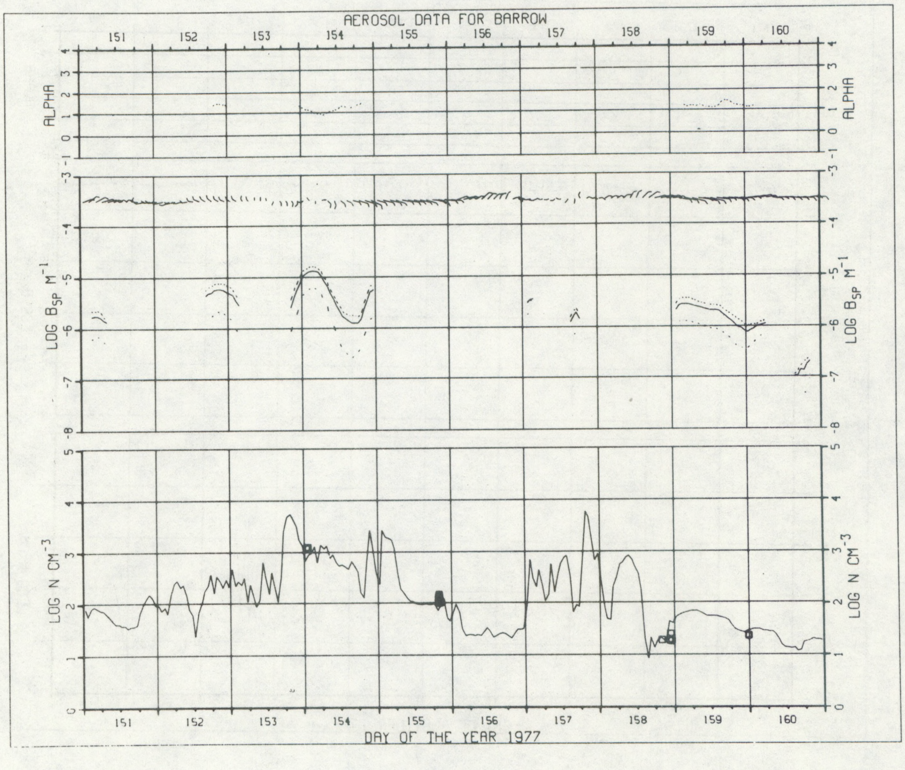
AEROSOL DATA FOR BARROW
ALPHA
LOG B$_{SP}$ M^{-1}
LOG N CM^{-3}
DAY OF THE YEAR 1977

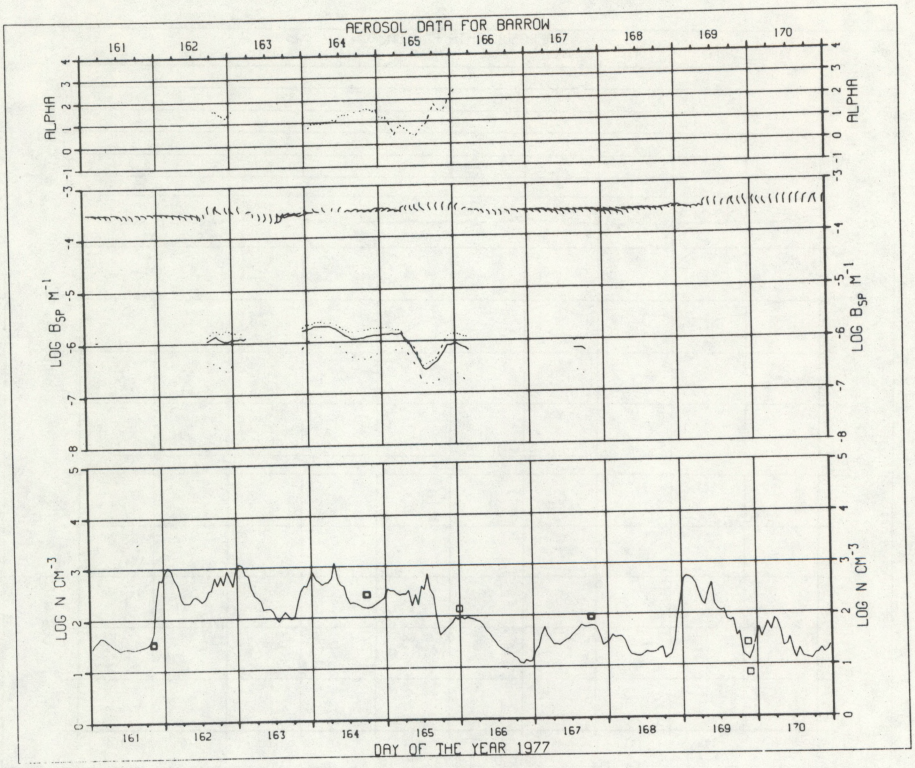
AEROSOL DATA FOR BARROW
ALPHA
LOG B_{SP} M^{-1}
LOG N CM^{-3}
DAY OF THE YEAR 1977

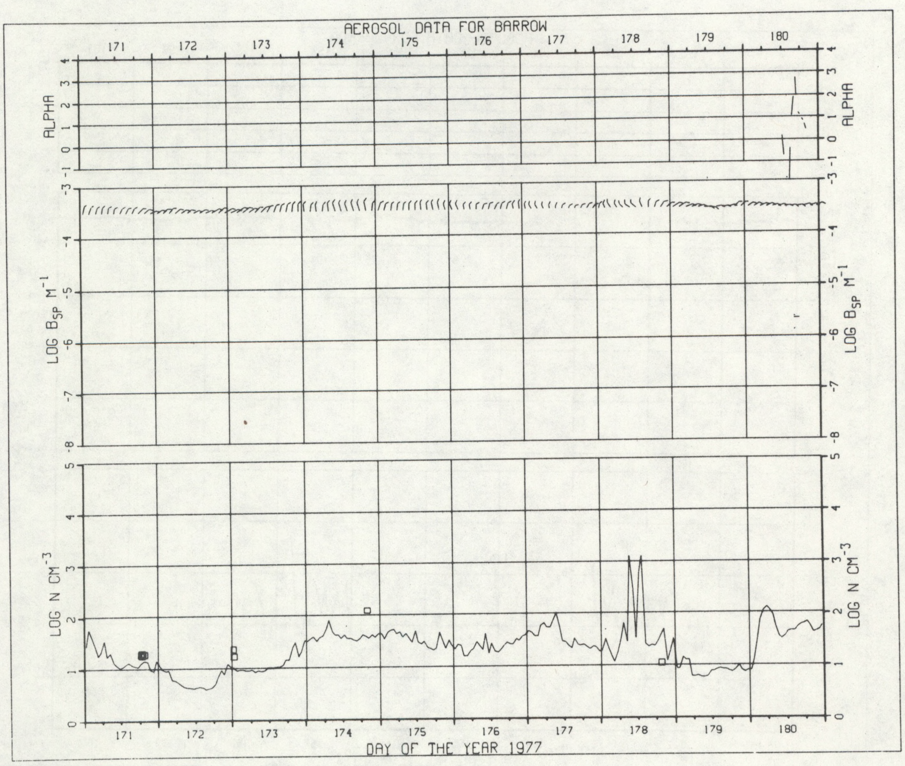
AEROSOL DATA FOR BARROW
ALPHA
LOG B_{SP} M^{-1}
LOG N CM^{-3}
DAY OF THE YEAR 1977

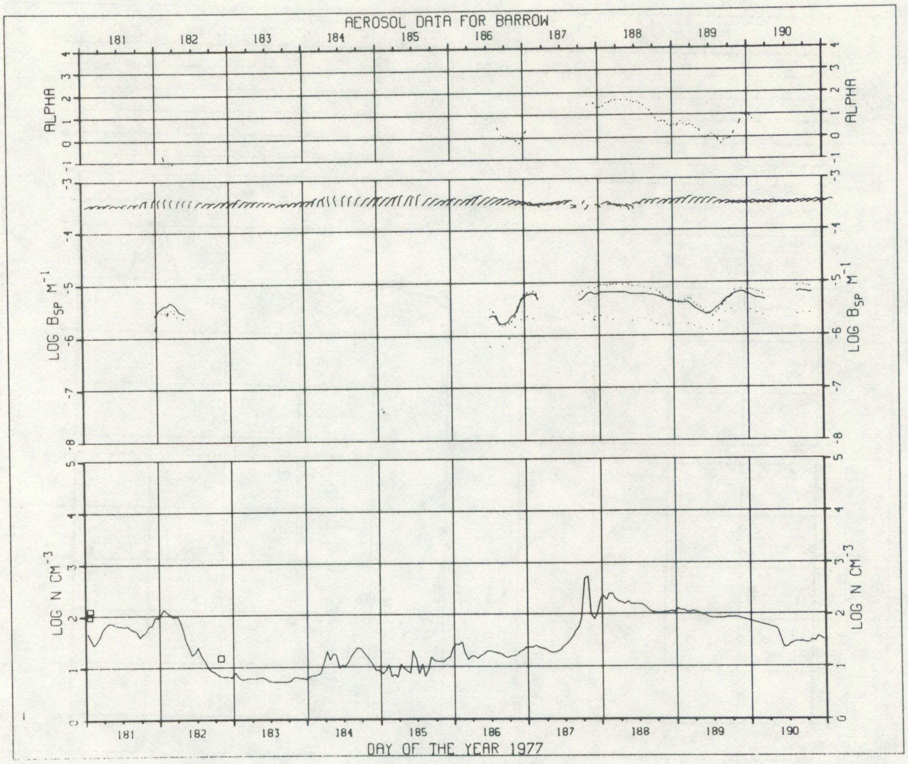
AEROSOL DATA FOR BARROW
ALPHA
LOG B_{SP} M^{-1}
LOG N CM^{-3}
DAY OF THE YEAR 1977

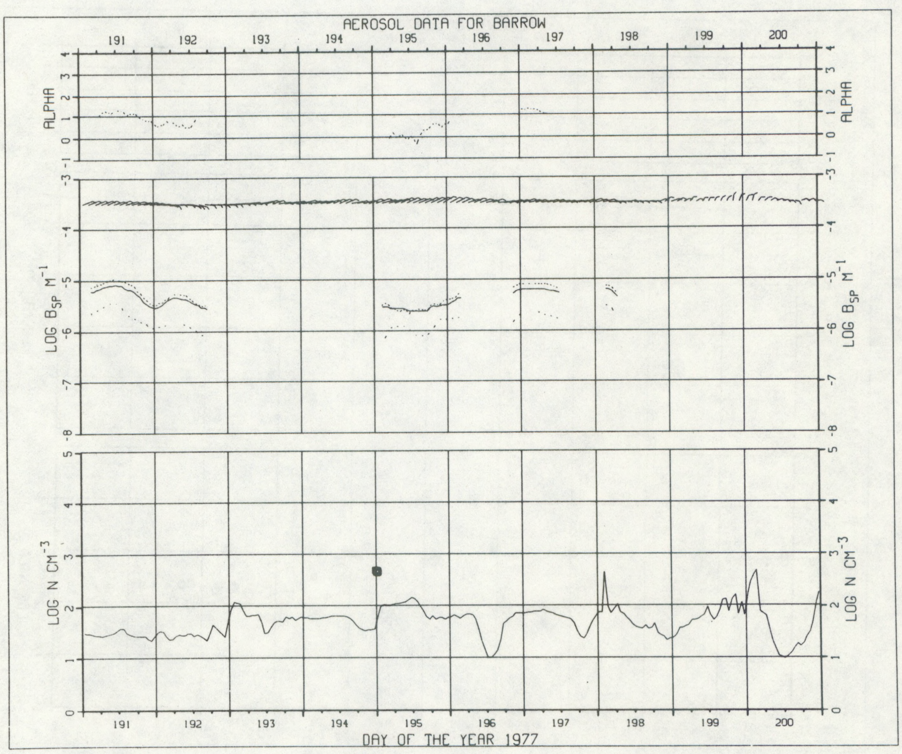
AEROSOL DATA FOR BARROW
ALPHA
LOG B_{SP} M^{-1}
LOG N CM^{-3}
DAY OF THE YEAR 1977

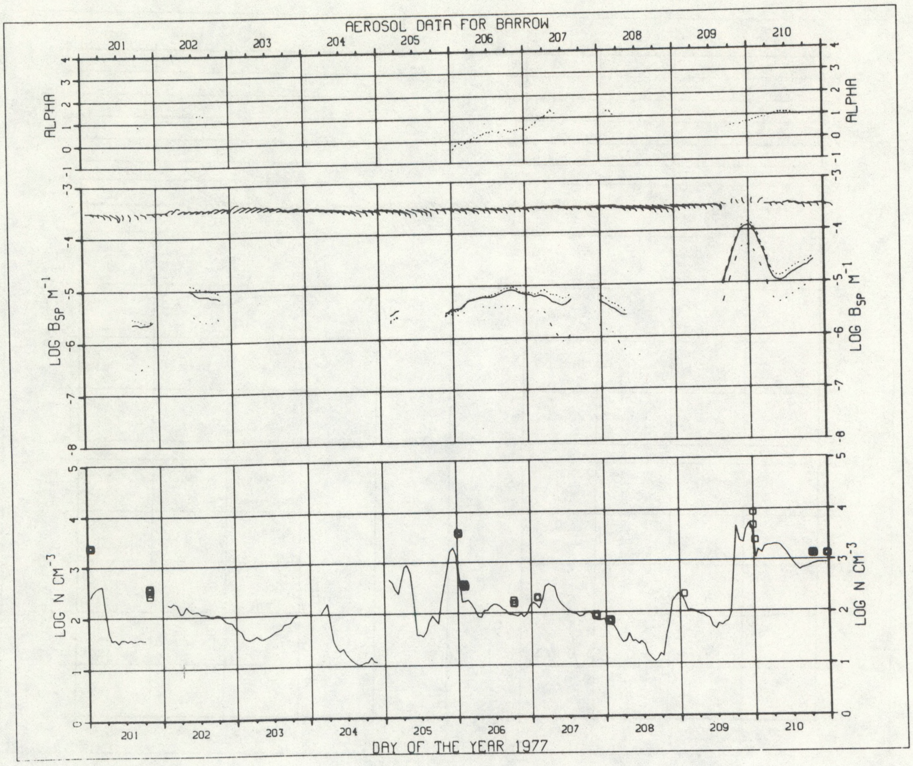
AEROSOL DATA FOR BARROW
ALPHA
LOG B_{SP} M^{-1}
LOG N CM^{-3}
DAY OF THE YEAR 1977
201
202
203
204
205
206
207
208
209
210

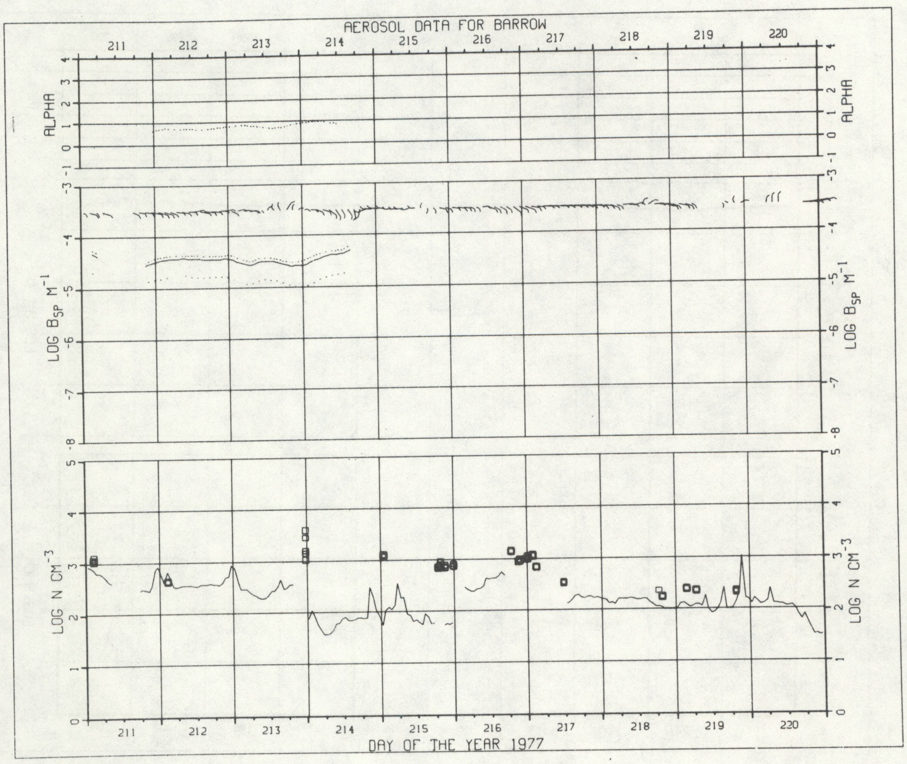
AEROSOL DATA FOR BARROW
ALPHA
LOG B_{SP} M^{-1}
LOG N CM^{-3}
DAY OF THE YEAR 1977
211
212
213
214
215
216
217
218
219
220

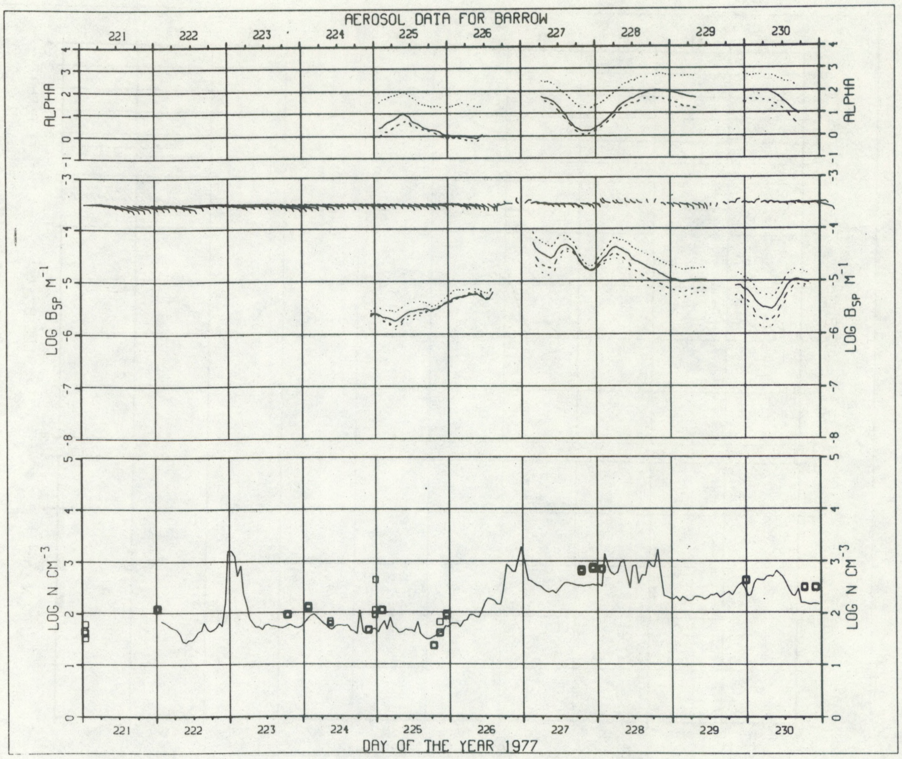
AEROSOL DATA FOR BARROW
221 222 223 224 225 226 227 228 229 230
ALPHA
LOG BSP M-1
LOG N CM-3
DAY OF THE YEAR 1977

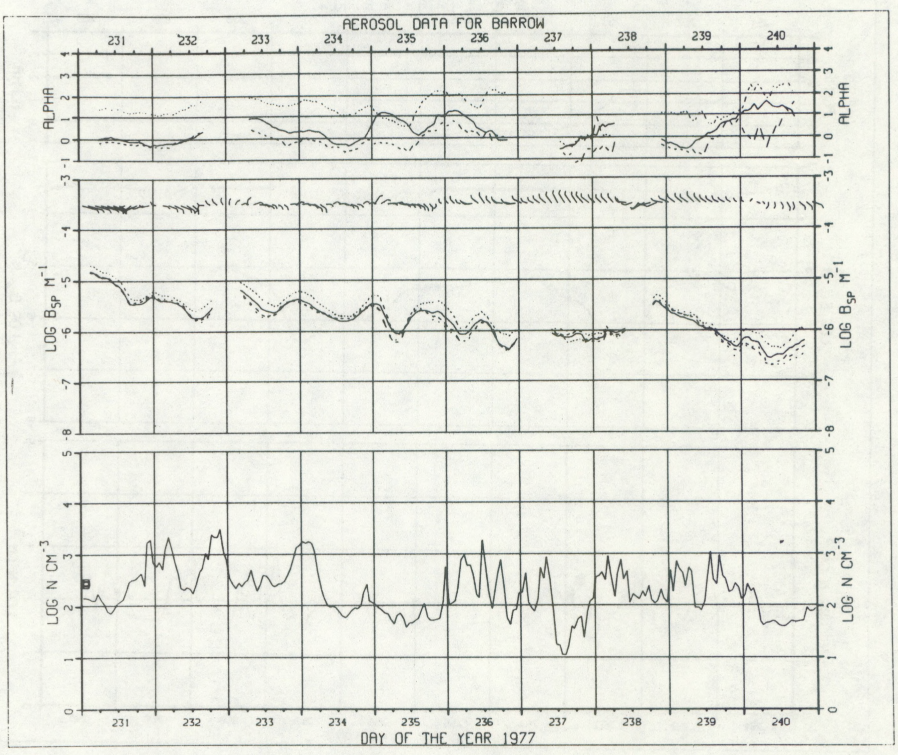
AEROSOL DATA FOR BARROW
231 232 233 234 235 236 237 238 239 240
ALPHA
LOG BSP M-1
LOG N CM-3
DAY OF THE YEAR 1977

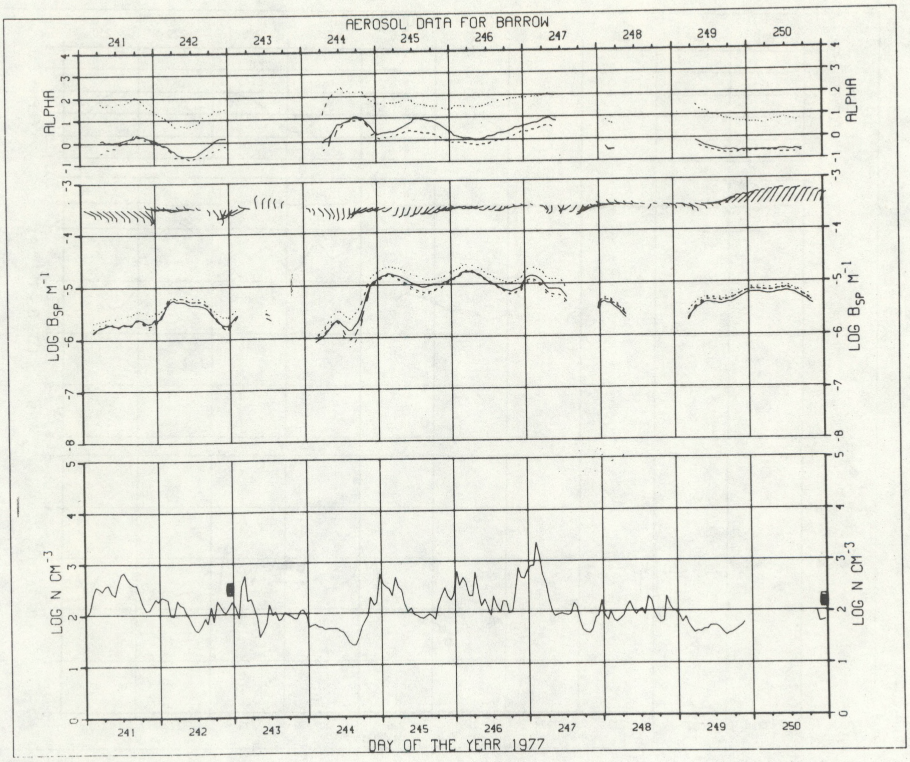
AEROSOL DATA FOR BARROW
ALPHA
LOG B SP M-1
LOG N CM-3
DAY OF THE YEAR 1977

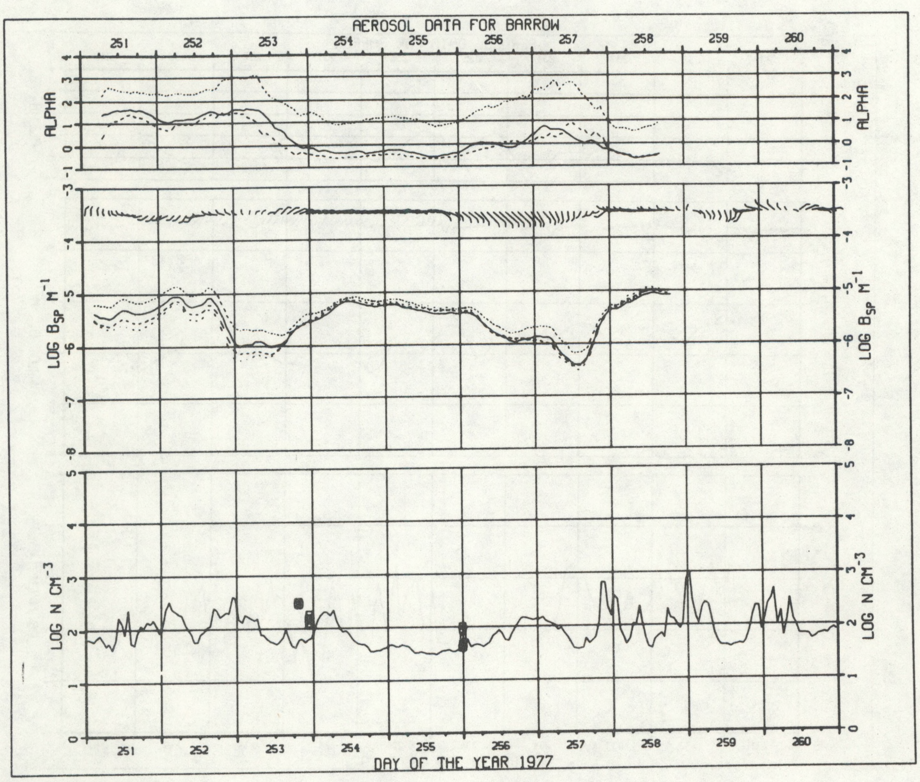
AEROSOL DATA FOR BARROW
ALPHA
LOG B SP M-1
LOG N CM-3
DAY OF THE YEAR 1977

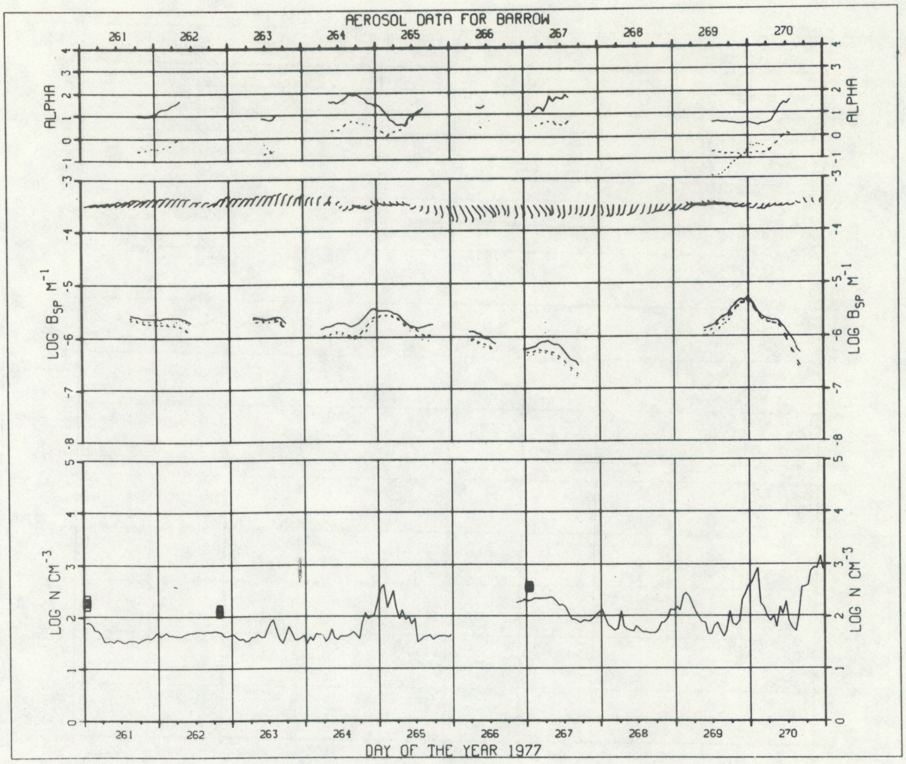
AEROSOL DATA FOR BARROW
ALPHA
LOG B_{SP} M^{-1}
LOG N CM^{-3}
DAY OF THE YEAR 1977

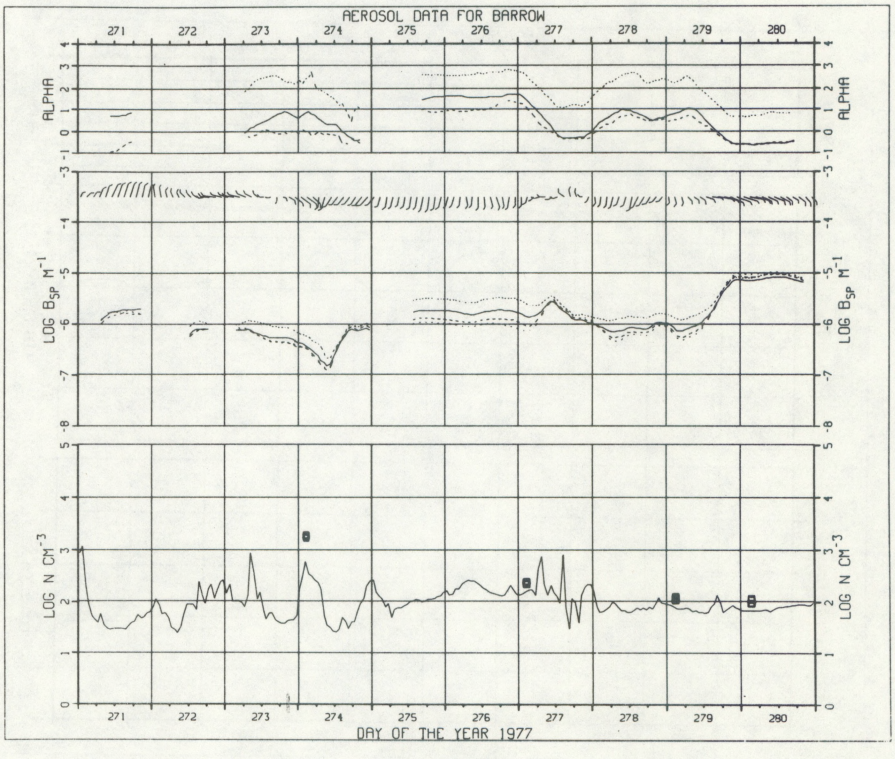
AEROSOL DATA FOR BARROW
ALPHA
LOG B_{SP} M^{-1}
LOG N CM^{-3}
DAY OF THE YEAR 1977

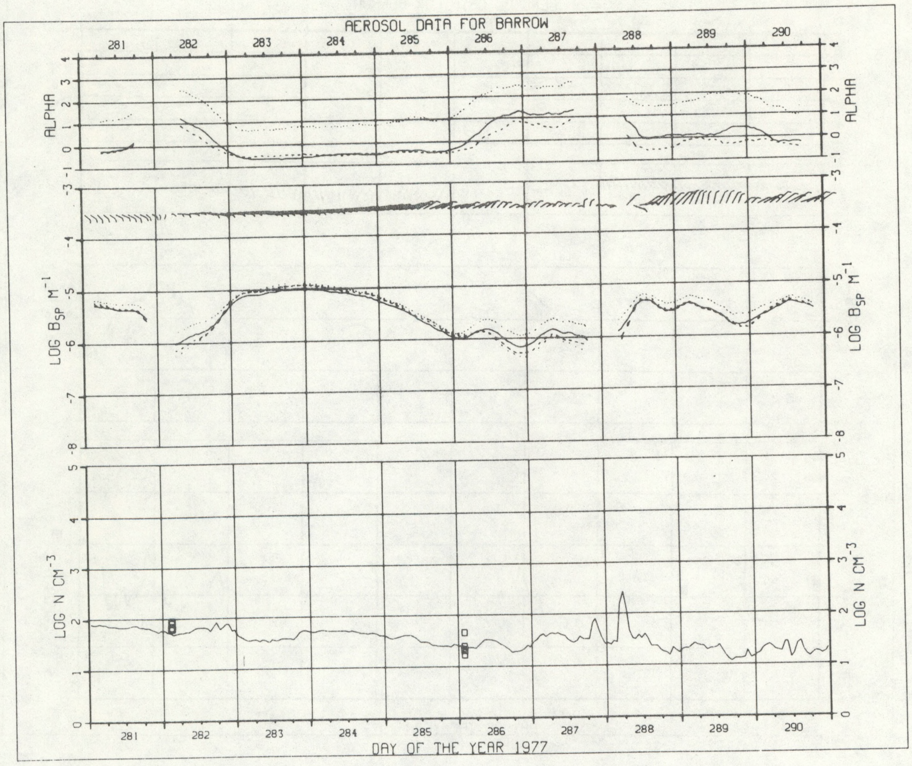
AEROSOL DATA FOR BARROW
ALPHA
LOG B_{SP} M^{-1}
LOG N CM^{-3}
DAY OF THE YEAR 1977

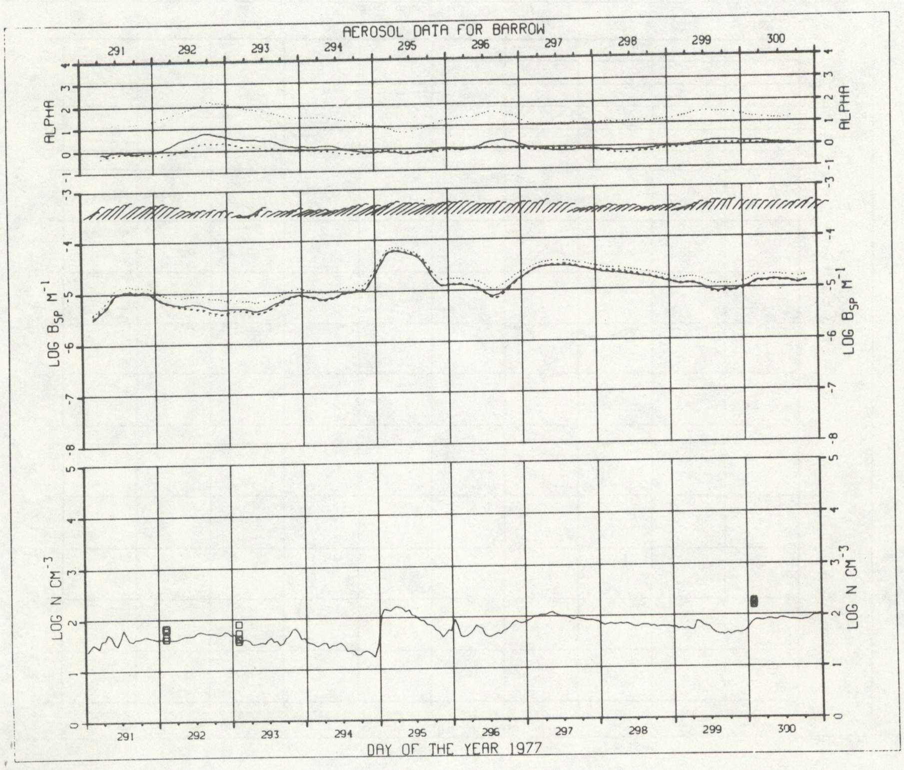
AEROSOL DATA FOR BARROW
ALPHA
LOG B_{SP} M^{-1}
LOG N CM^{-3}
DAY OF THE YEAR 1977

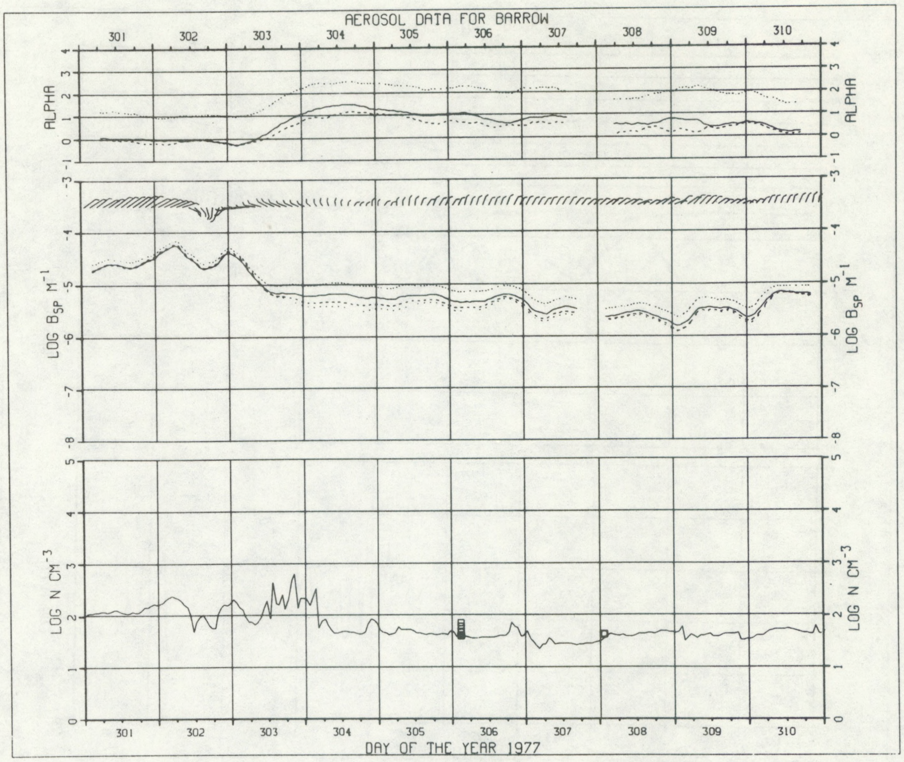
AEROSOL DATA FOR BARROW
301 302 303 304 305 306 307 308 309 310
ALPHA
LOG B_{SP} M^{-1}
LOG N CM^{-3}
DAY OF THE YEAR 1977

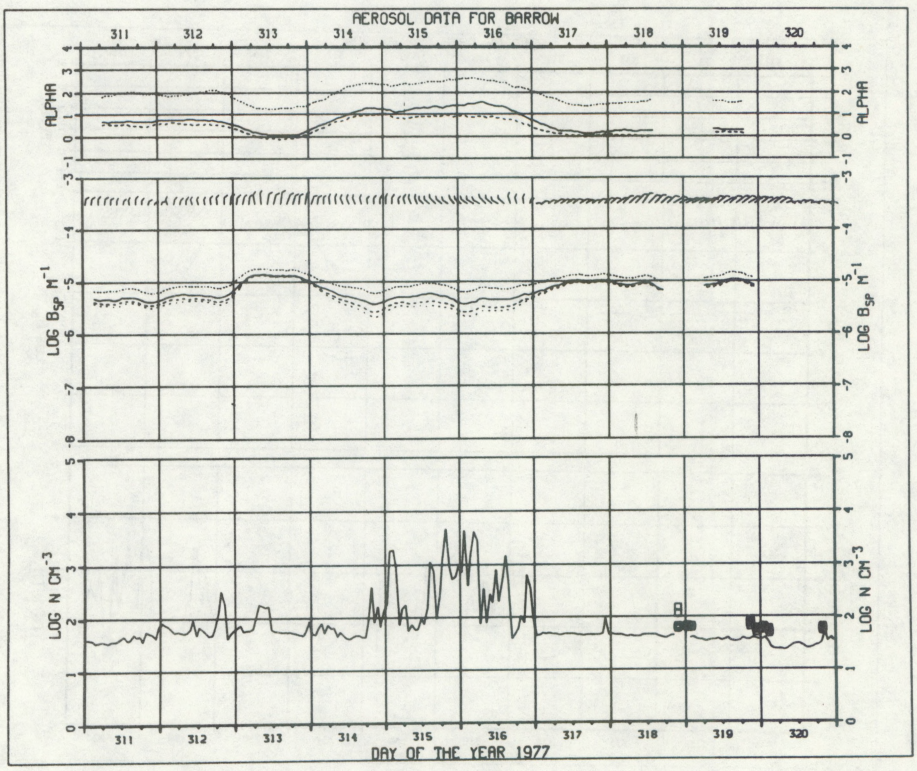
AEROSOL DATA FOR BARROW
311 312 313 314 315 316 317 318 319 320
ALPHA
LOG B_{SP} M^{-1}
LOG N CM^{-3}
DAY OF THE YEAR 1977

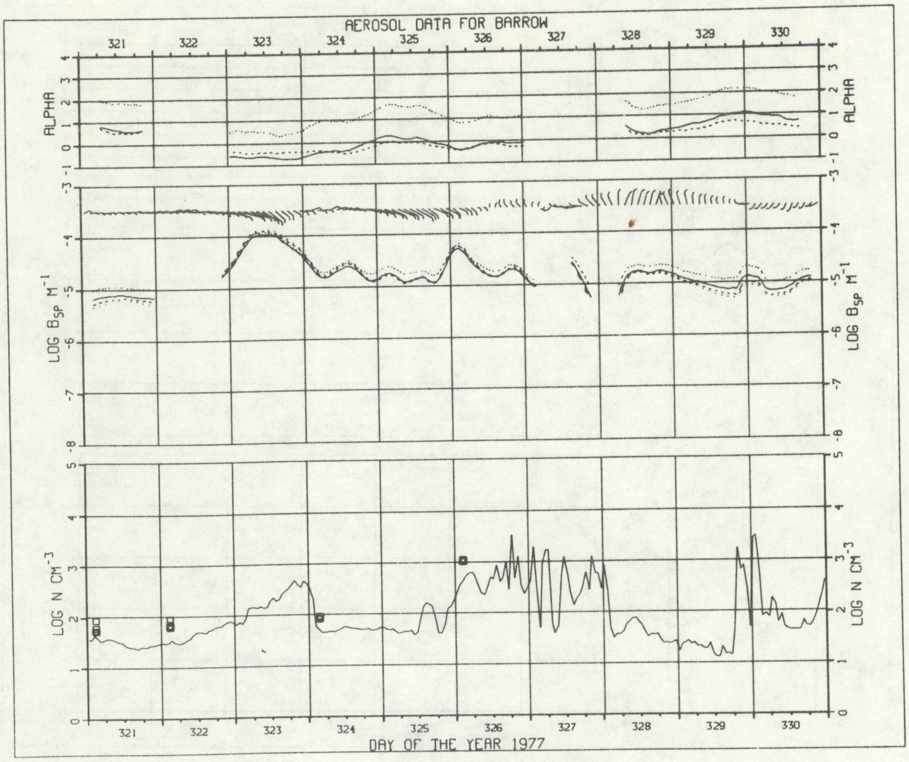
AEROSOL DATA FOR BARROW
ALPHA
LOG B_{SP} M^{-1}
LOG N CM^{-3}
DAY OF THE YEAR 1977

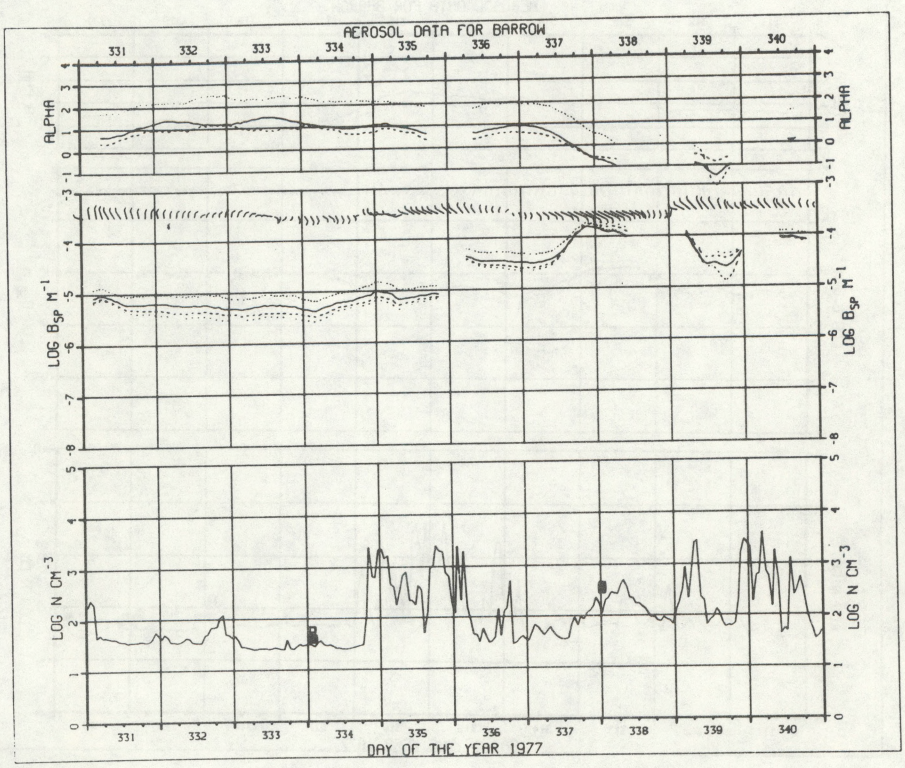
AEROSOL DATA FOR BARROW
ALPHA
LOG B_{SP} M^{-1}
LOG N CM^{-3}
DAY OF THE YEAR 1977

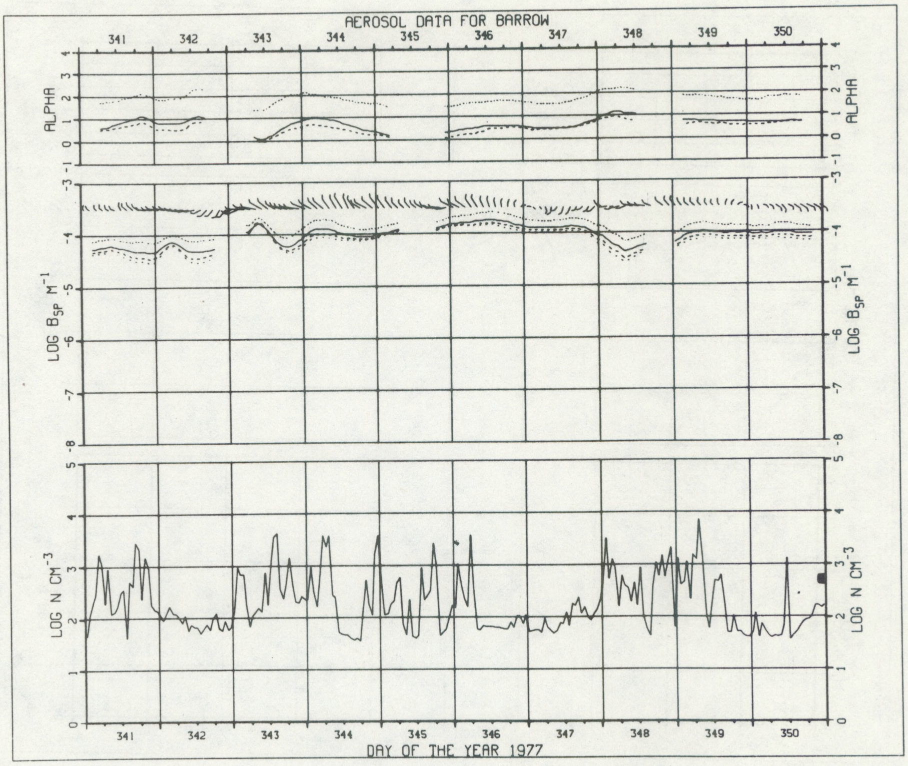
AEROSOL DATA FOR BARROW
ALPHA
LOG B_{SP} M^{-1}
LOG N CM^{-3}
DAY OF THE YEAR 1977

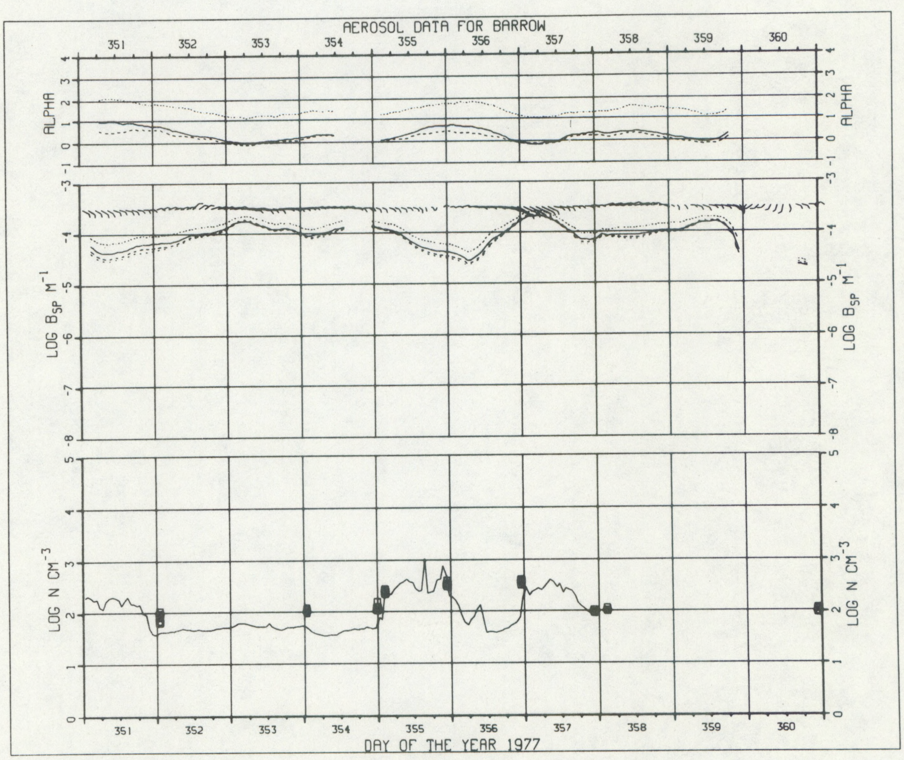
AEROSOL DATA FOR BARROW
ALPHA
LOG B_{SP} M^{-1}
LOG N CM^{-3}
DAY OF THE YEAR 1977

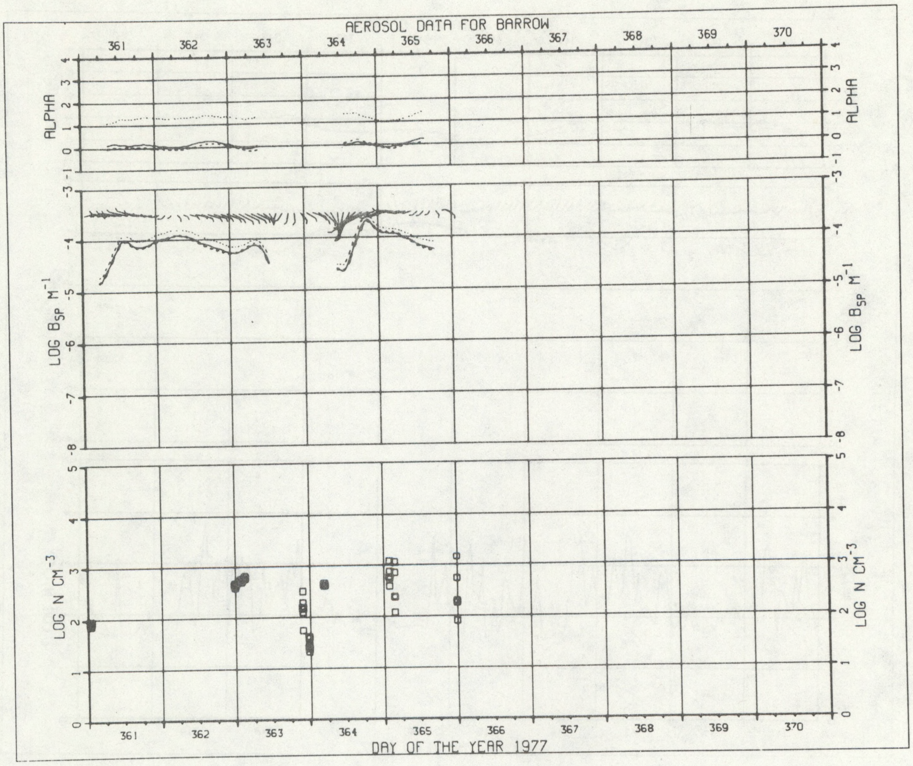
AEROSOL DATA FOR BARROW
ALPHA
LOG B_{SP} M^{-1}
LOG N CM^{-3}
361 362 363 364 365 366 367 368 369 370
DAY OF THE YEAR 1977

APPENDIX C

Appendix C contains the hourly mean nuclei concentrations, Pollak counter observations, light scattering data, and Angstrom exponents plotted on a logarithmic scale for 1978. A histogram of successive one minute voltage differences for each month was generated and the variability criterion was determined to be ±0.0335 volts.

The data pairs were obtained from the minute data and grouped into periods where the G.E. counter was operating. The scaling factors generated are:

Day	Scaling Factor
1006-8820	1.00
8821-10818	1.25356739
16202-18101	0.91277479
18102-23602	3.4238591
25020-31300	0.836304445
31400-36523	0.797598917

The G.E. counter was down during days 00-1006, 10819-16201, and 23913-25019.

Scaled graphical display of aerosol data for 1978.
for each plot;

the top graph contains: Angstrom exponents
Alpha (1-2): dashed line
Alpha (2-3): solid line
Alpha (3-4): long dashed line

the center graph contains: light scattering and wind data
wavelength 450 nm: dashed line
wavelength 550 nm: solid line
wavelength 700 nm: long dashed line
wavelength 850 nm: short dashed line

the lower graph contains: nuclei concentrations
G.E. counter: solid line
Pollak counter: squares

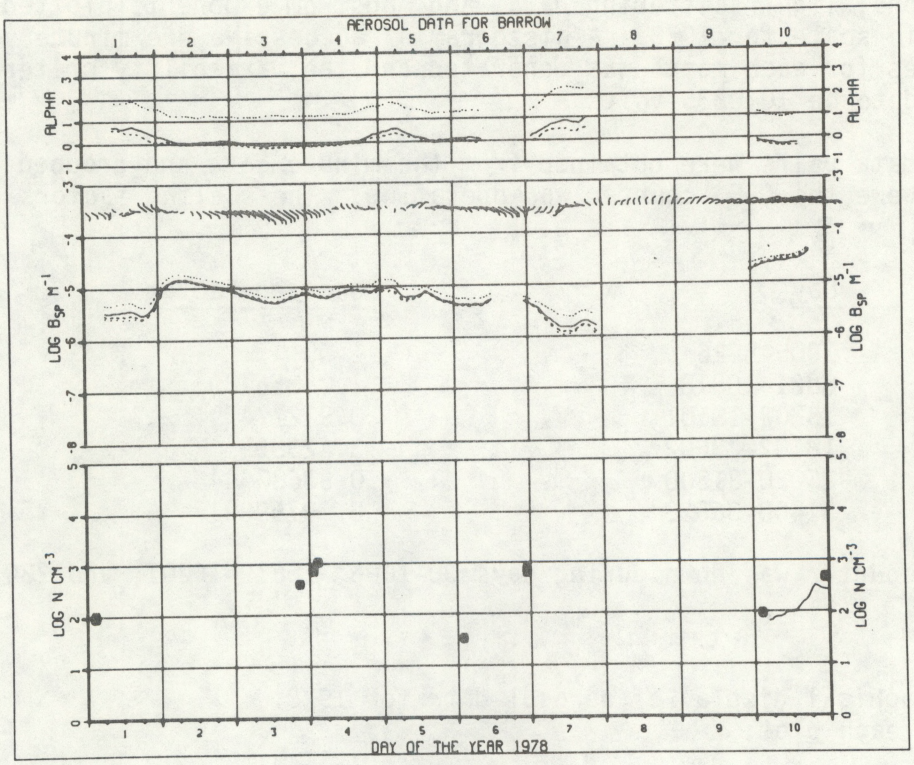
AEROSOL DATA FOR BARROW
ALPHA
LOG B_SP M^-1
LOG N CM^-3
DAY OF THE YEAR 1978

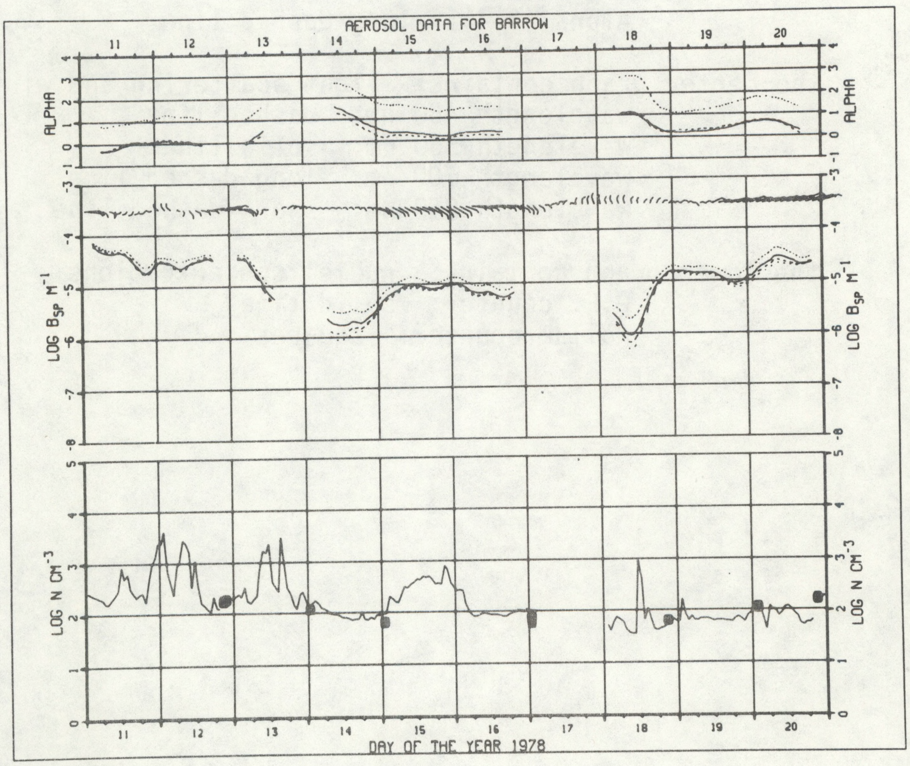
AEROSOL DATA FOR BARROW
ALPHA
LOG B_SP M^-1
LOG N CM^-3
DAY OF THE YEAR 1978

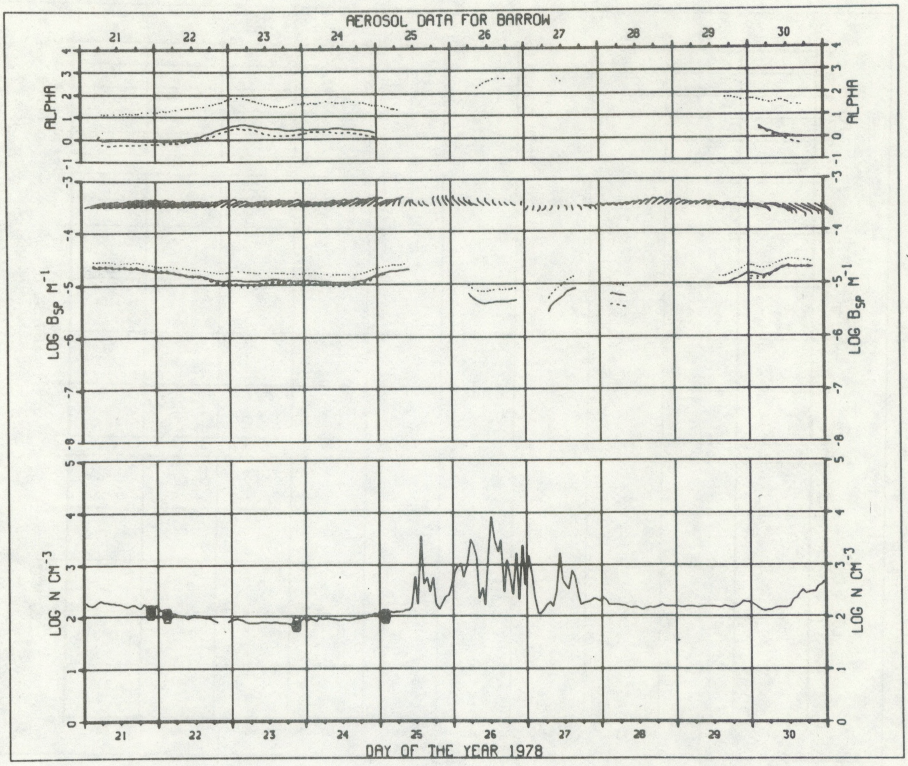
AEROSOL DATA FOR BARROW
ALPHA
LOG B$_{SP}$ M^{-1}
LOG N CM^{-3}
DAY OF THE YEAR 1978

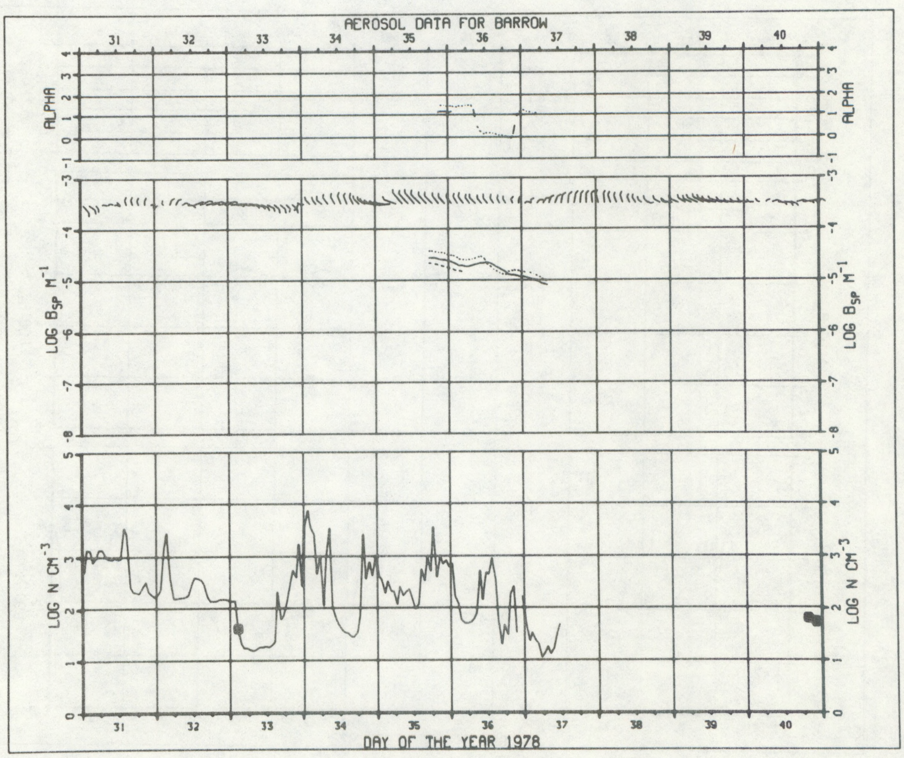
AEROSOL DATA FOR BARROW
ALPHA
LOG B$_{SP}$ M^{-1}
LOG N CM^{-3}
DAY OF THE YEAR 1978

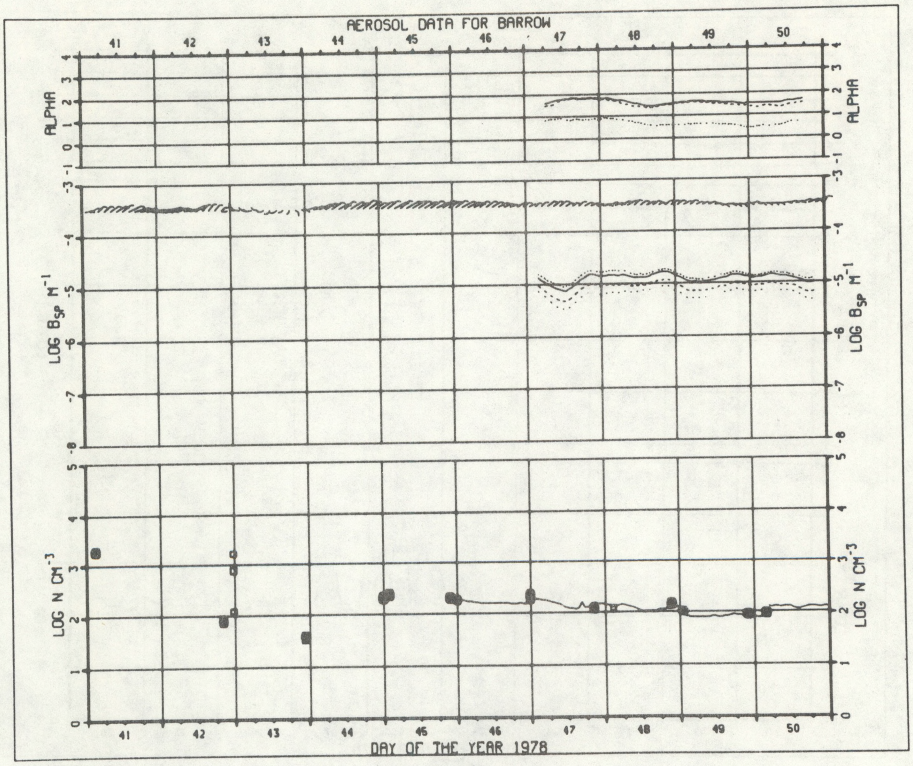
AEROSOL DATA FOR BARROW
ALPHA
LOG B_{SP} M^{-1}
LOG N CM^{-3}
DAY OF THE YEAR 1978

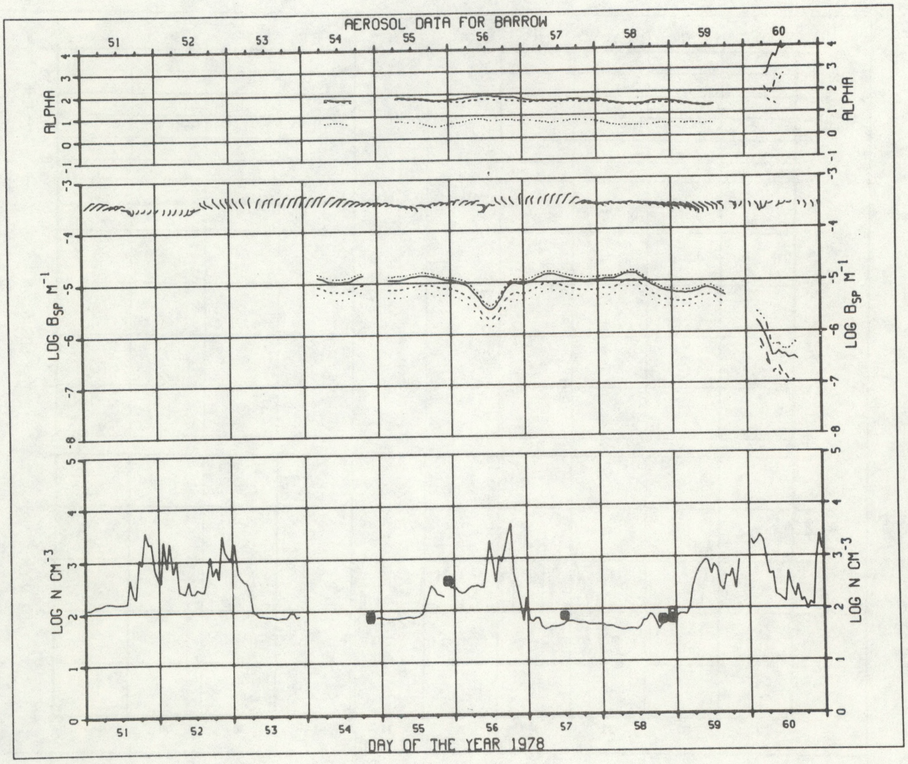
AEROSOL DATA FOR BARROW
ALPHA
LOG B_{SP} M^{-1}
LOG N CM^{-3}
DAY OF THE YEAR 1978

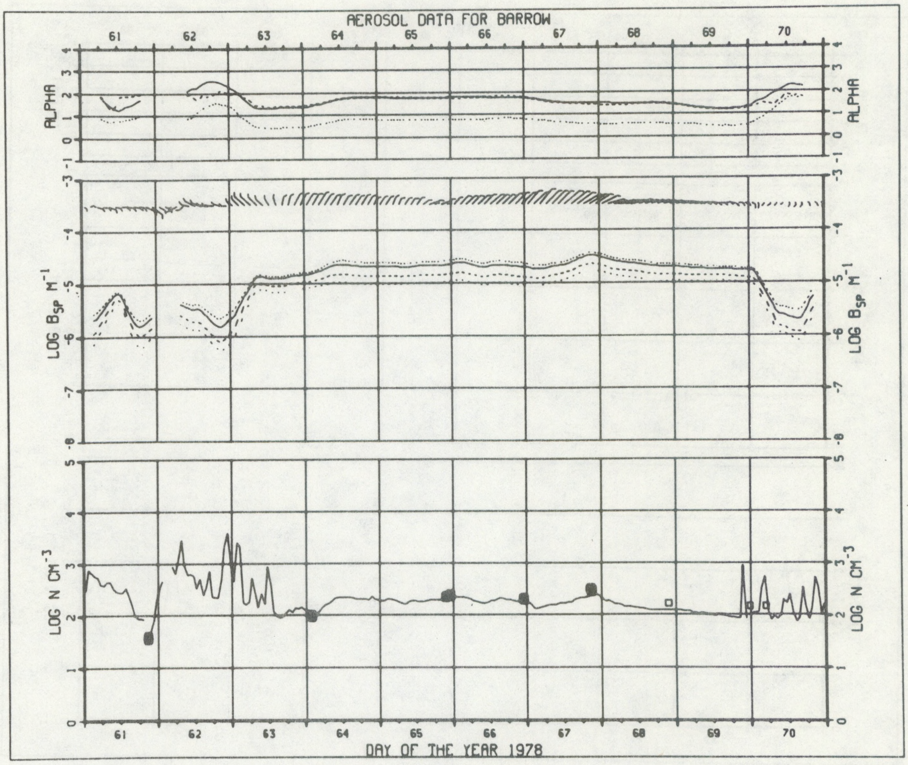

AEROSOL DATA FOR BARROW
ALPHA
LOG B$_{SP}$ M^{-1}
LOG N CM^{-3}
DAY OF THE YEAR 1978

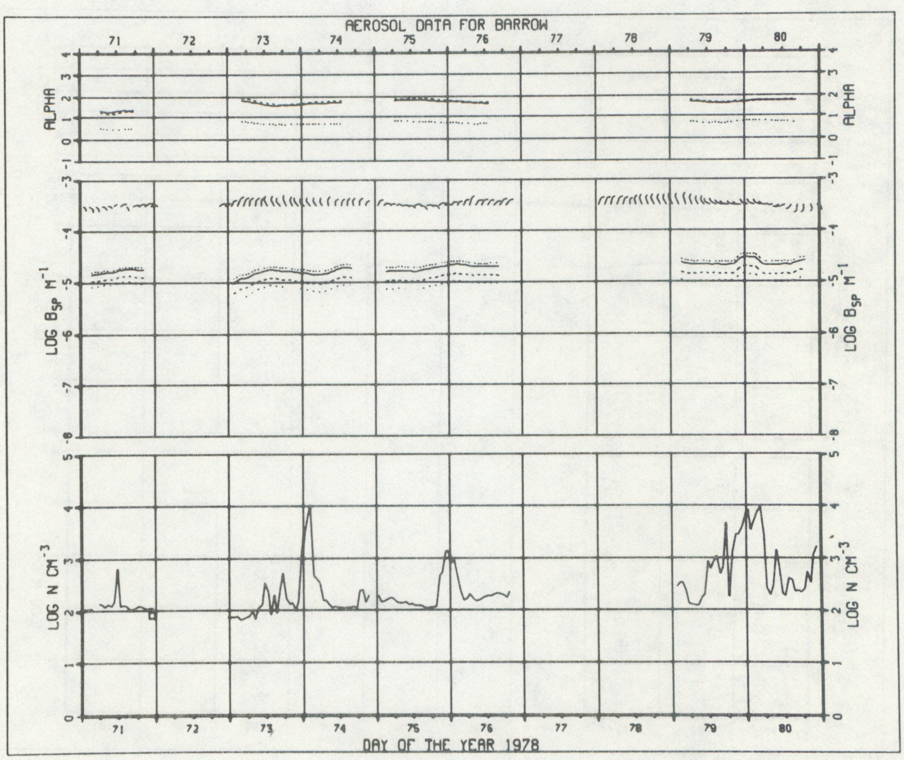

AEROSOL DATA FOR BARROW
ALPHA
LOG B$_{SP}$ M^{-1}
LOG N CM^{-3}
DAY OF THE YEAR 1978

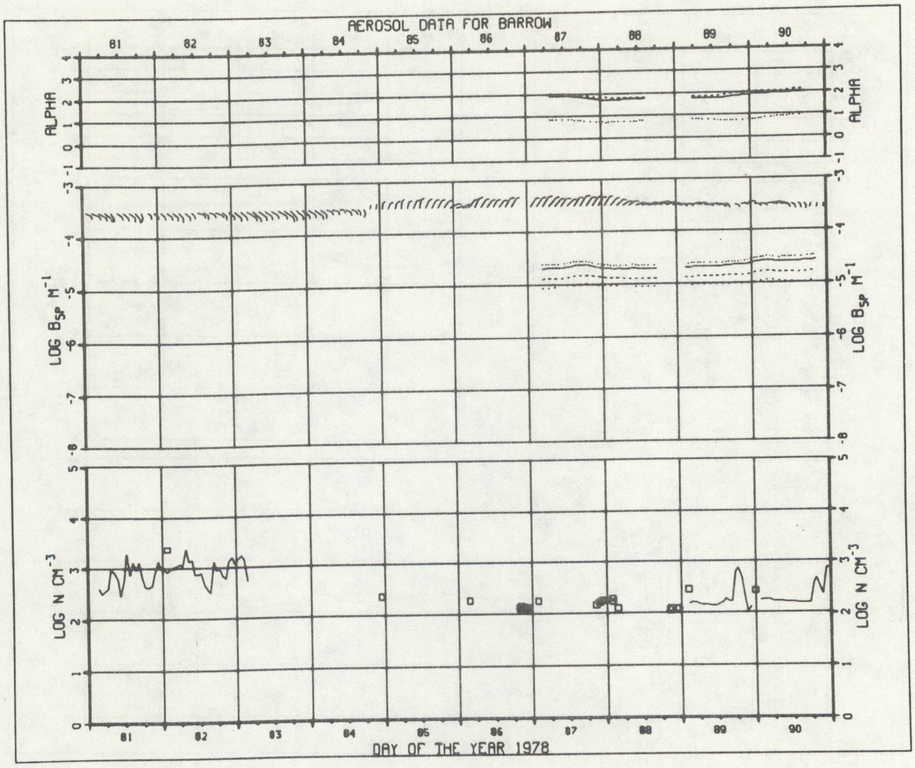
AEROSOL DATA FOR BARROW
ALPHA
LOG B$_{SP}$ M^{-1}
LOG N CM^{-3}
DAY OF THE YEAR 1978

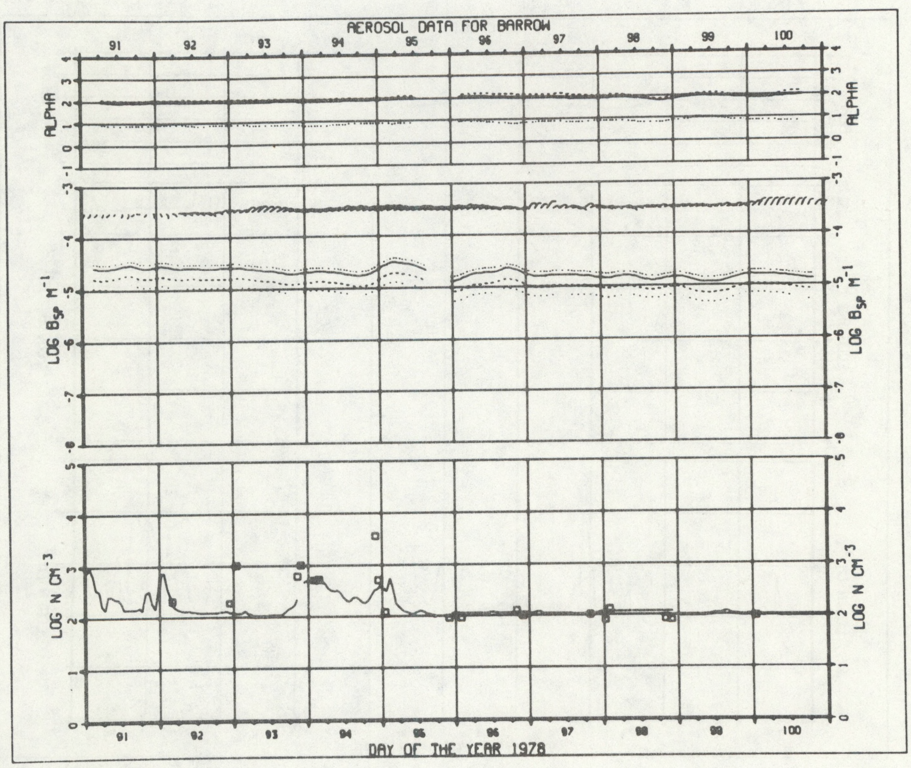
AEROSOL DATA FOR BARROW
ALPHA
LOG B$_{SP}$ M^{-1}
LOG N CM^{-3}
DAY OF THE YEAR 1978

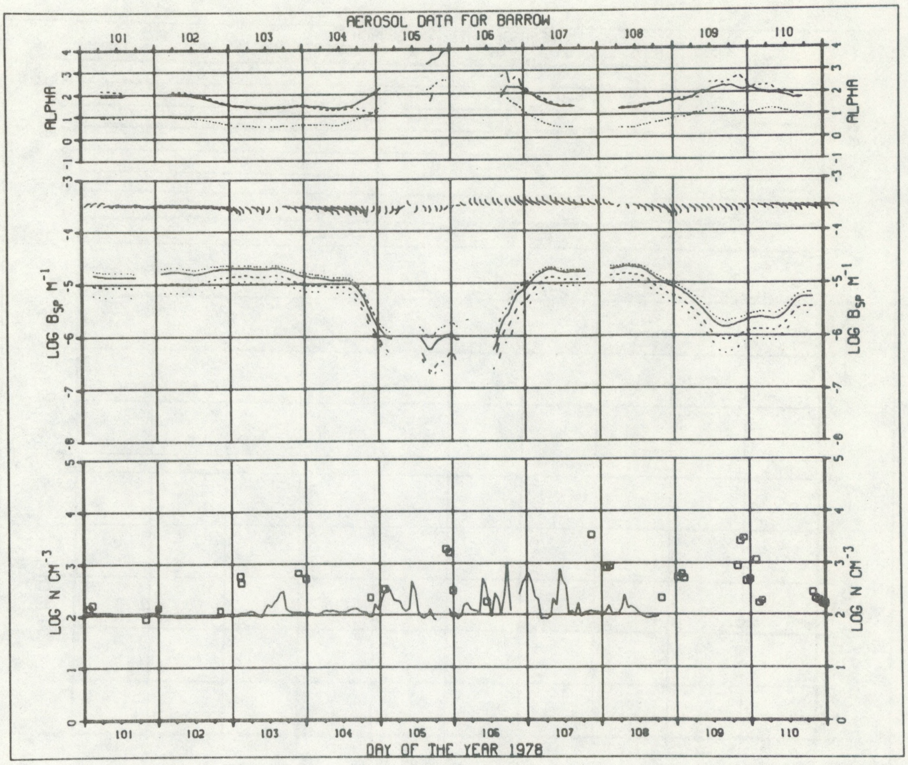

AEROSOL DATA FOR BARROW
ALPHA
LOG B_SP M^-1
LOG N CM^-3
DAY OF THE YEAR 1978

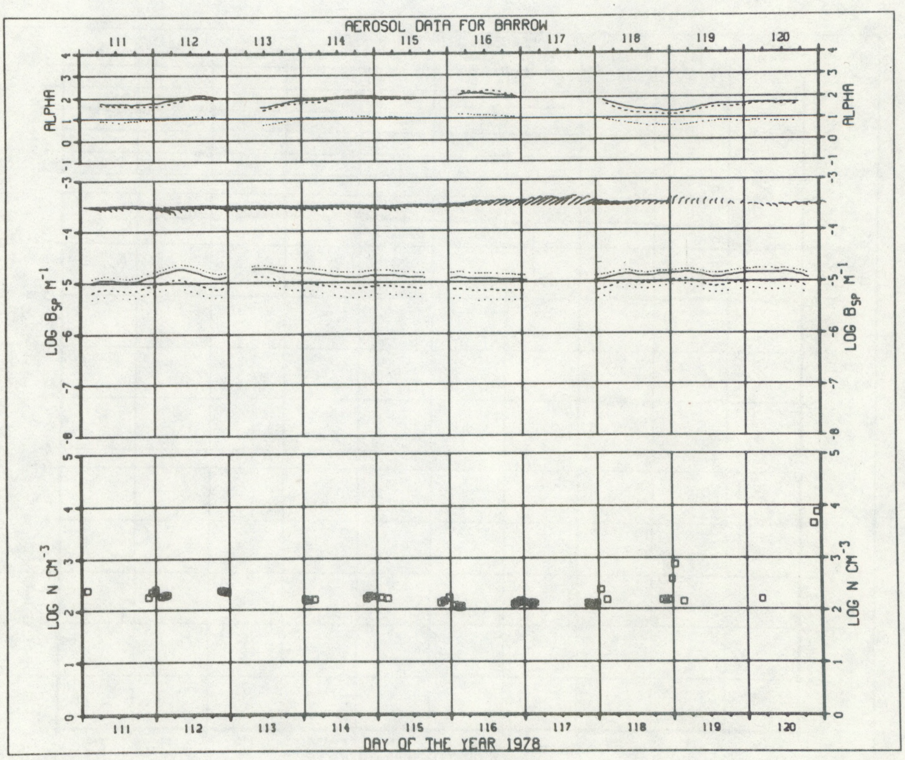

AEROSOL DATA FOR BARROW
ALPHA
LOG B_SP M^-1
LOG N CM^-3
DAY OF THE YEAR 1978

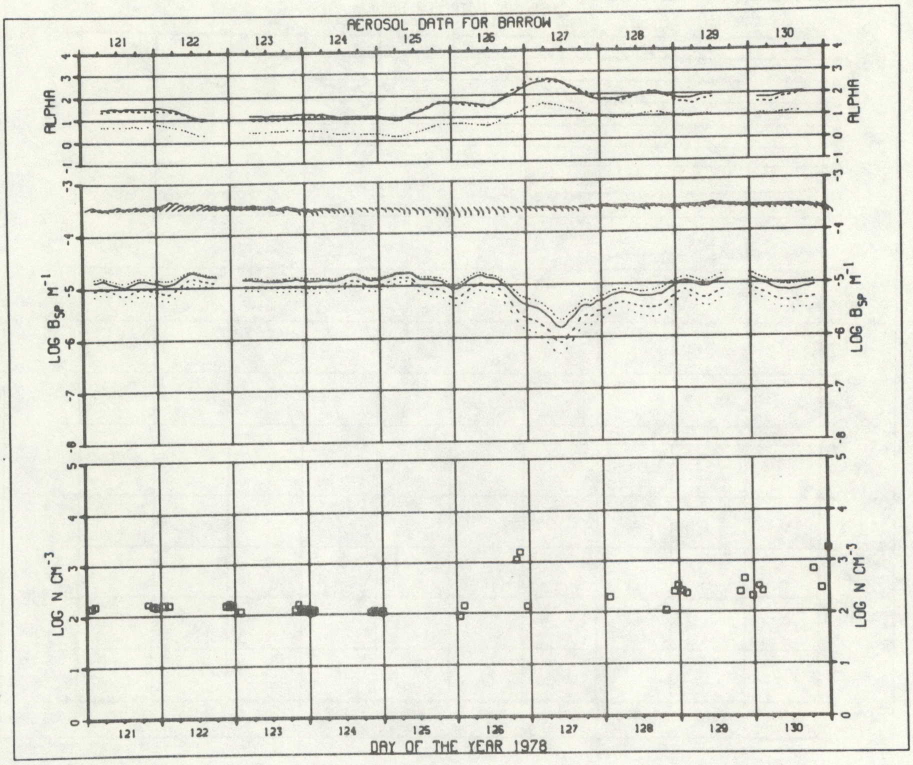
AEROSOL DATA FOR BARROW
ALPHA
LOG B_{SP} M^{-1}
LOG N CM^{-3}
DAY OF THE YEAR 1978

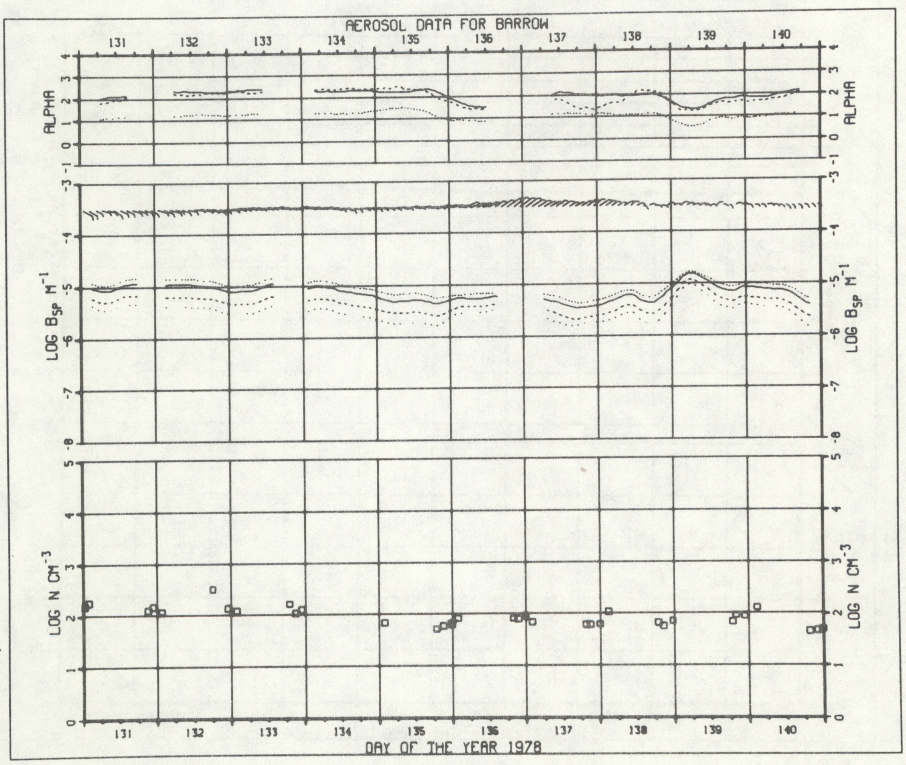
AEROSOL DATA FOR BARROW
ALPHA
LOG B_{SP} M^{-1}
LOG N CM^{-3}
DAY OF THE YEAR 1978

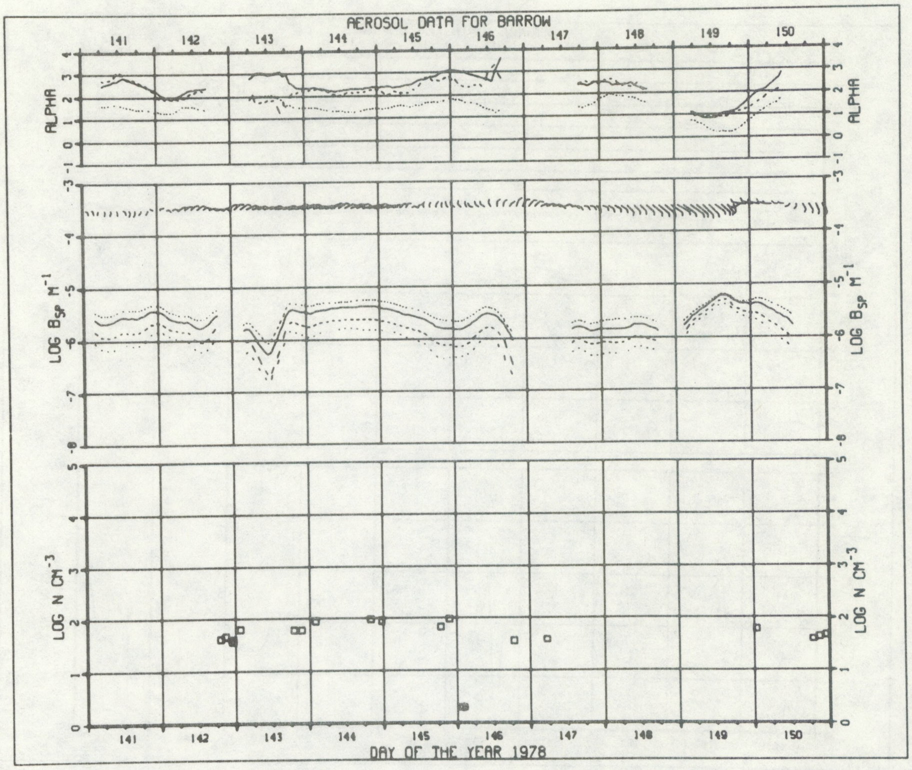
AEROSOL DATA FOR BARROW
ALPHA
LOG B$_{SP}$ M^{-1}
LOG N CM^{-3}
DAY OF THE YEAR 1978

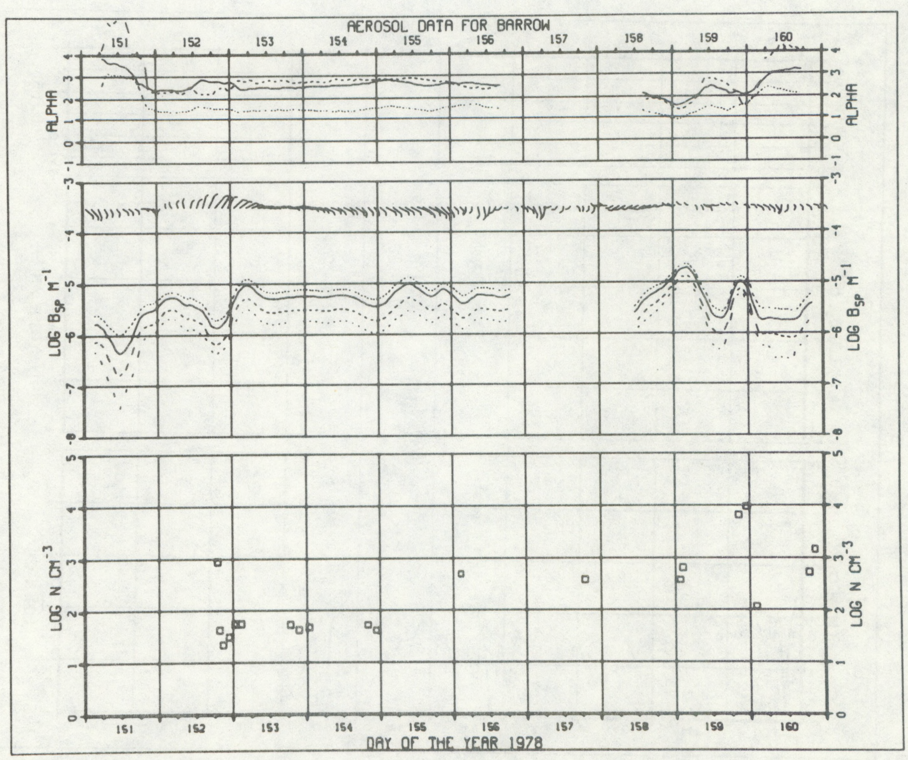
AEROSOL DATA FOR BARROW
ALPHA
LOG B$_{SP}$ M^{-1}
LOG N CM^{-3}
DAY OF THE YEAR 1978

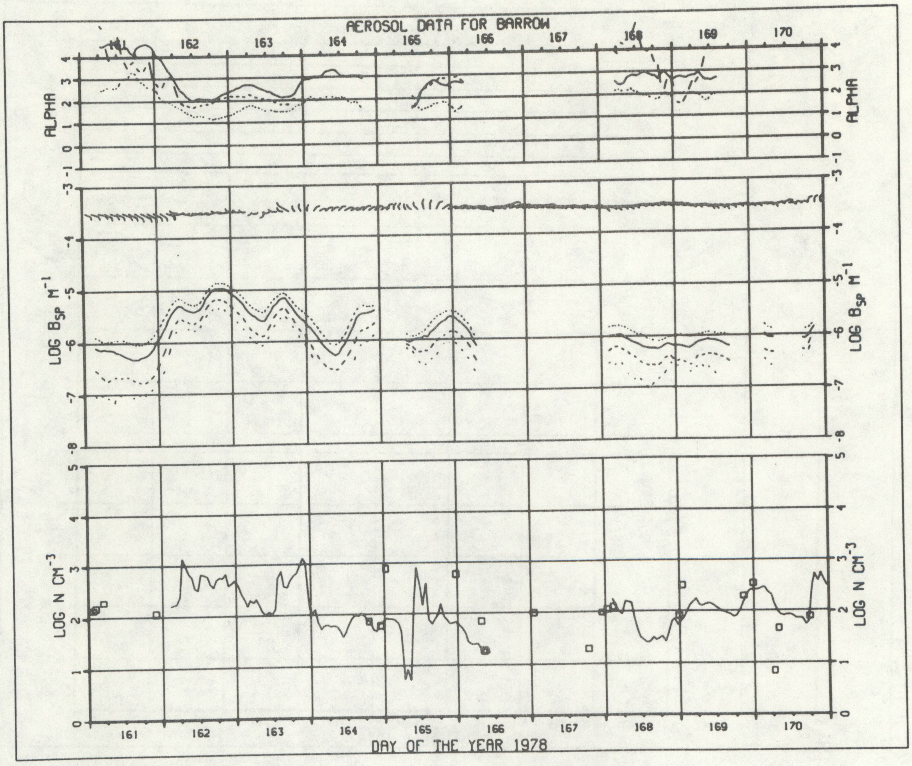
AEROSOL DATA FOR BARROW
ALPHA
LOG B_{SP} M^{-1}
LOG N CM^{-3}
DAY OF THE YEAR 1978

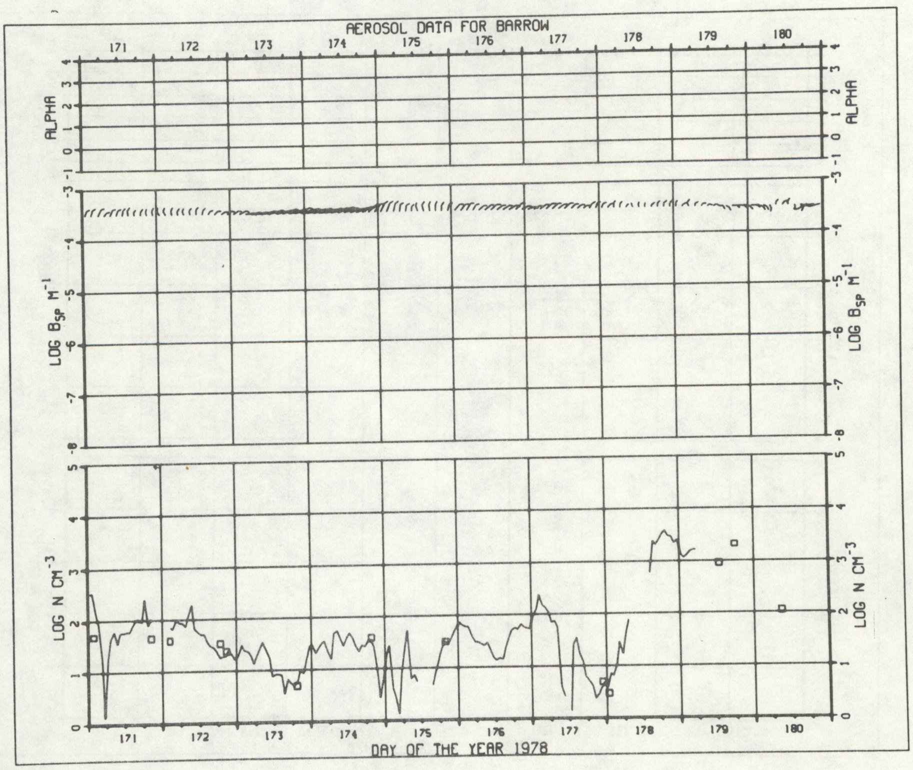
AEROSOL DATA FOR BARROW
ALPHA
LOG B_{SP} M^{-1}
LOG N CM^{-3}
DAY OF THE YEAR 1978

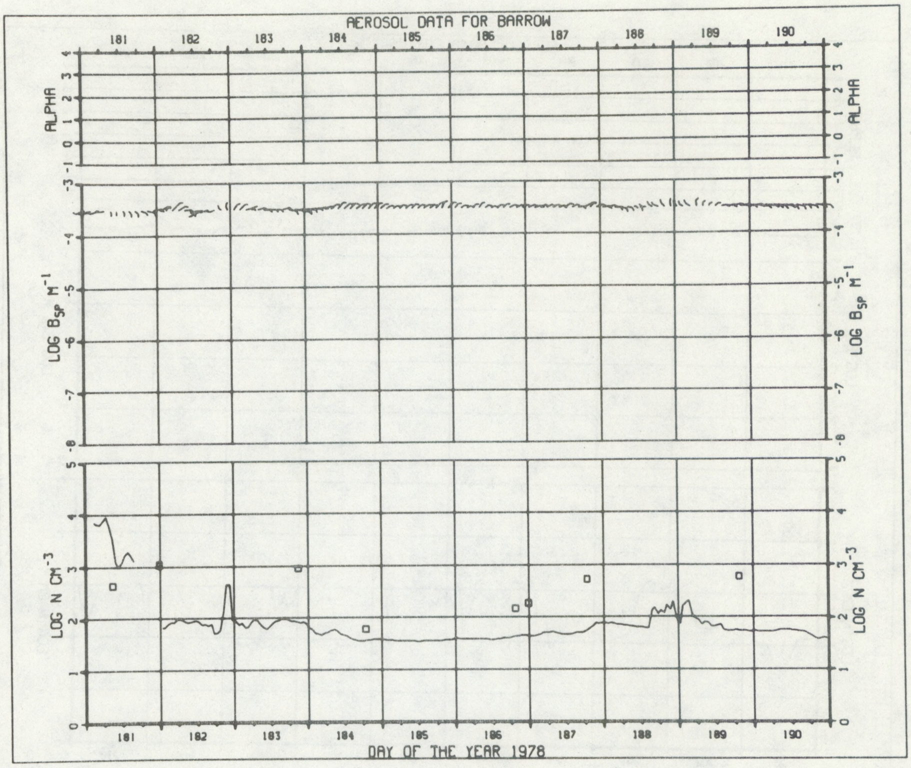
AEROSOL DATA FOR BARROW
ALPHA
LOG B_{SP} M^{-1}
LOG N CM^{-3}
DAY OF THE YEAR 1978

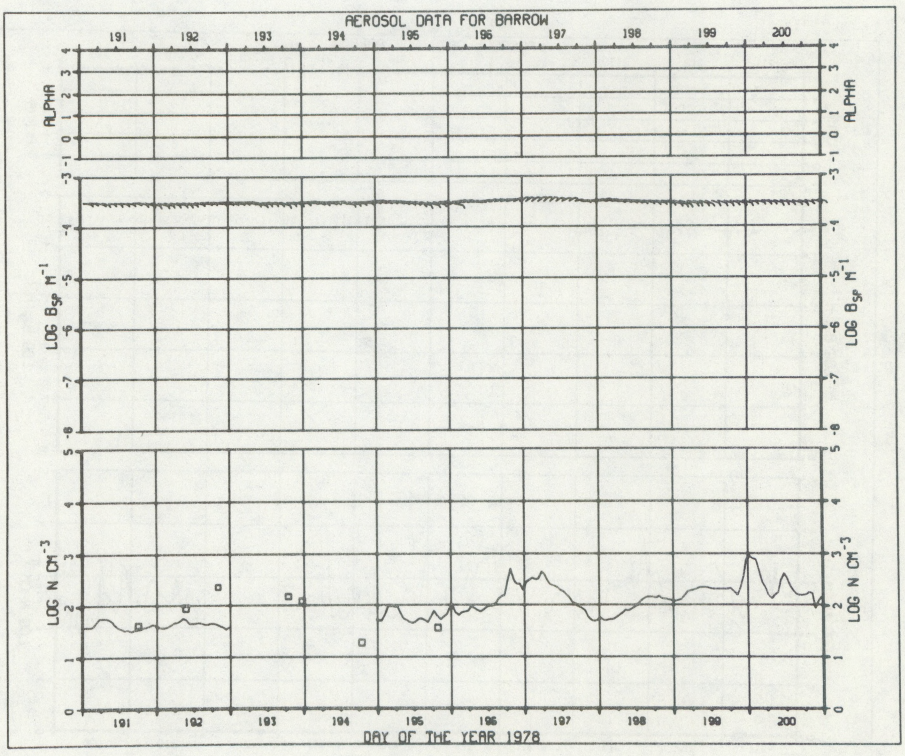
AEROSOL DATA FOR BARROW
ALPHA
LOG B_{SP} M^{-1}
LOG N CM^{-3}
DAY OF THE YEAR 1978

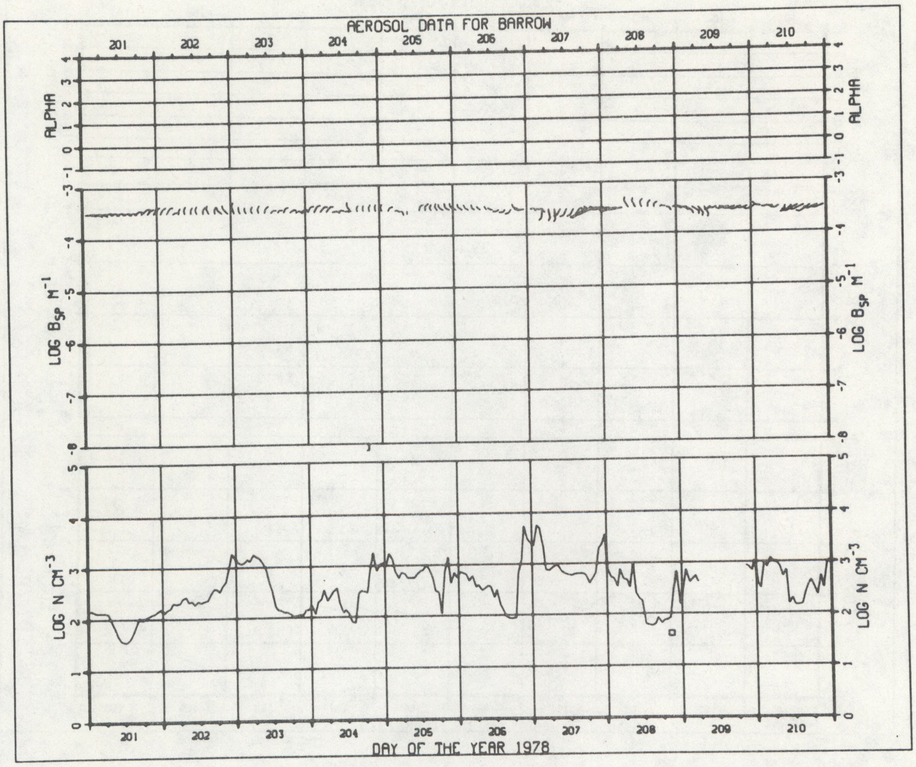
AEROSOL DATA FOR BARROW
ALPHA
LOG BSP M-1
LOG N CM-3
DAY OF THE YEAR 1978

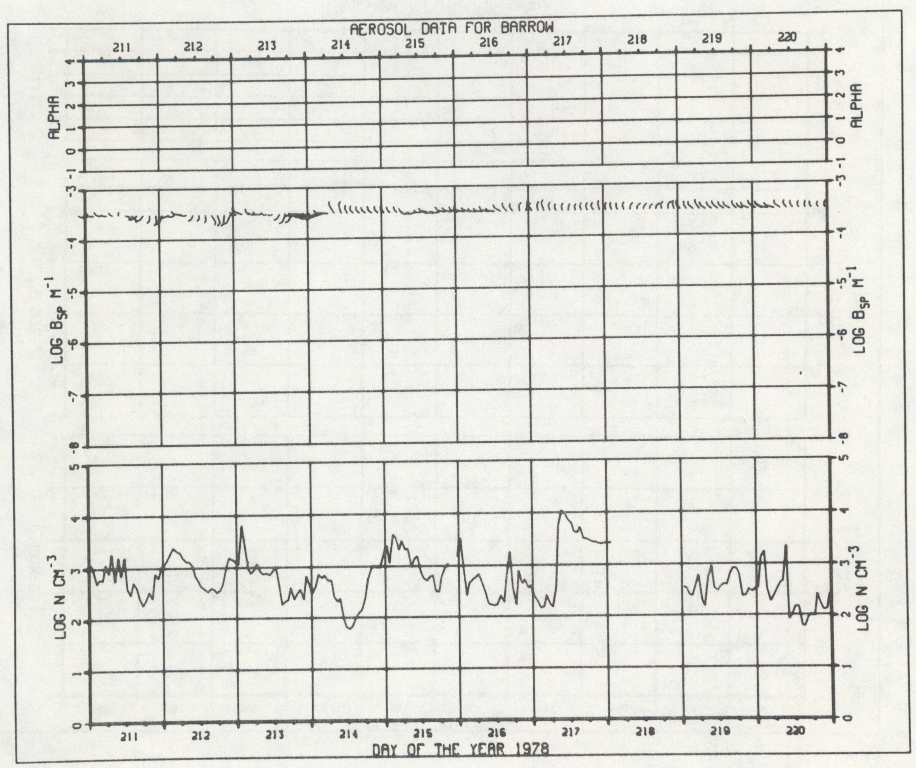
AEROSOL DATA FOR BARROW
ALPHA
LOG BSP M-1
LOG N CM-3
DAY OF THE YEAR 1978

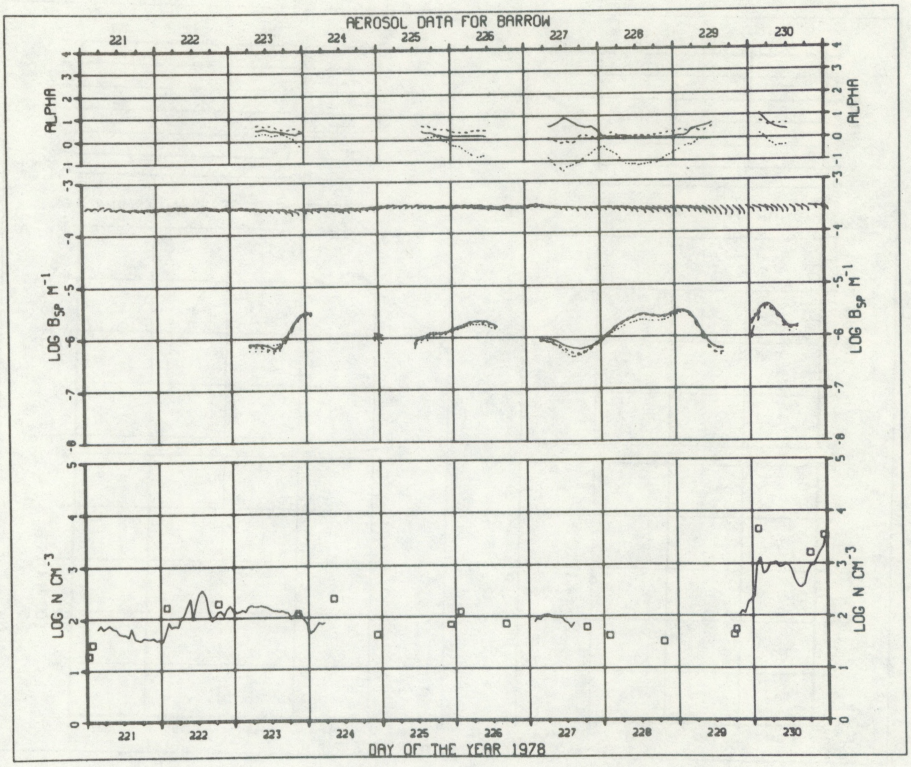
AEROSOL DATA FOR BARROW
ALPHA
LOG B_{SP} M^{-1}
LOG N CM^{-3}
DAY OF THE YEAR 1978

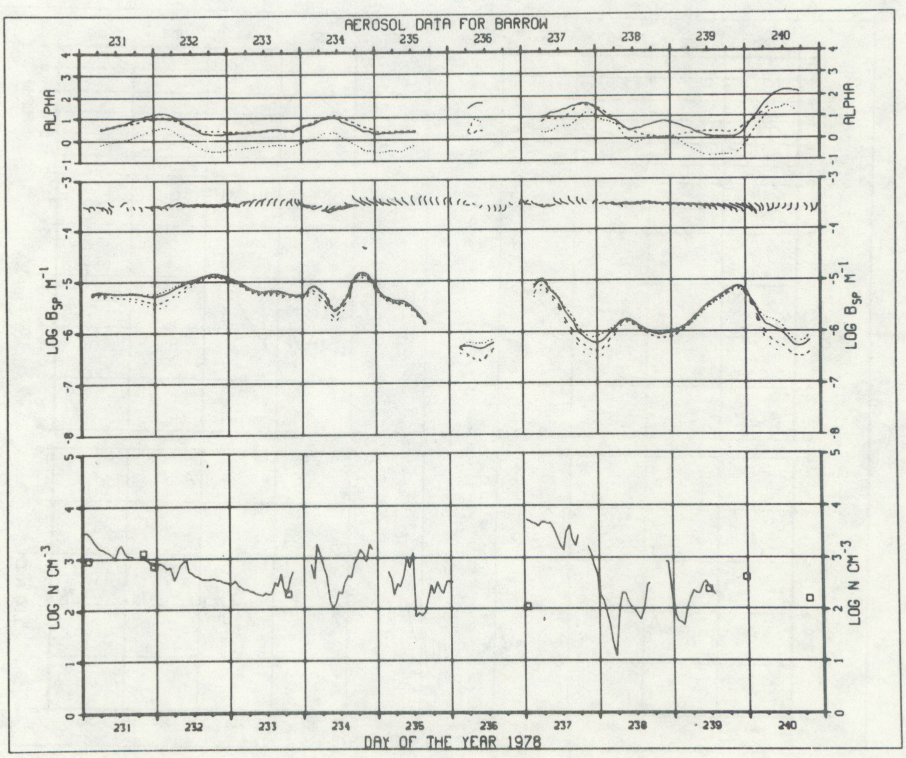
AEROSOL DATA FOR BARROW
ALPHA
LOG B_{SP} M^{-1}
LOG N CM^{-3}
DAY OF THE YEAR 1978

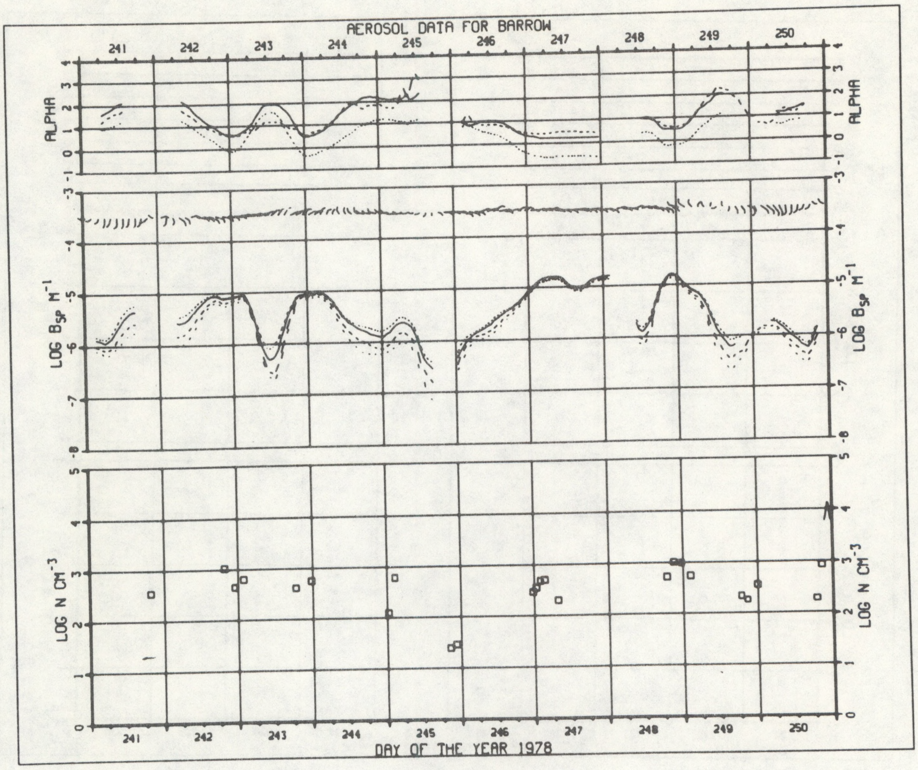
AEROSOL DATA FOR BARROW
ALPHA
LOG B$_{SP}$ M^{-1}
LOG N CM^{-3}
DAY OF THE YEAR 1978

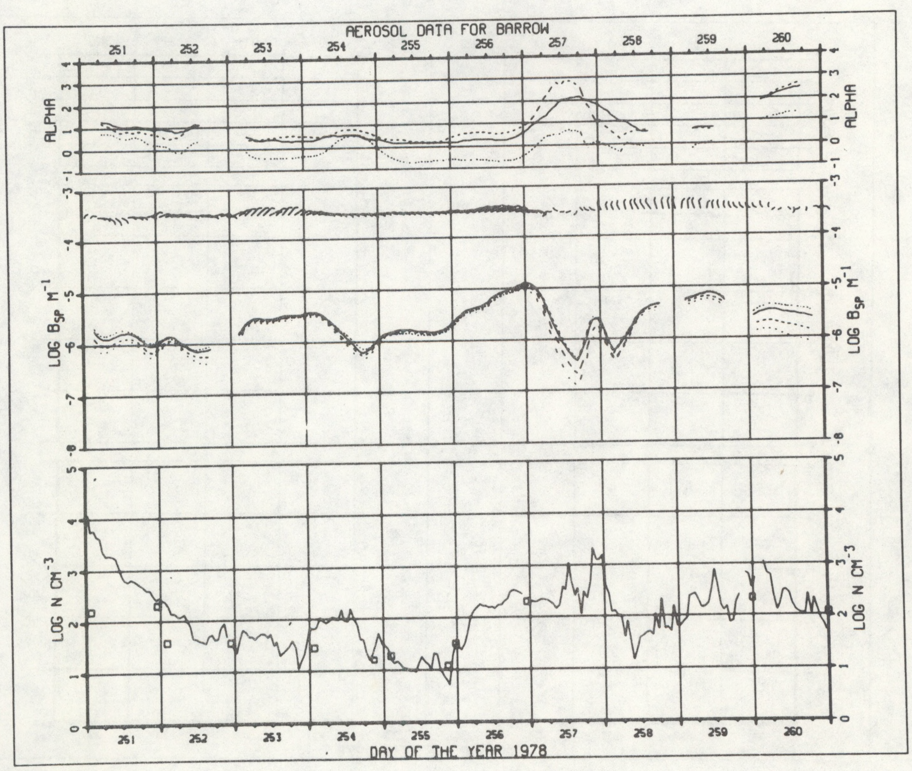
AEROSOL DATA FOR BARROW
ALPHA
LOG B$_{SP}$ M^{-1}
LOG N CM^{-3}
DAY OF THE YEAR 1978

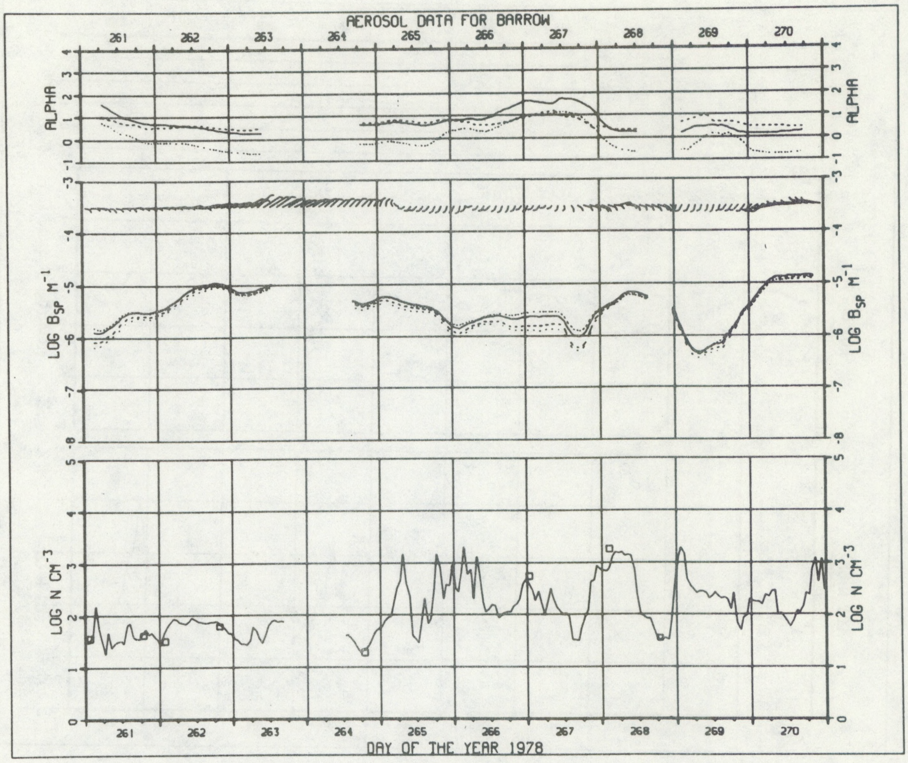
AEROSOL DATA FOR BARROW
ALPHA
LOG B_SP M^-1
LOG N CM^-3
DAY OF THE YEAR 1978

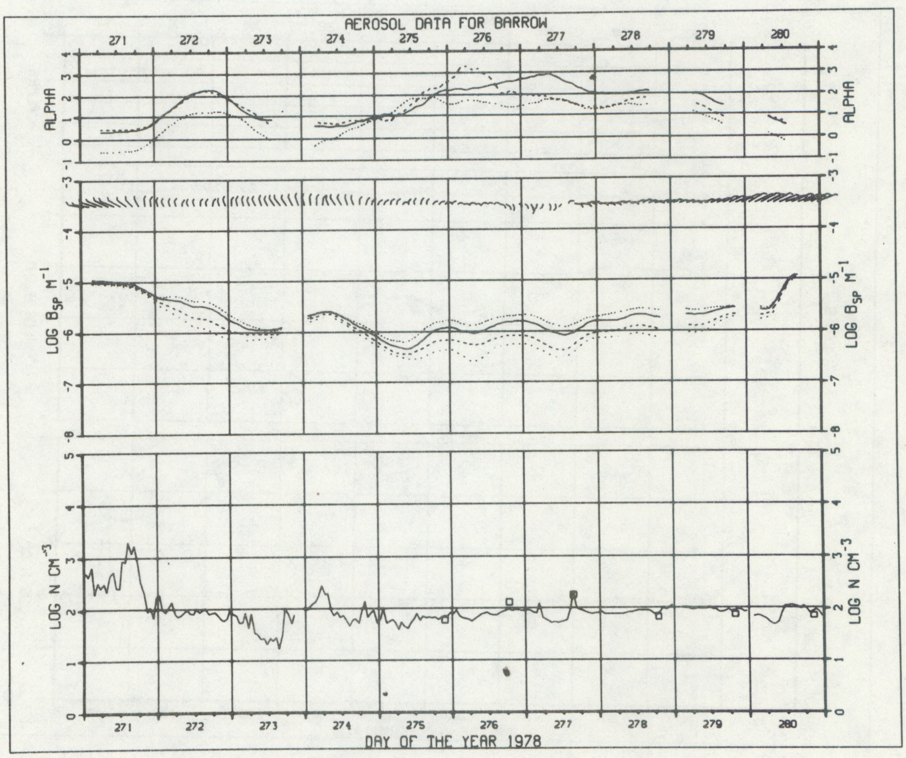
AEROSOL DATA FOR BARROW
ALPHA
LOG B_SP M^-1
LOG N CM^-3
DAY OF THE YEAR 1978

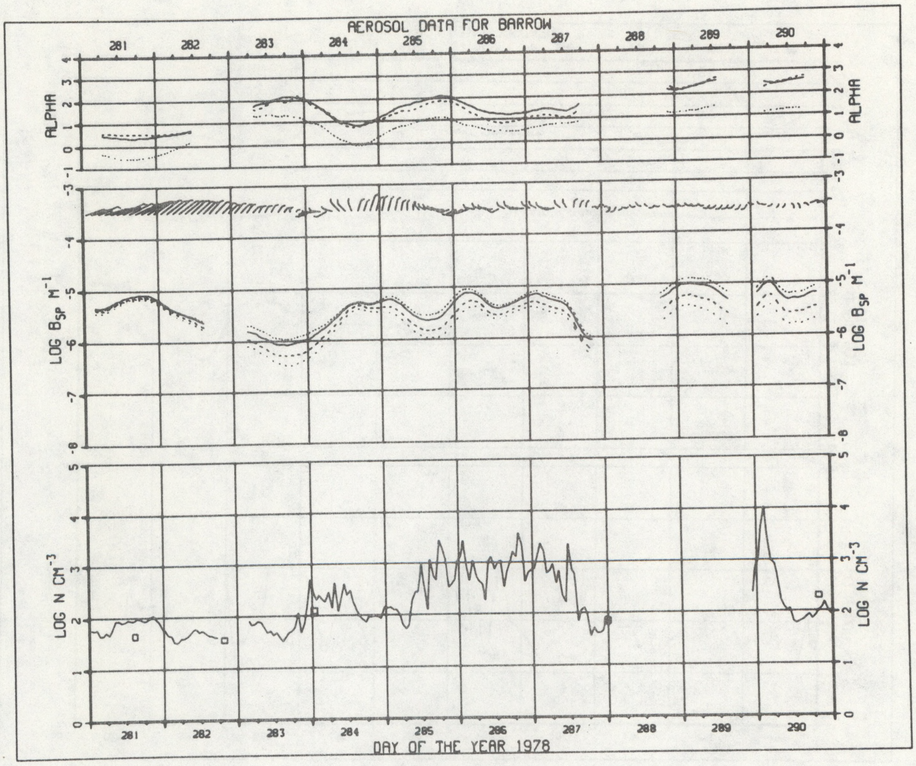
AEROSOL DATA FOR BARROW
ALPHA
LOG B_{SP} M^{-1}
LOG N CM^{-3}
DAY OF THE YEAR 1978

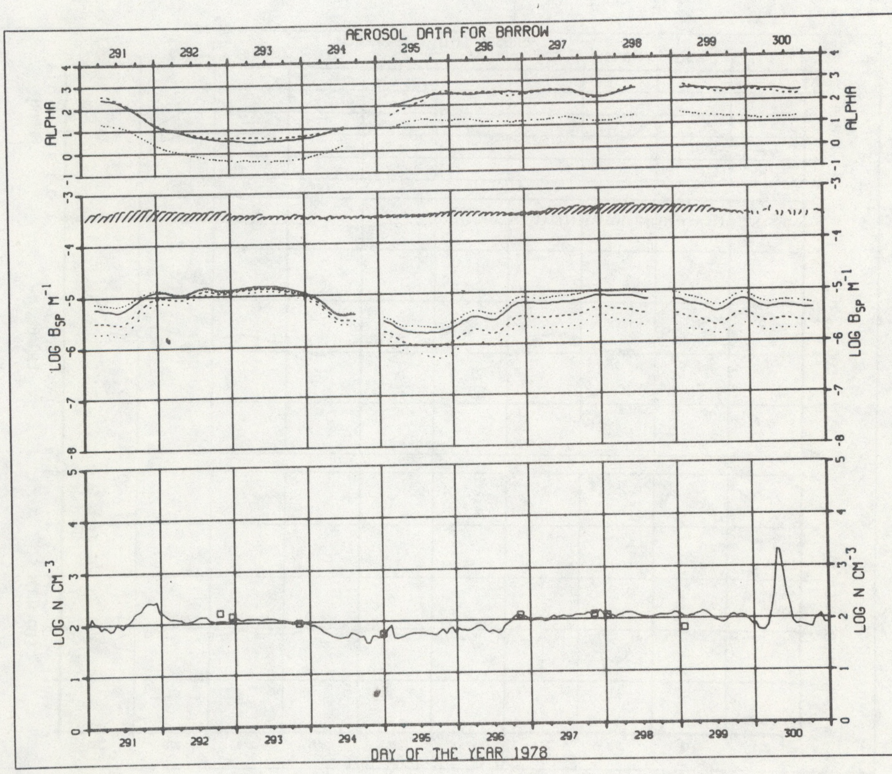
AEROSOL DATA FOR BARROW
ALPHA
LOG B_{SP} M^{-1}
LOG N CM^{-3}
DAY OF THE YEAR 1978

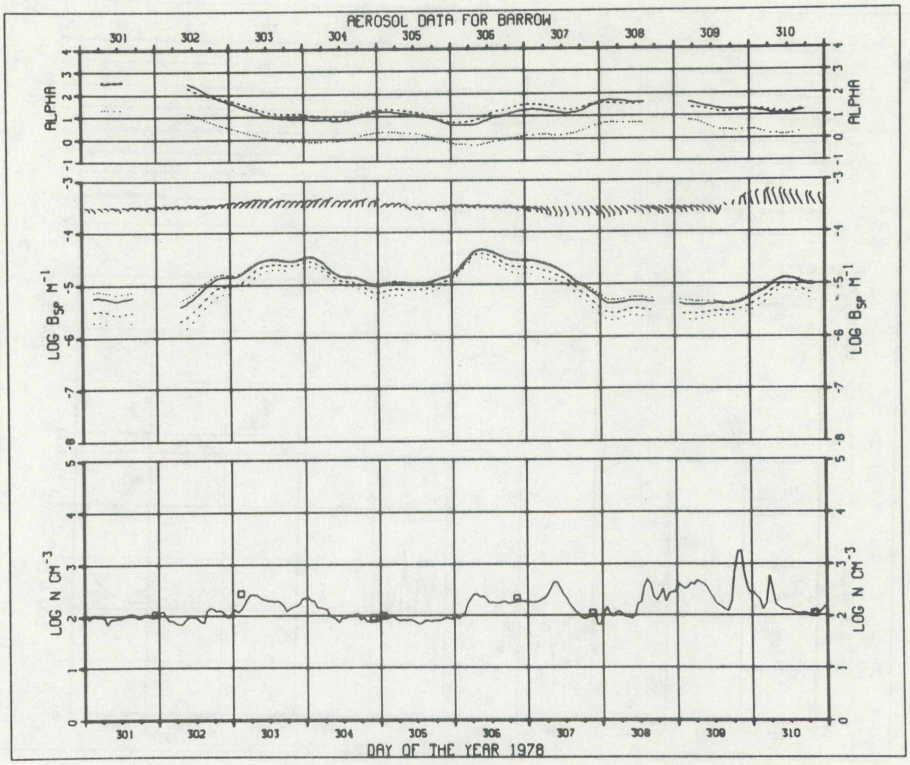
AEROSOL DATA FOR BARROW
ALPHA
LOG B_{SP} M^{-1}
LOG N CM^{-3}
DAY OF THE YEAR 1978

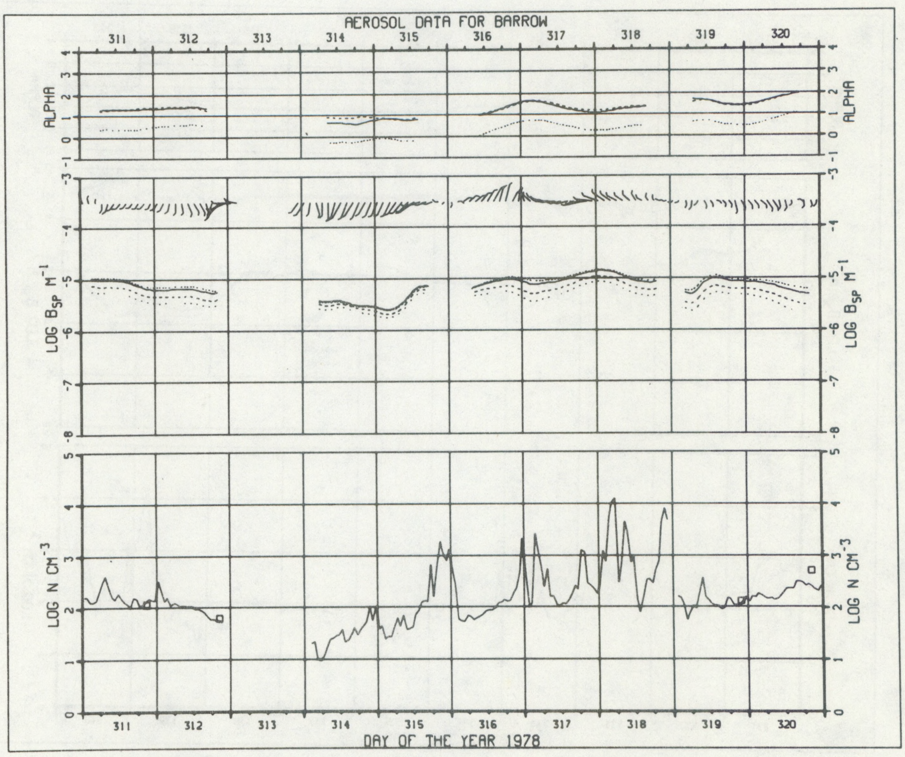
AEROSOL DATA FOR BARROW
ALPHA
LOG B_{SP} M^{-1}
LOG N CM^{-3}
DAY OF THE YEAR 1978

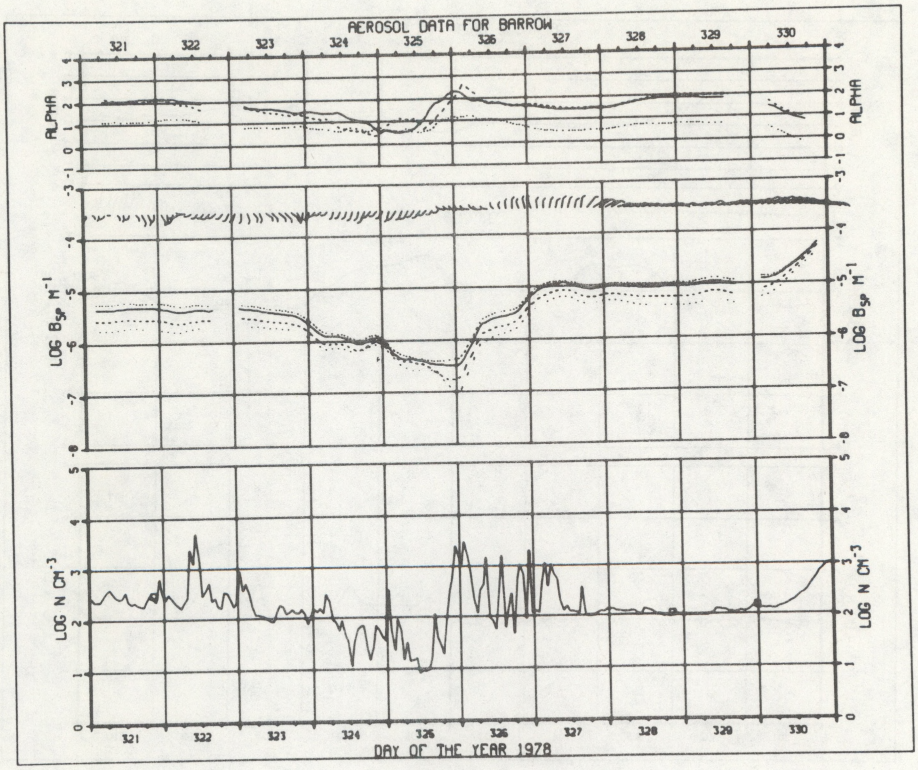
AEROSOL DATA FOR BARROW
ALPHA
LOG B$_{SP}$ M^{-1}
LOG N CM^{-3}
DAY OF THE YEAR 1978

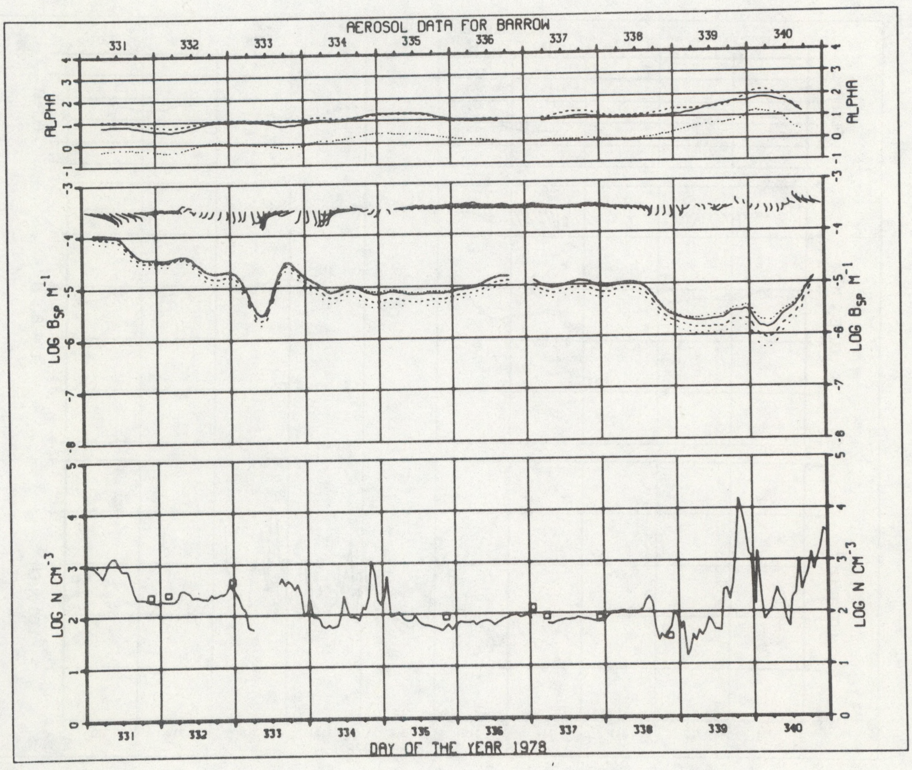
AEROSOL DATA FOR BARROW
ALPHA
LOG B$_{SP}$ M^{-1}
LOG N CM^{-3}
DAY OF THE YEAR 1978

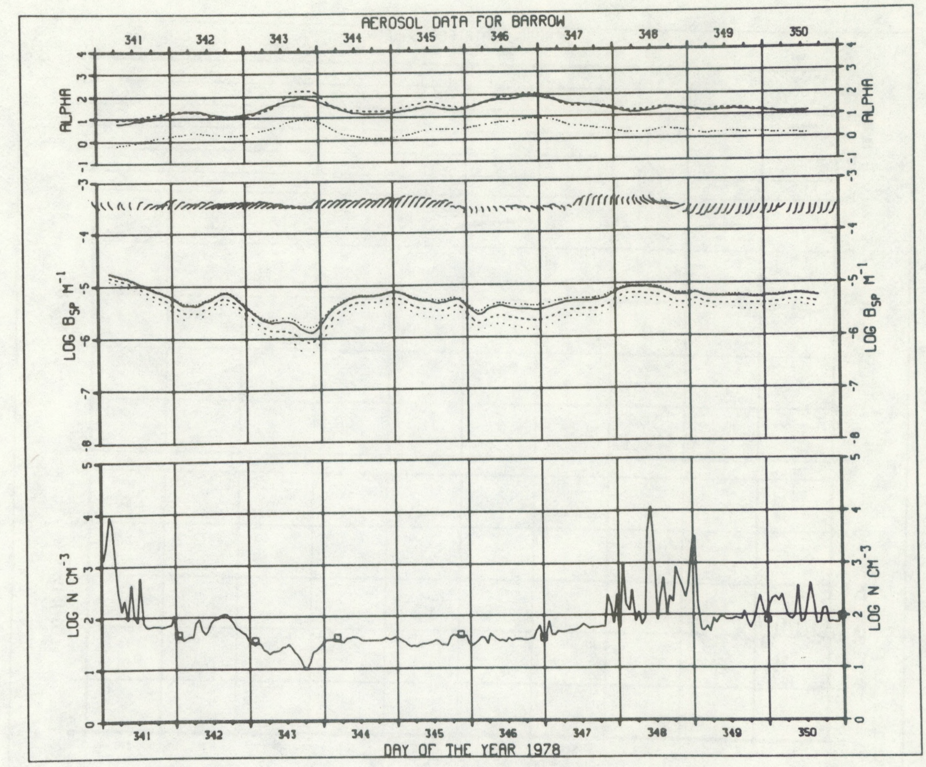
AEROSOL DATA FOR BARROW
ALPHA
LOG B_{SP} M^{-1}
LOG N CM^{-3}
DAY OF THE YEAR 1978

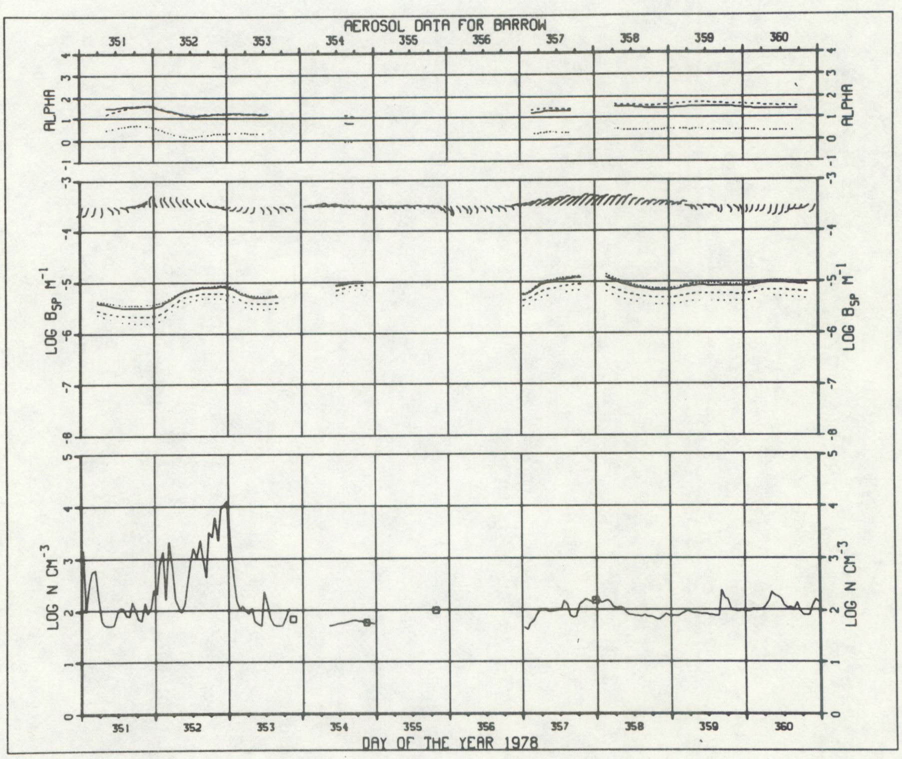
AEROSOL DATA FOR BARROW
ALPHA
LOG B_{SP} M^{-1}
LOG N CM^{-3}
DAY OF THE YEAR 1978

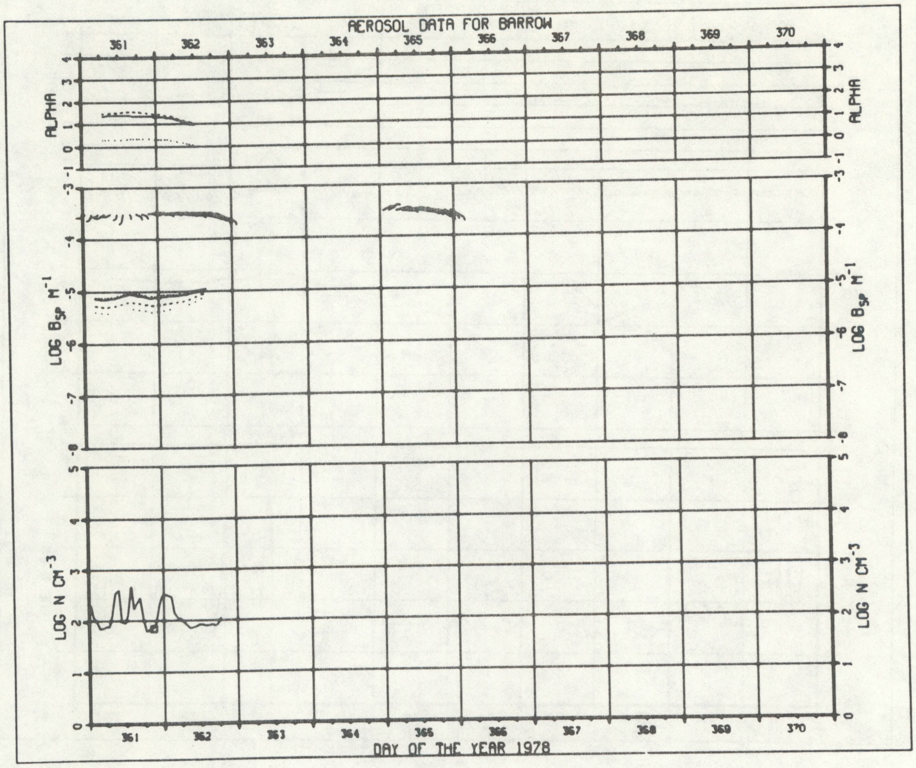
AEROSOL DATA FOR BARROW
361
362
363
364
365
366
367
368
369
370
ALPHA
LOG B_{sp} M^{-1}
LOG N CM^{-3}
DAY OF THE YEAR 1978

APPENDIX D

Appendix D contains the hourly mean nuclei concentrations, Pollak counter observations, light scattering data, and Angstrom exponents plotted on a logarithmic scale for 1979. A histogram of successive one minute voltage differences for each month was generated and the variability criterion was determined to be ±0.0367 volts.

The data pairs were obtained from the minute data and grouped into periods where the G.E. counter was operating. The scaling factors generated are:

Day	Scaling Factor
00-1416	0.987590904
1417-4523	1.26469707
4600-5814	1.027947025
5815-10322	1.07397945
10323-12218	1.18969160
12219-13700	0.7964008
13701-16423	0.955291811
16500-20819	1.30319718
20820-29221	0.953110995
29222-29517	1.00
29518-36523	0.761895322

Scaled graphical display of aerosol data for 1979.
for each plot;

the top graph contains: Angstrom exponents
Alpha (1-2): dashed line
Alpha (2-3): solid line
Alpha (3-4): long dashed line

the center graph contains: light scattering and wind data
wavelength 450 nm: dashed line
wavelength 550 nm: solid line
wavelength 700 nm: long dashed line
wavelength 850 nm: short dashed line

the lower graph contains: nuclei concentrations
G.E. counter: solid line
Pollak counter: squares

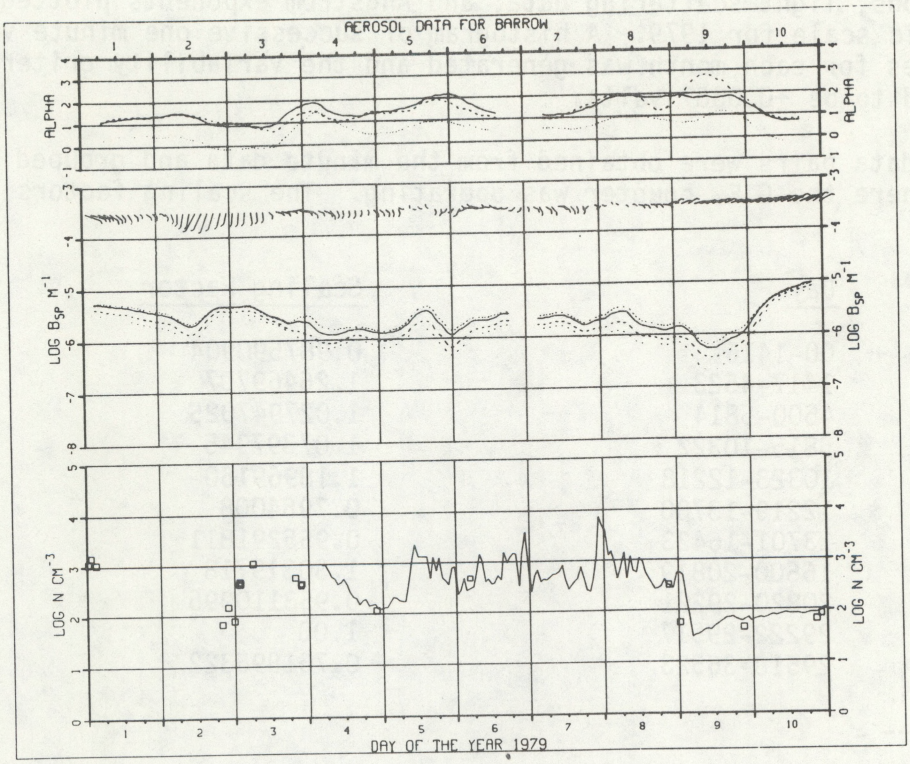
AEROSOL DATA FOR BARROW
ALPHA
LOG B_SP M^-1
LOG N CM^-3
DAY OF THE YEAR 1979

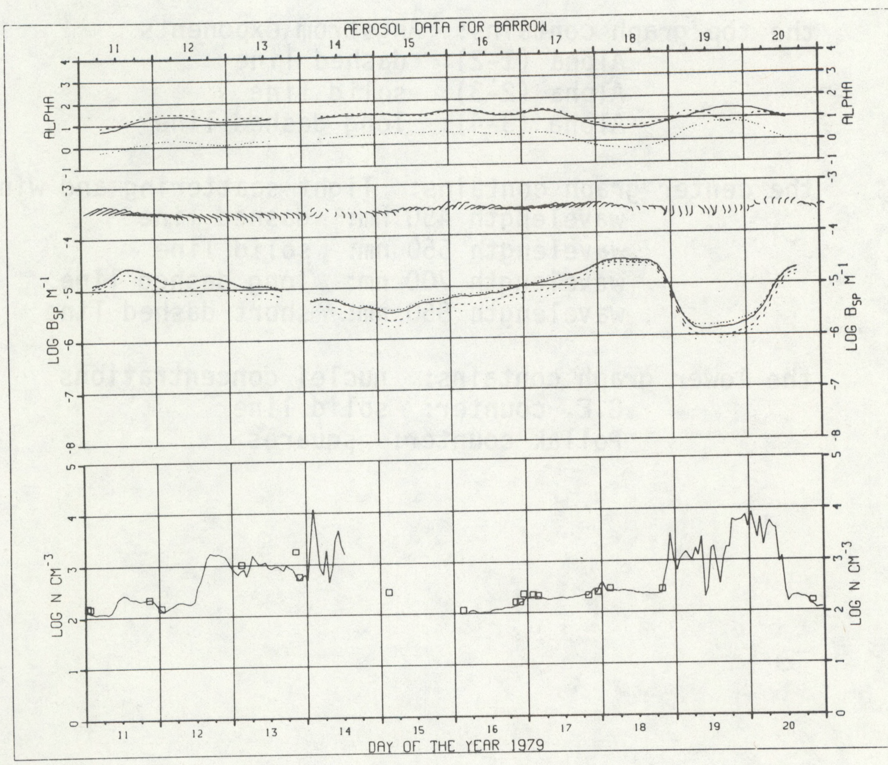
AEROSOL DATA FOR BARROW
ALPHA
LOG B_SP M^-1
LOG N CM^-3
DAY OF THE YEAR 1979

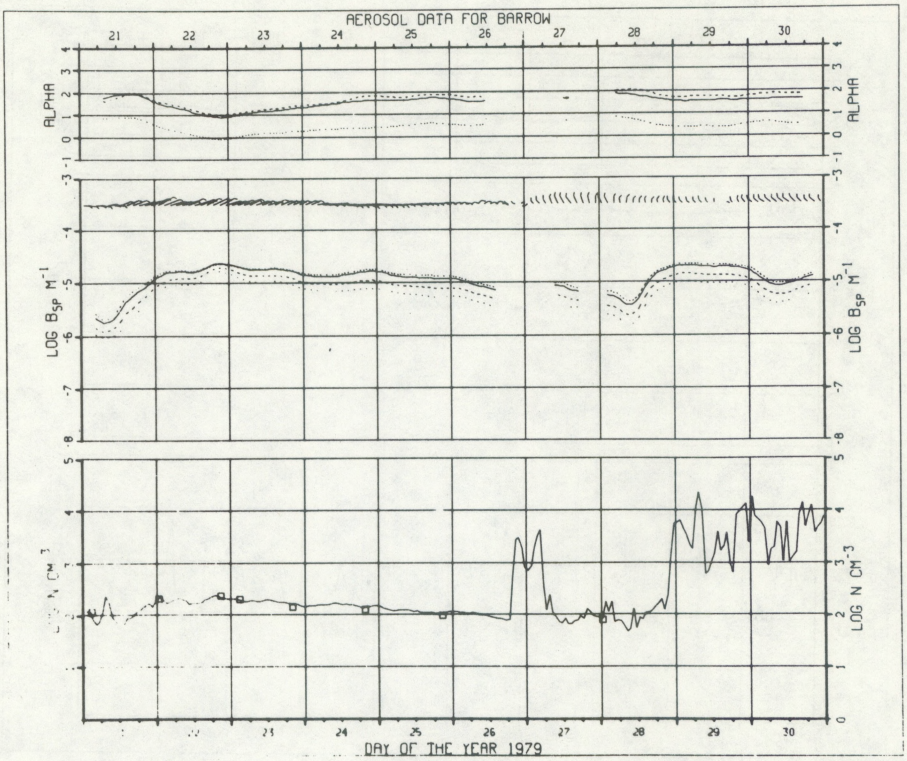
AEROSOL DATA FOR BARROW
ALPHA
LOG B_{SP} M^{-1}
LOG N CM^{-3}
DAY OF THE YEAR 1979

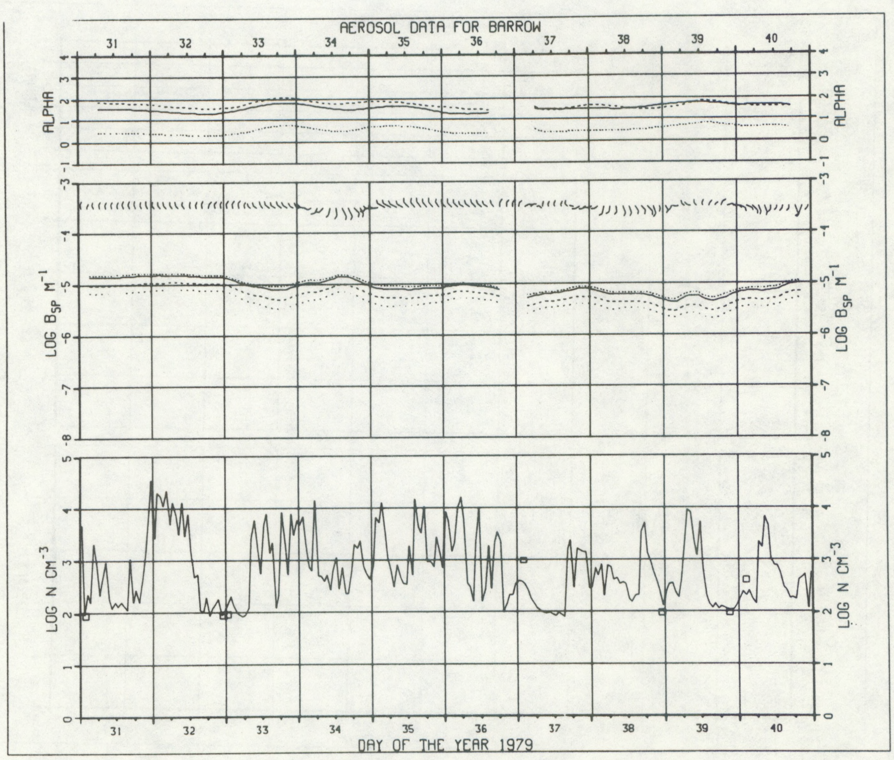
AEROSOL DATA FOR BARROW
ALPHA
LOG B_{SP} M^{-1}
LOG N CM^{-3}
DAY OF THE YEAR 1979

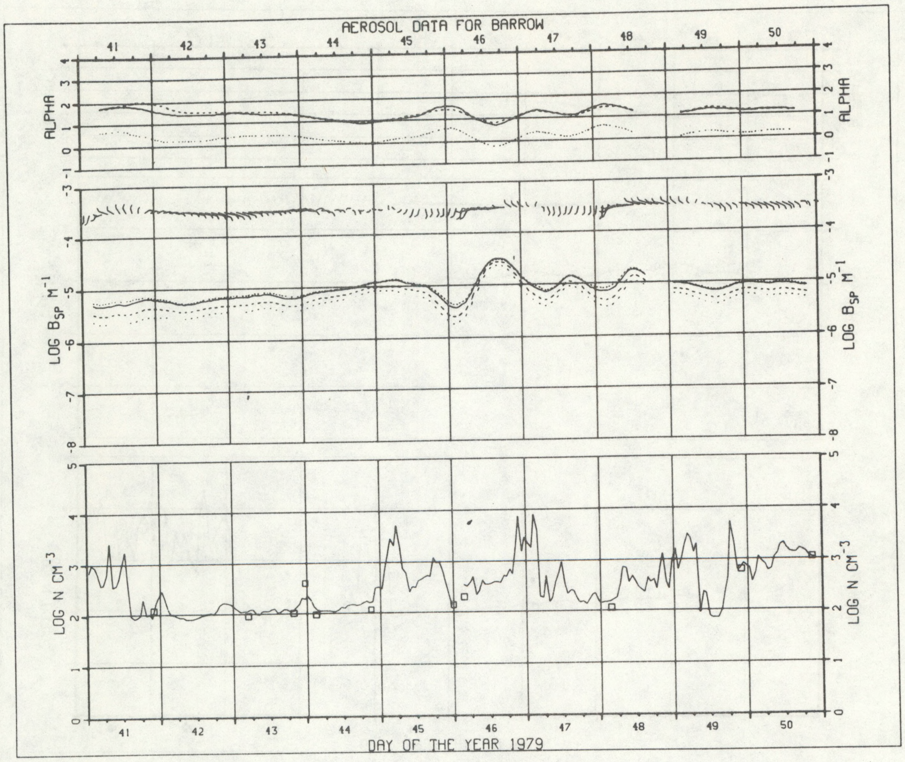

AEROSOL DATA FOR BARROW
ALPHA
LOG B_{SP} M^{-1}
LOG N CM^{-3}
DAY OF THE YEAR 1979

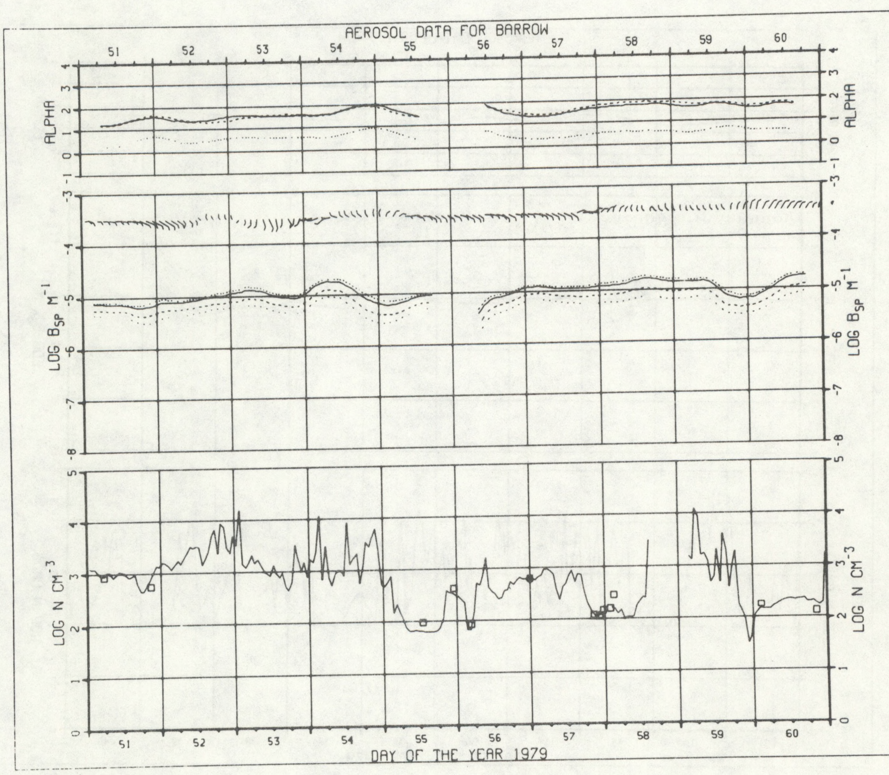

AEROSOL DATA FOR BARROW
ALPHA
LOG B_{SP} M^{-1}
LOG N CM^{-3}
DAY OF THE YEAR 1979

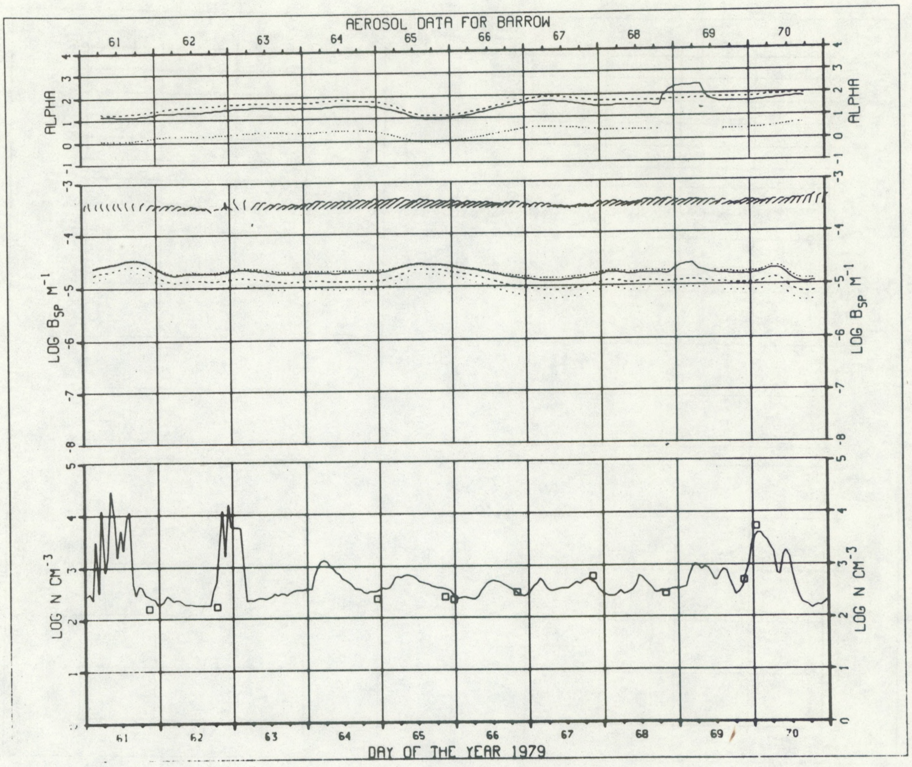
AEROSOL DATA FOR BARROW
ALPHA
LOG B$_{SP}$ M^{-1}
LOG N CM^{-3}
DAY OF THE YEAR 1979

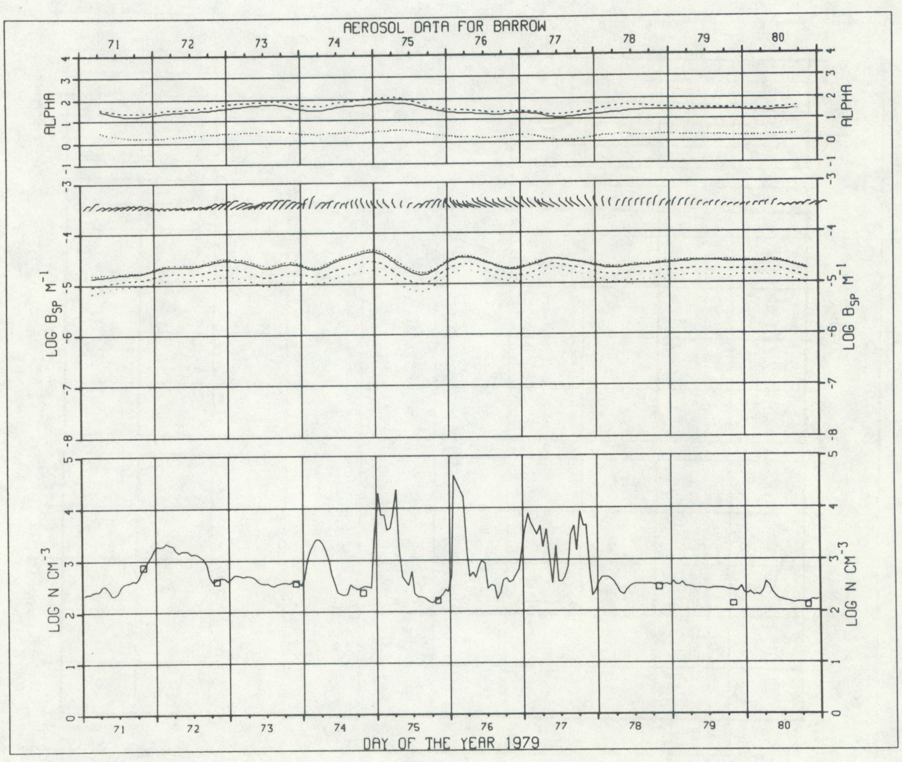
AEROSOL DATA FOR BARROW
ALPHA
LOG B$_{SP}$ M^{-1}
LOG N CM^{-3}
DAY OF THE YEAR 1979

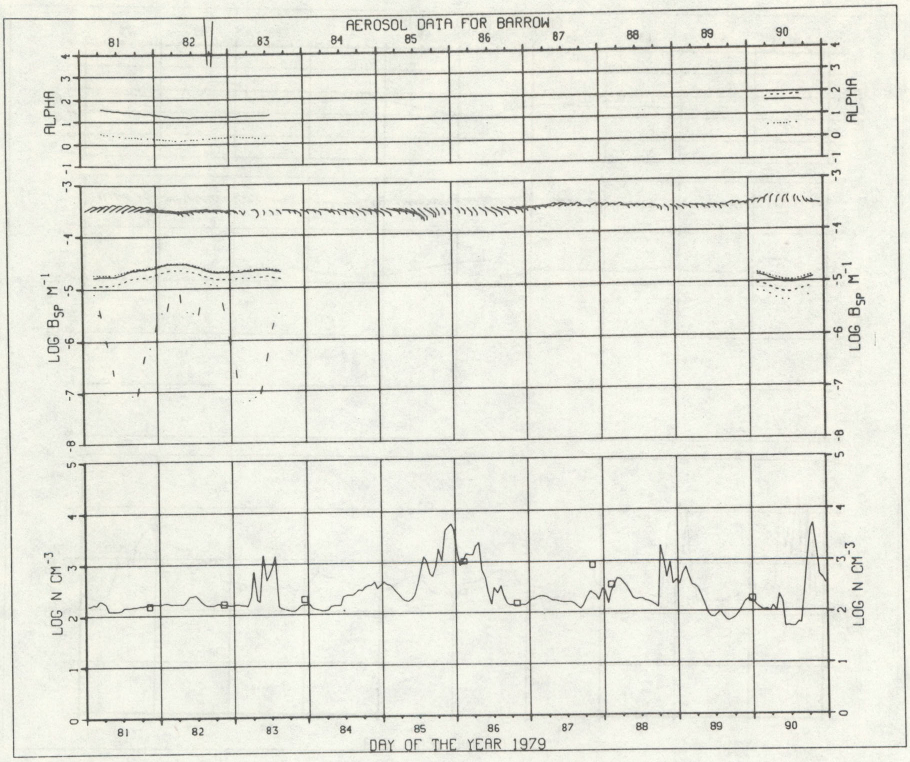
AEROSOL DATA FOR BARROW
ALPHA
LOG B_{SP} M^{-1}
LOG N CM^{-3}
DAY OF THE YEAR 1979

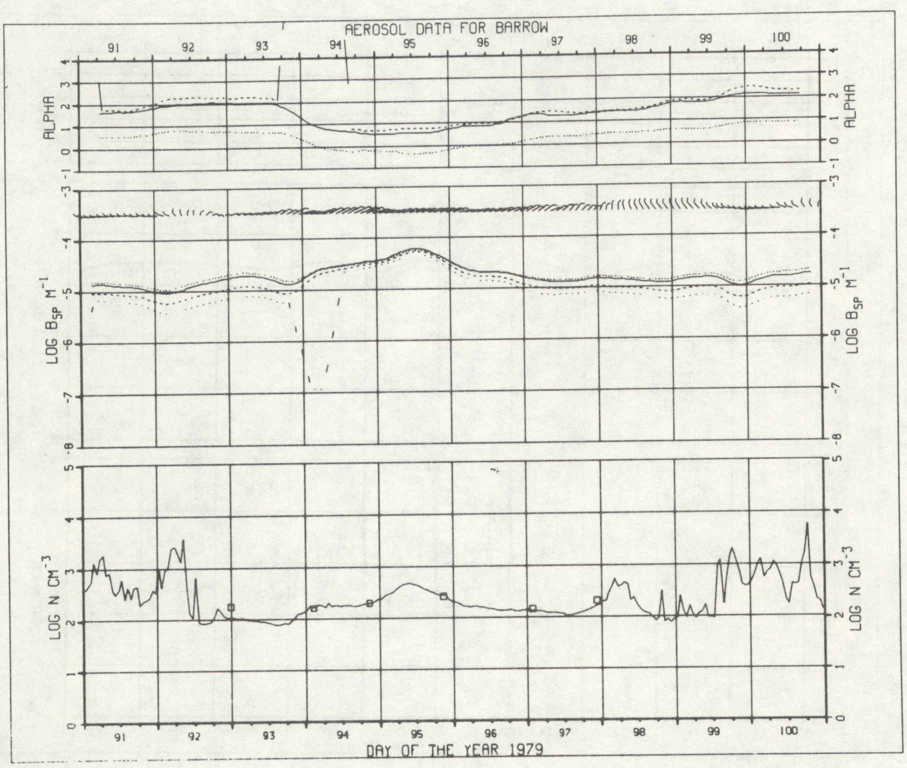
AEROSOL DATA FOR BARROW
ALPHA
LOG B_{SP} M^{-1}
LOG N CM^{-3}
DAY OF THE YEAR 1979

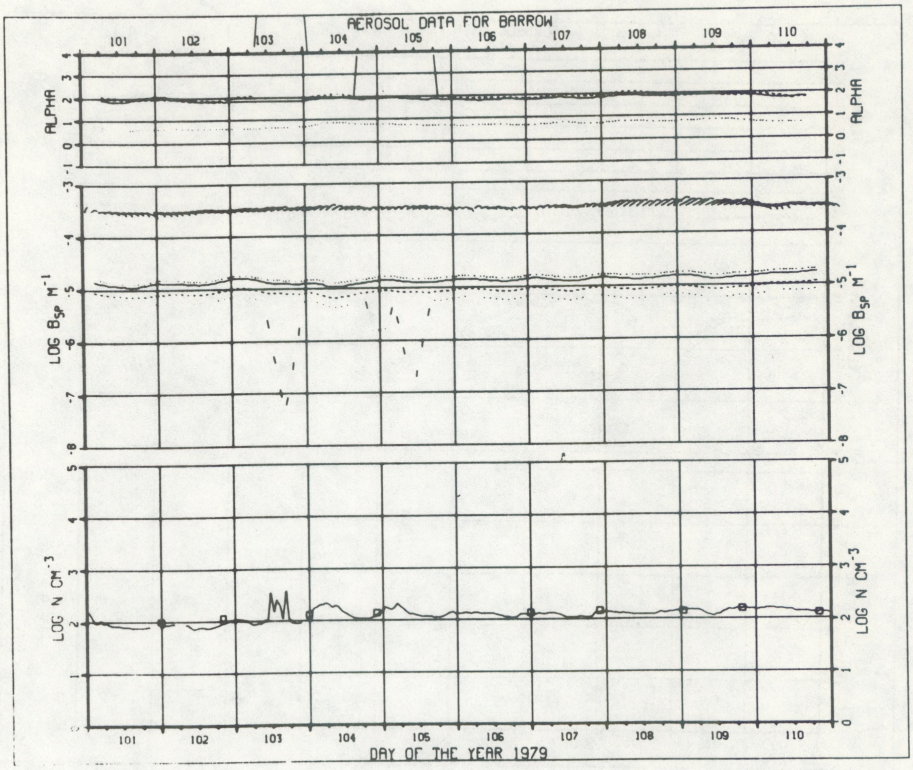
AEROSOL DATA FOR BARROW
ALPHA
LOG B_{SP} M^{-1}
LOG N CM^{-3}
DAY OF THE YEAR 1979

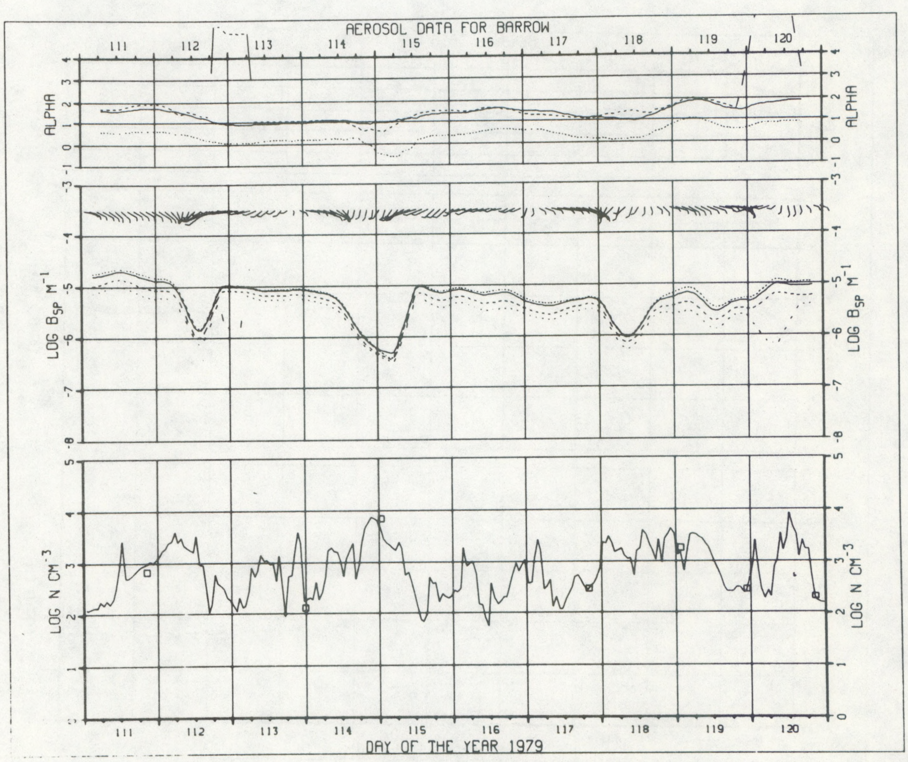
AEROSOL DATA FOR BARROW
ALPHA
LOG B_{SP} M^{-1}
LOG N CM^{-3}
DAY OF THE YEAR 1979

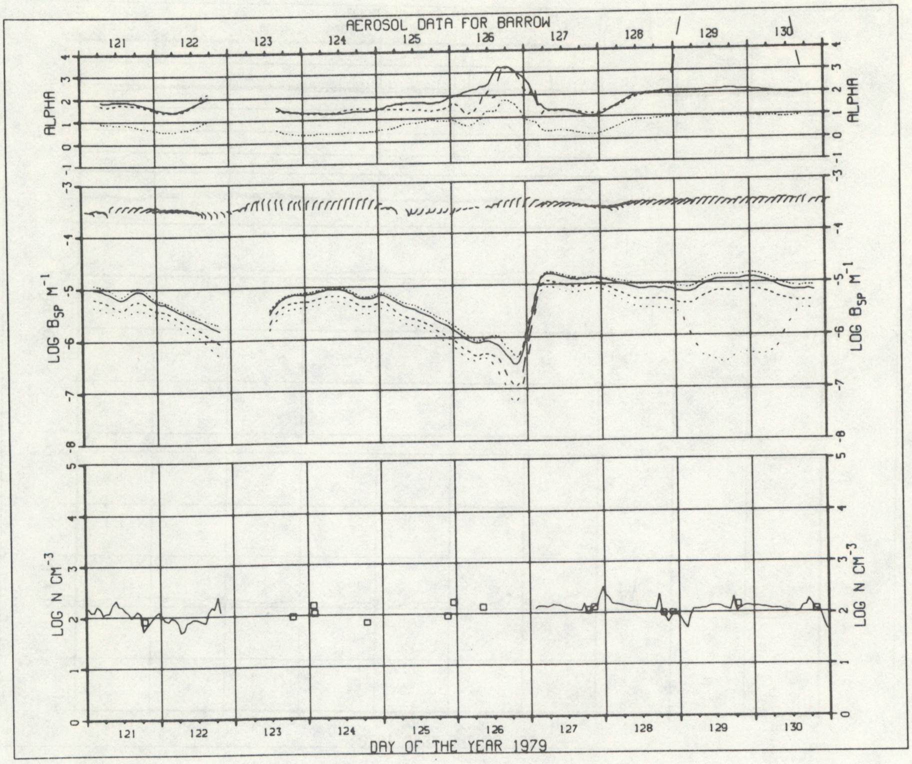
AEROSOL DATA FOR BARROW
ALPHA
LOG B_{SP} M^{-1}
LOG N CM^{-3}
DAY OF THE YEAR 1979

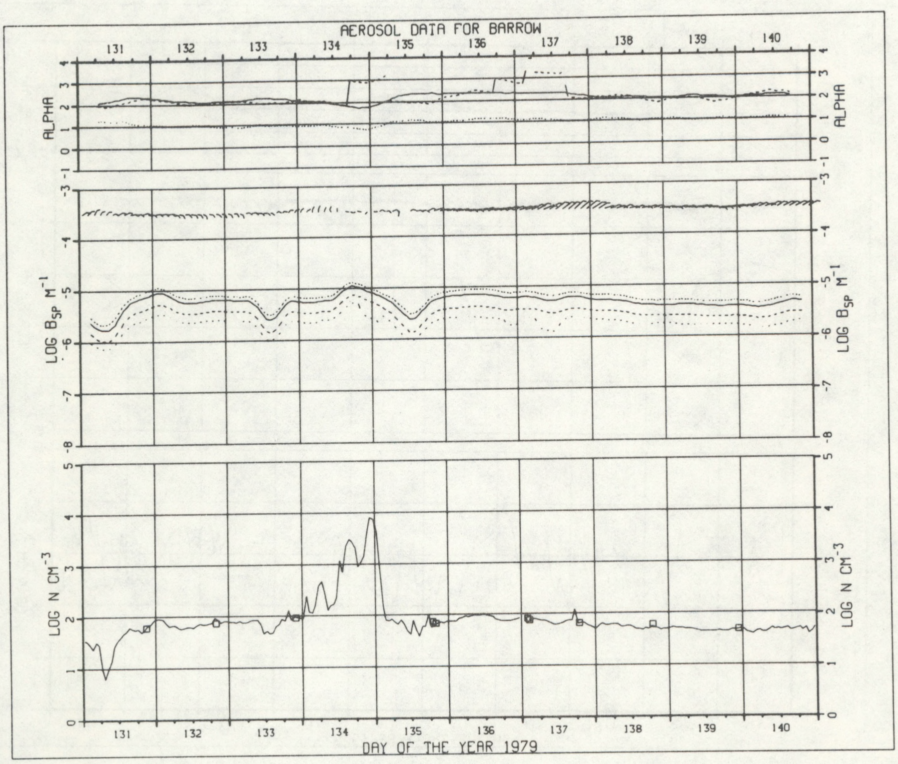
AEROSOL DATA FOR BARROW
ALPHA
LOG B_{SP} M^{-1}
LOG N CM^{-3}
DAY OF THE YEAR 1979

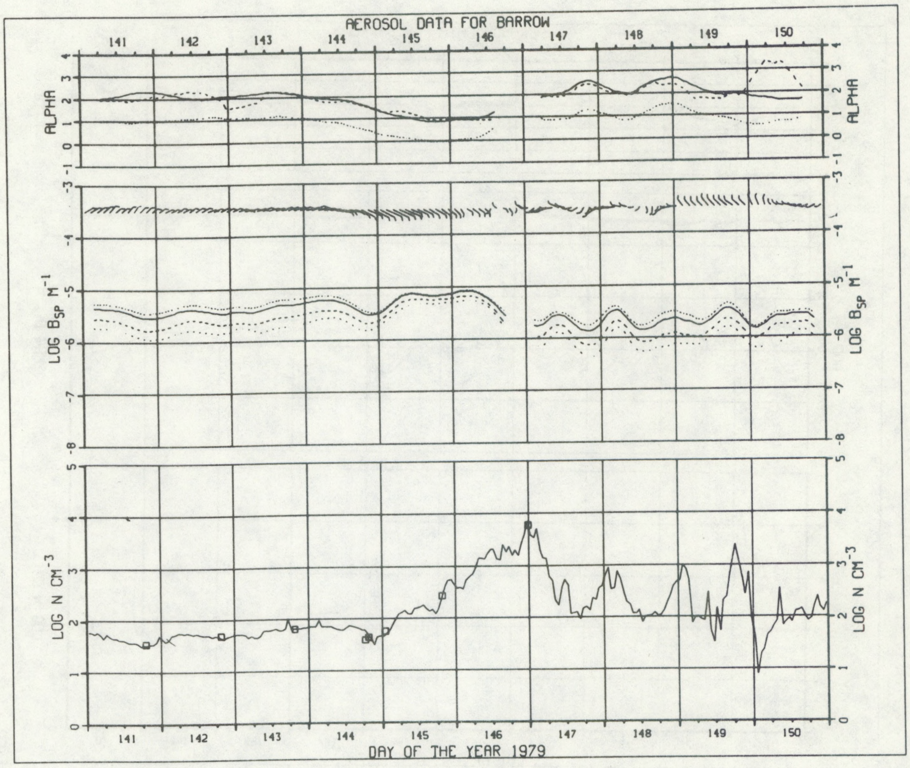
AEROSOL DATA FOR BARROW
ALPHA
LOG B_{SP} M^{-1}
LOG N CM^{-3}
DAY OF THE YEAR 1979

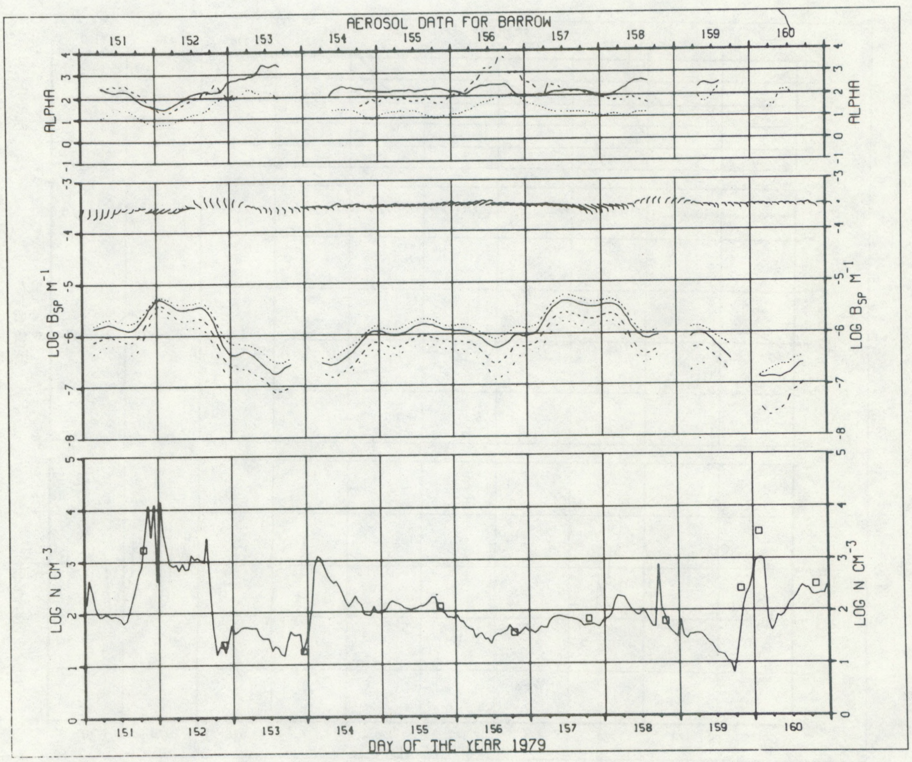
AEROSOL DATA FOR BARROW
ALPHA
LOG B_{SP} M^{-1}
LOG N CM^{-3}
DAY OF THE YEAR 1979

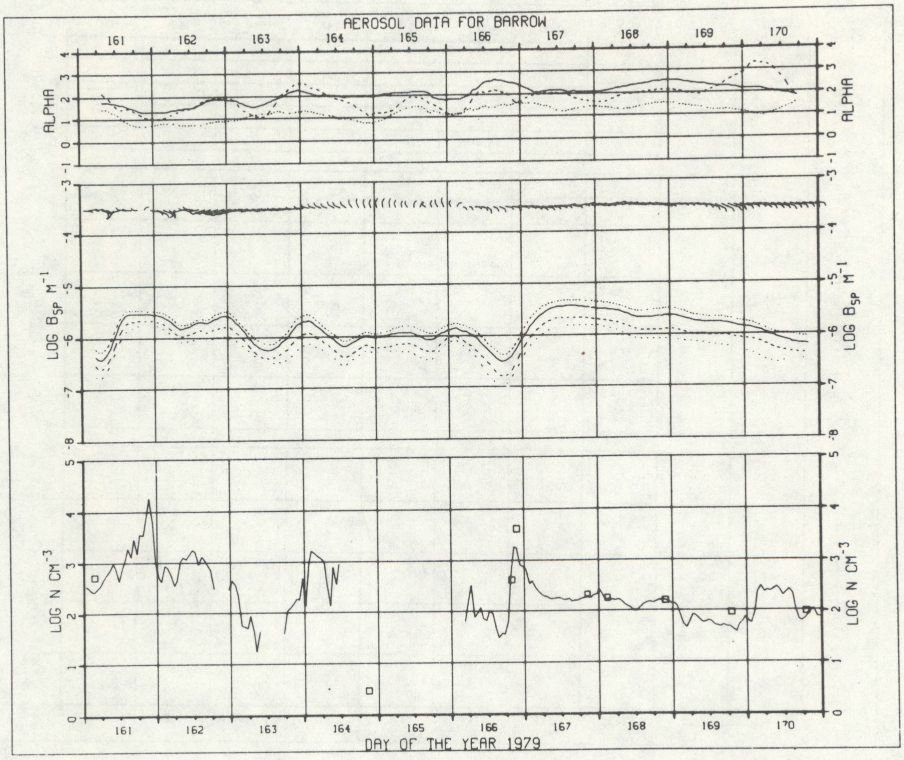
AEROSOL DATA FOR BARROW
ALPHA
LOG B_SP M^-1
LOG N CM^-3
DAY OF THE YEAR 1979

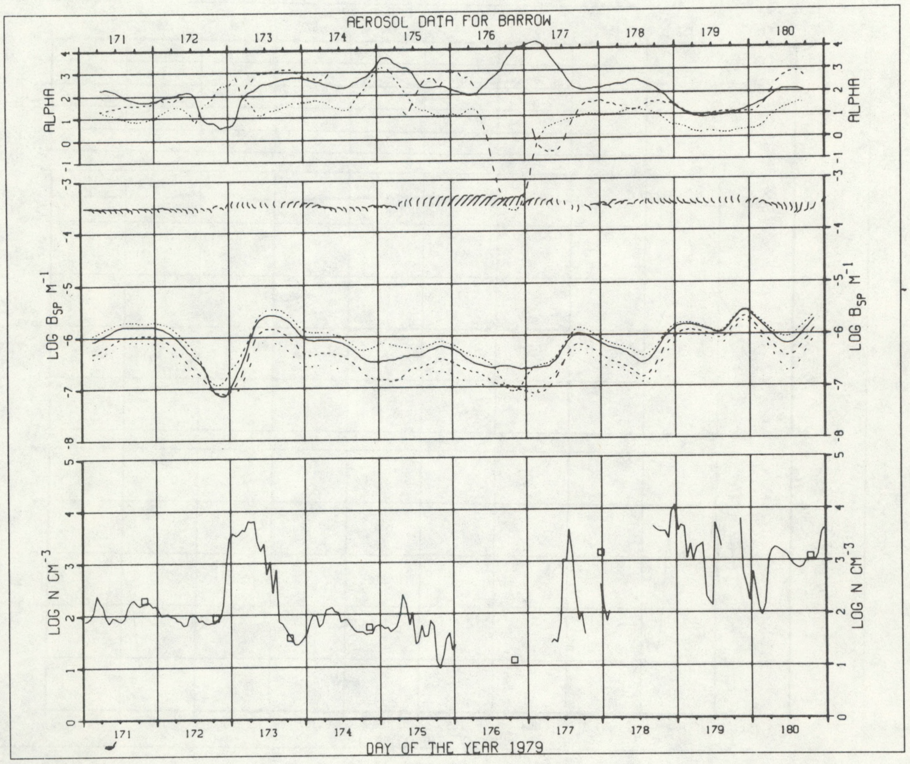
AEROSOL DATA FOR BARROW
ALPHA
LOG B_SP M^-1
LOG N CM^-3
DAY OF THE YEAR 1979

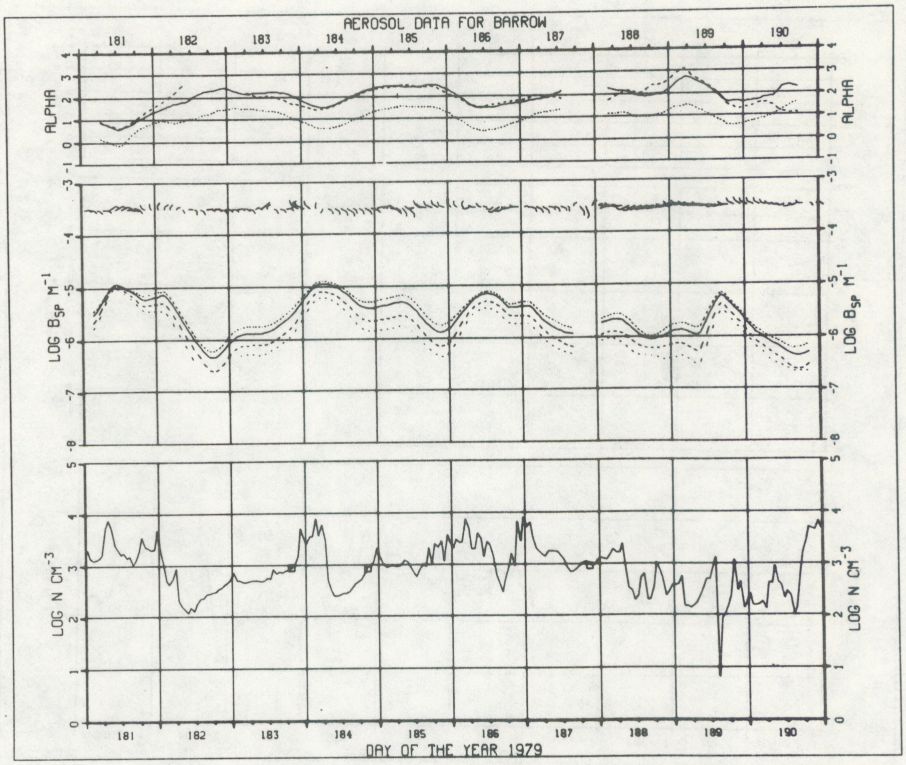
AEROSOL DATA FOR BARROW
ALPHA
LOG B_{SP} M^{-1}
LOG N CM^{-3}
DAY OF THE YEAR 1979

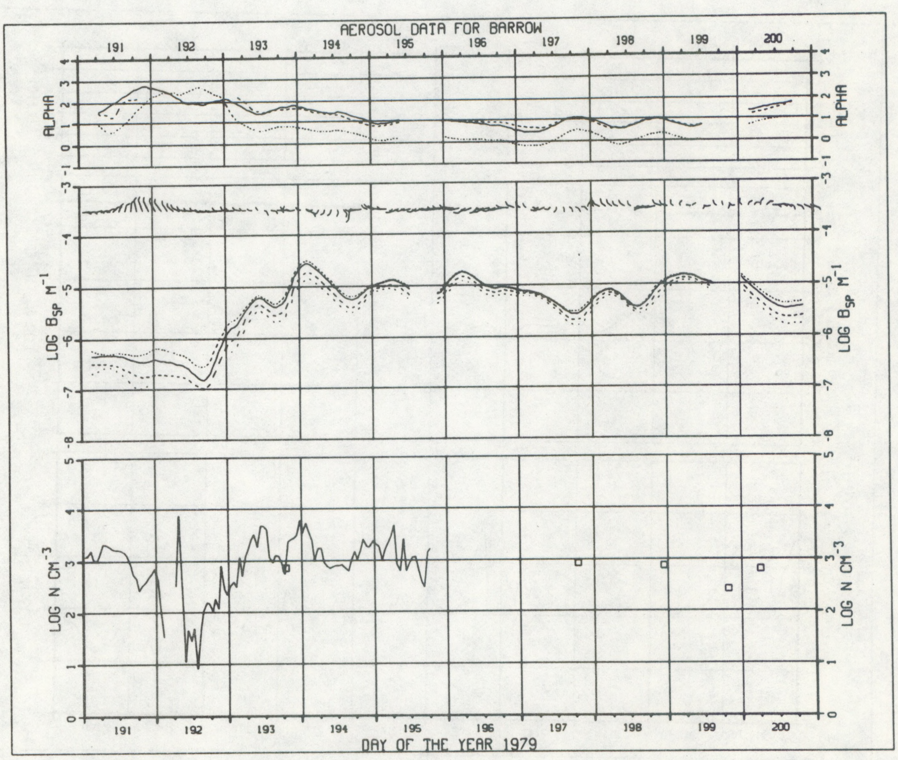
AEROSOL DATA FOR BARROW
ALPHA
LOG B_{SP} M^{-1}
LOG N CM^{-3}
DAY OF THE YEAR 1979

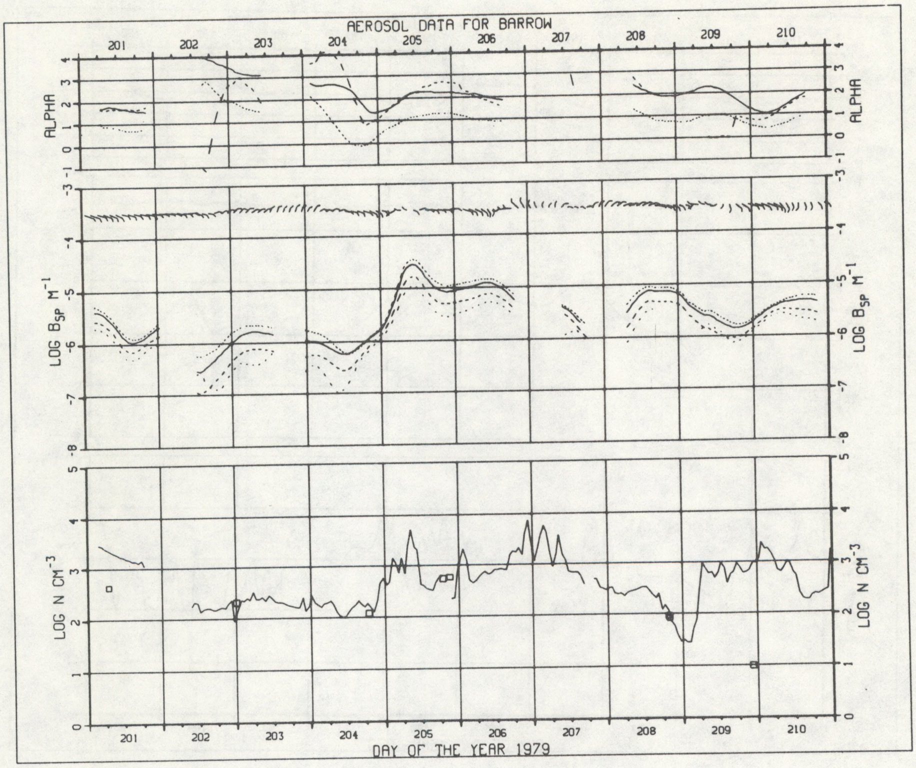
AEROSOL DATA FOR BARROW
ALPHA
LOG B_{SP} M^{-1}
LOG N CM^{-3}
201 202 203 204 205 206 207 208 209 210
DAY OF THE YEAR 1979

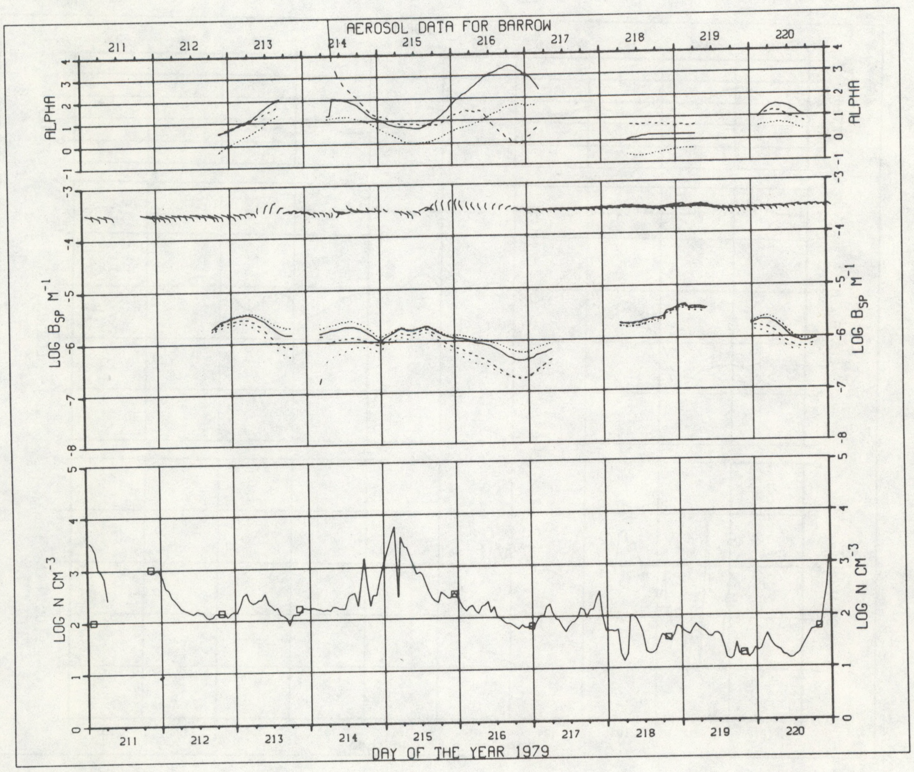
AEROSOL DATA FOR BARROW
ALPHA
LOG B_{SP} M^{-1}
LOG N CM^{-3}
211 212 213 214 215 216 217 218 219 220
DAY OF THE YEAR 1979

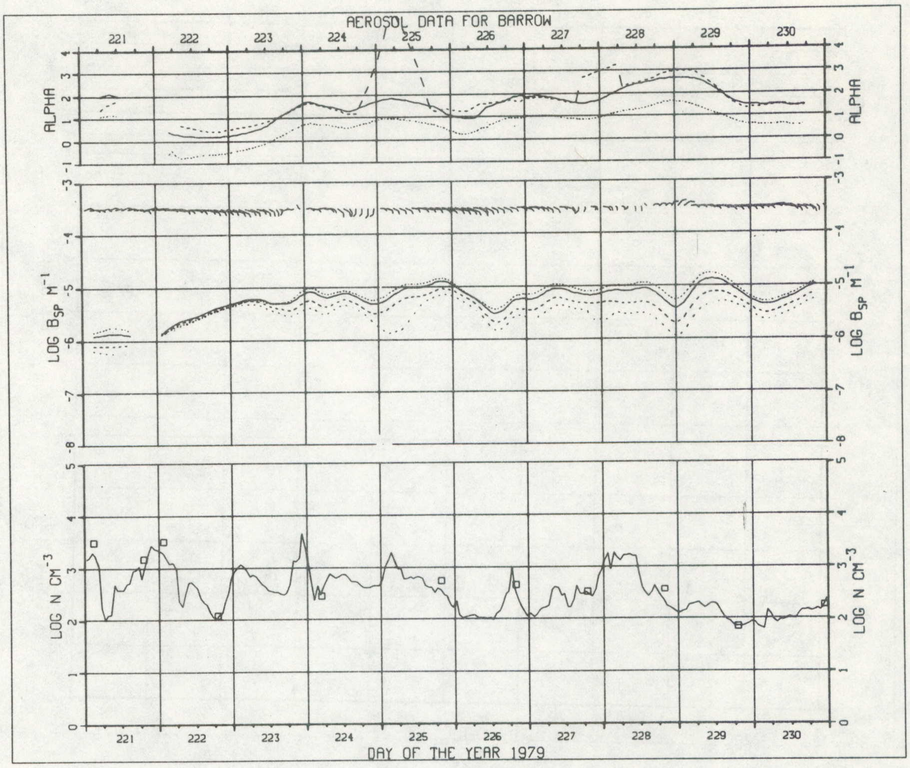
AEROSOL DATA FOR BARROW
ALPHA
LOG BSP M-1
LOG N CM-3
DAY OF THE YEAR 1979

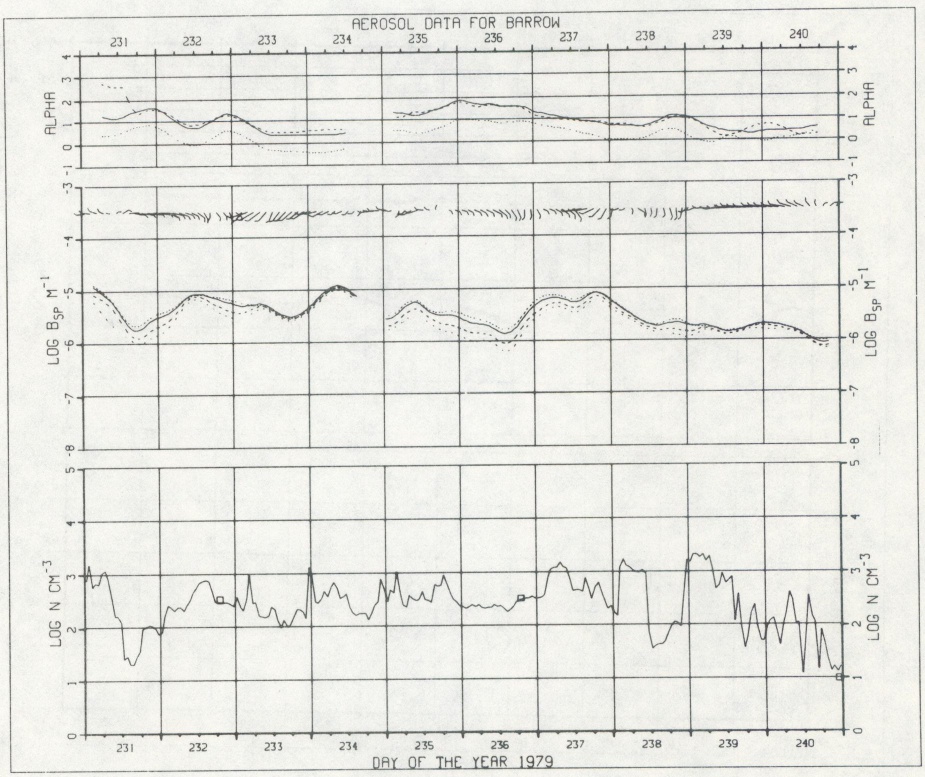
AEROSOL DATA FOR BARROW
ALPHA
LOG BSP M-1
LOG N CM-3
DAY OF THE YEAR 1979

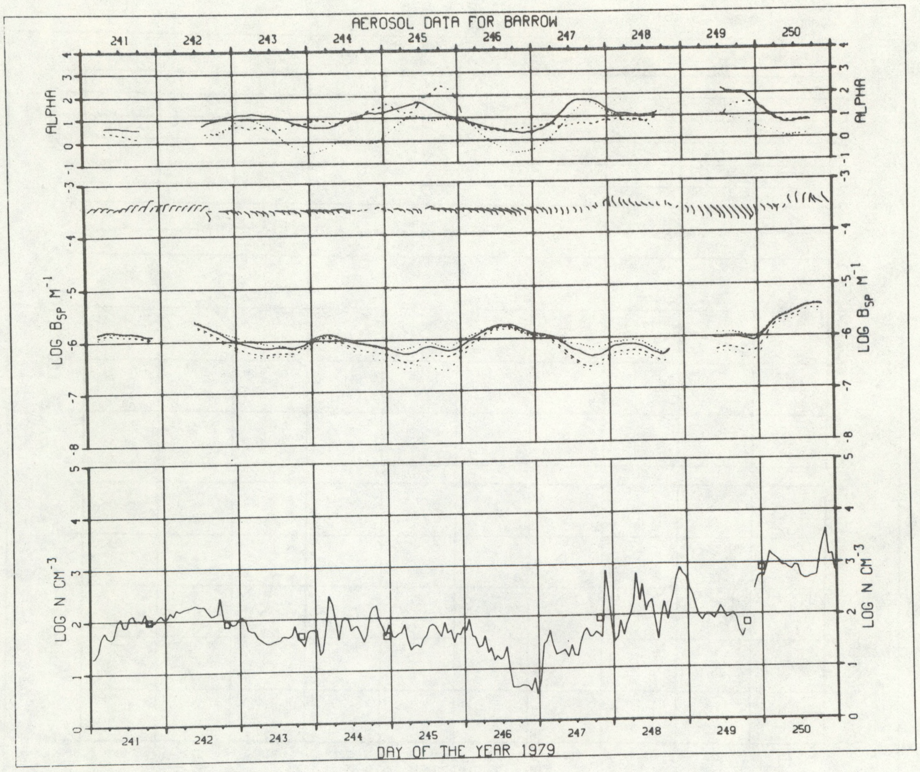
AEROSOL DATA FOR BARROW
ALPHA
LOG B_{SP} M^{-1}
LOG N CM^{-3}
DAY OF THE YEAR 1979

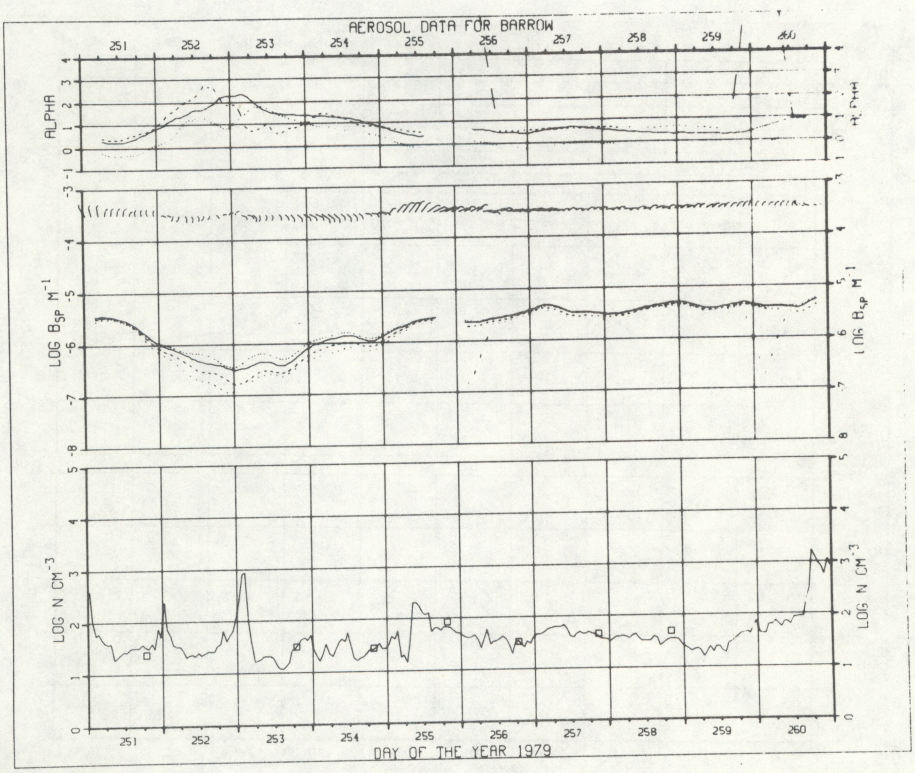
AEROSOL DATA FOR BARROW
ALPHA
LOG B_{SP} M^{-1}
LOG N CM^{-3}
DAY OF THE YEAR 1979

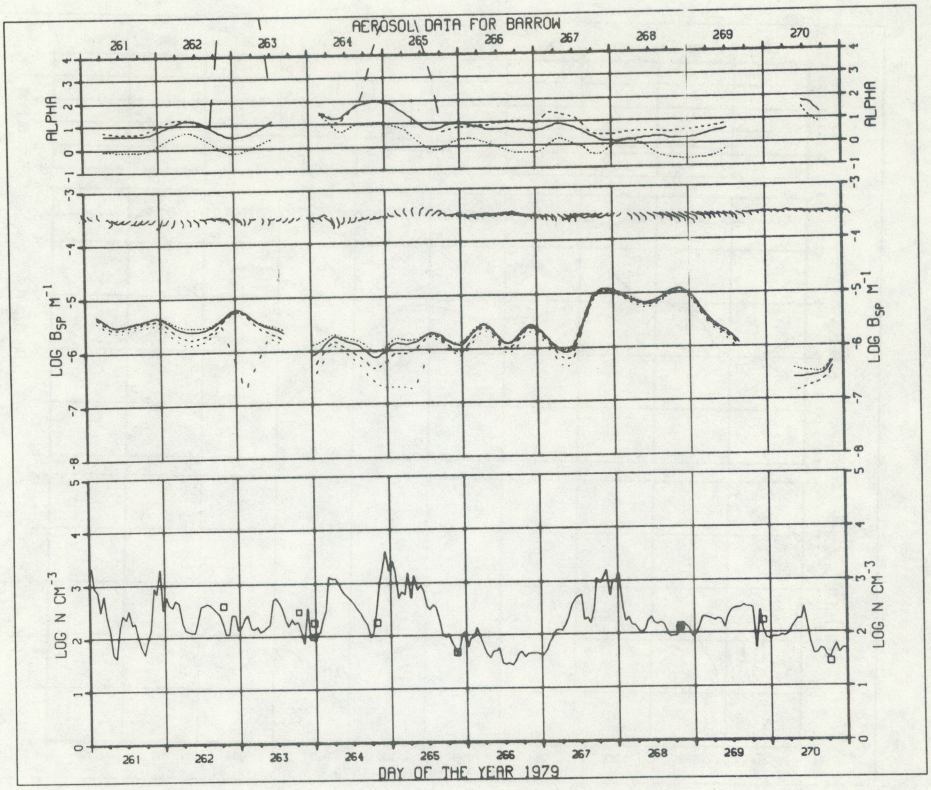
AEROSOL DATA FOR BARROW
ALPHA
LOG B_{SP} M^{-1}
LOG N CM^{-3}
DAY OF THE YEAR 1979

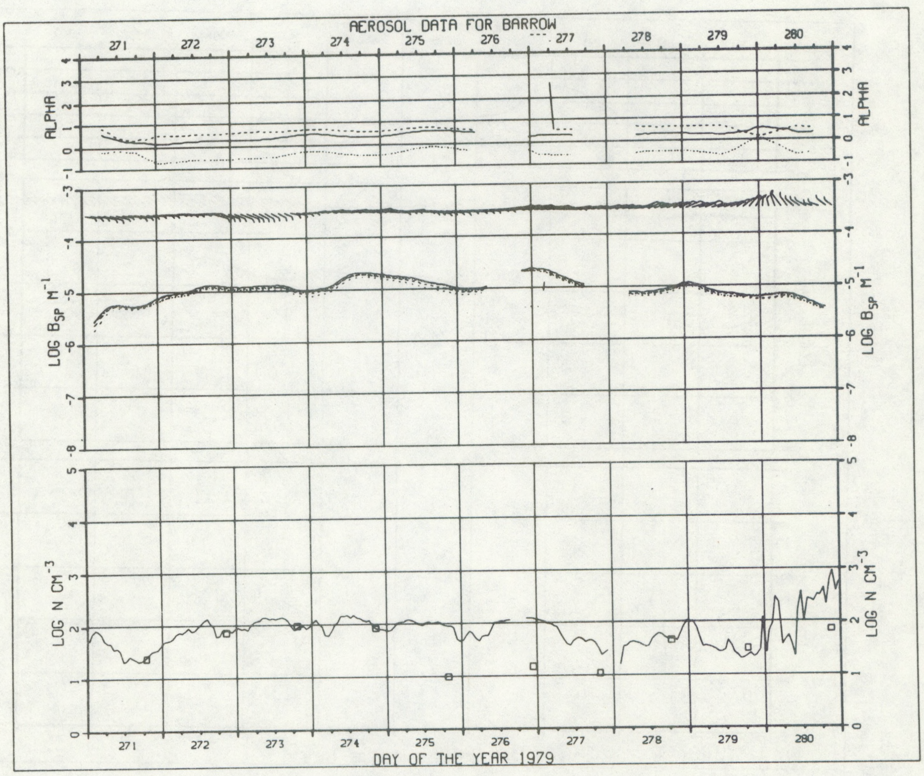
AEROSOL DATA FOR BARROW
ALPHA
LOG B_{SP} M^{-1}
LOG N CM^{-3}
DAY OF THE YEAR 1979

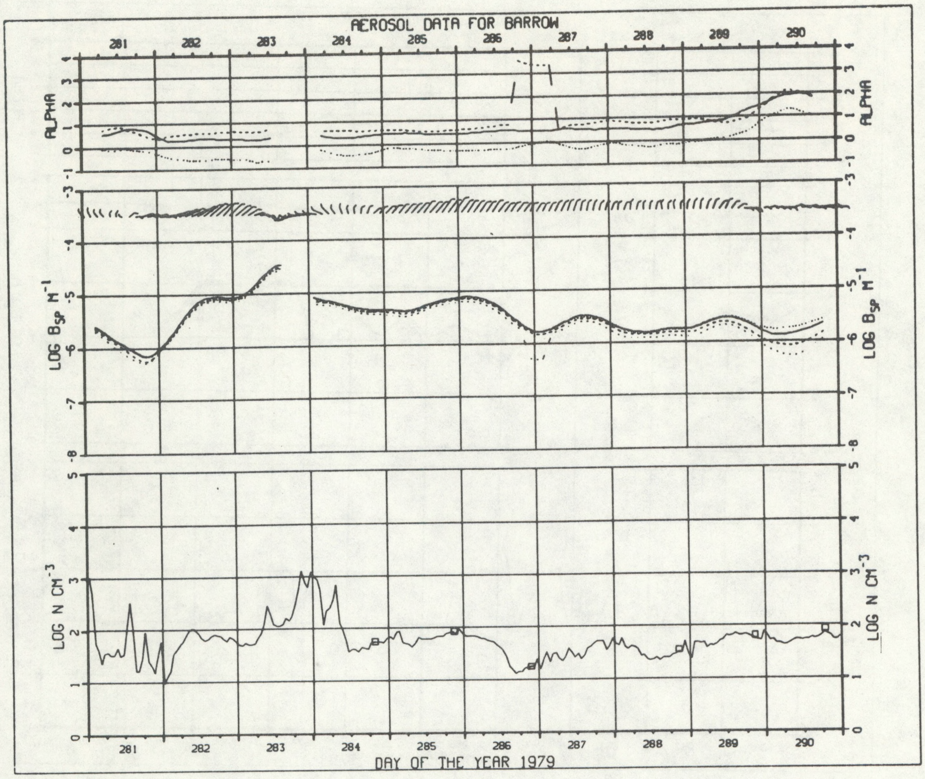
AEROSOL DATA FOR BARROW
ALPHA
LOG B_{SP} M^{-1}
LOG N CM^{-3}
DAY OF THE YEAR 1979

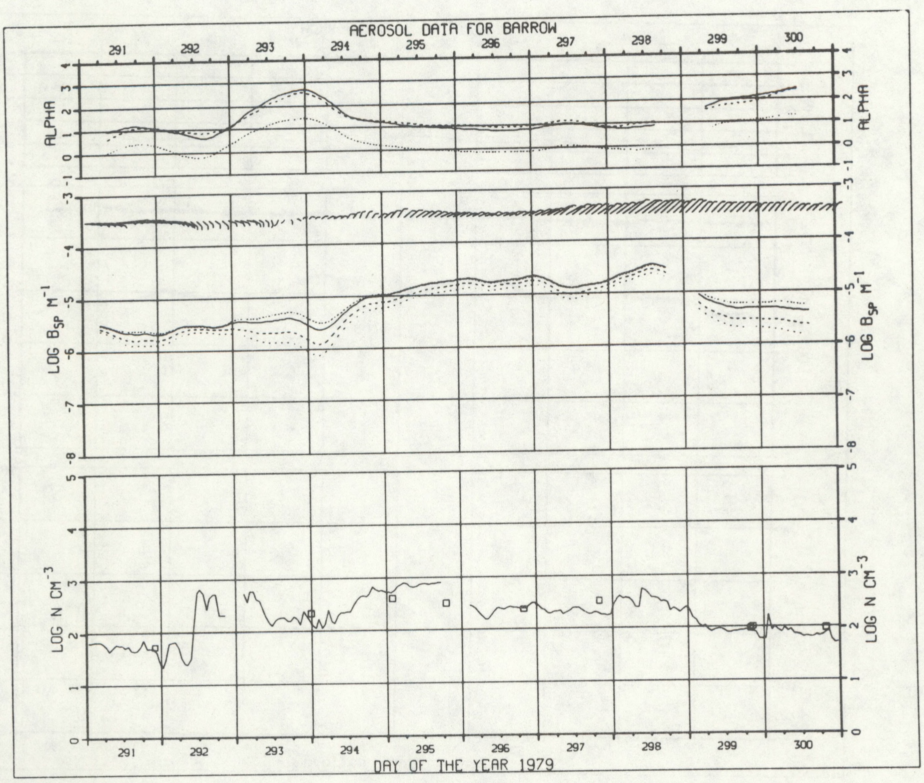
AEROSOL DATA FOR BARROW
ALPHA
LOG B_{SP} M^{-1}
LOG N CM^{-3}
DAY OF THE YEAR 1979

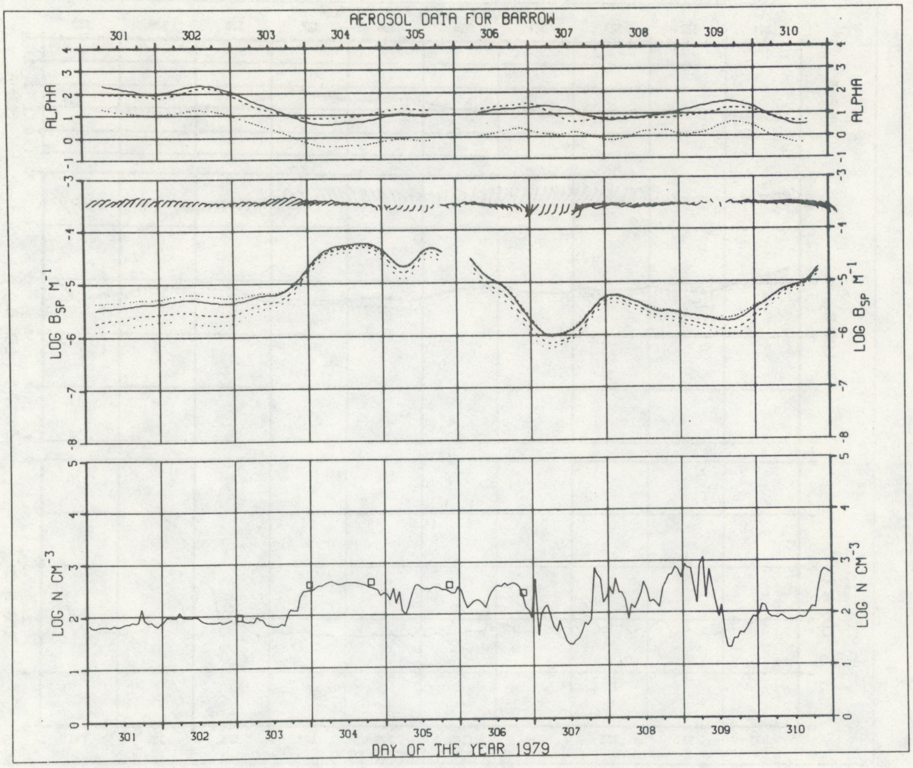
AEROSOL DATA FOR BARROW
ALPHA
LOG B_{SP} M^{-1}
LOG N CM^{-3}
DAY OF THE YEAR 1979

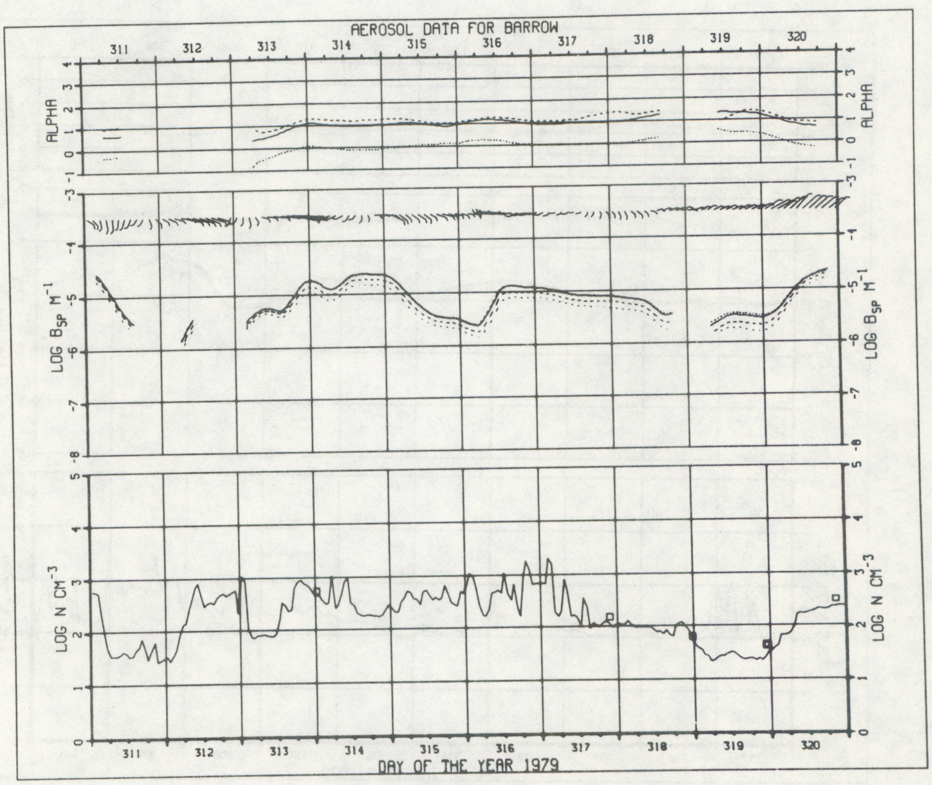
AEROSOL DATA FOR BARROW
ALPHA
LOG B_{SP} M^{-1}
LOG N CM^{-3}
DAY OF THE YEAR 1979

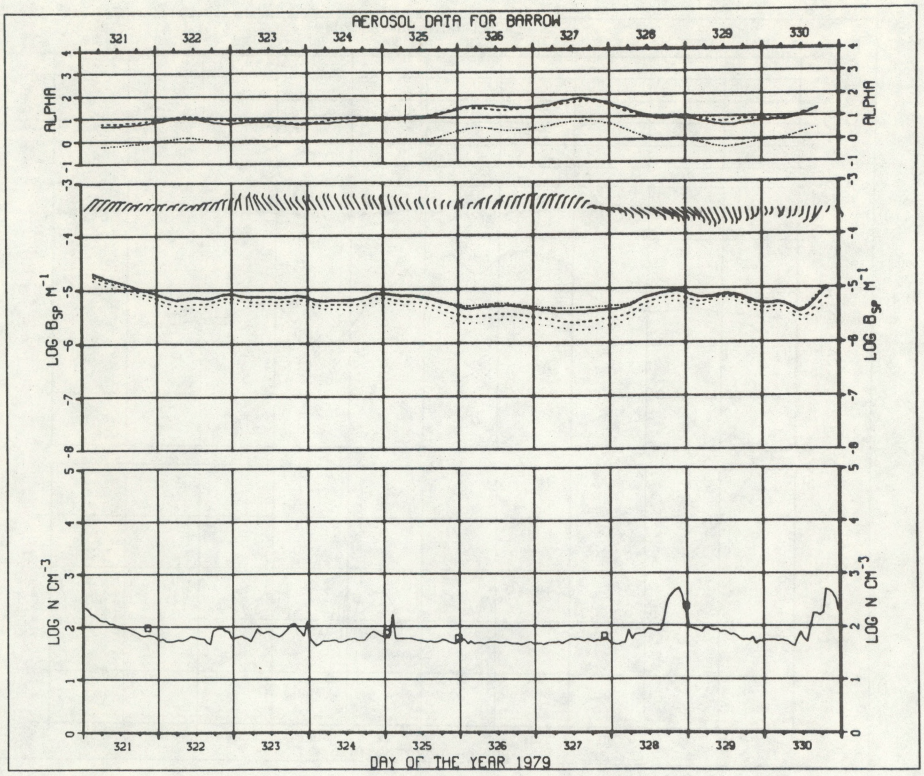
AEROSOL DATA FOR BARROW
ALPHA
LOG B_SP M^-1
LOG N CM^-3
DAY OF THE YEAR 1979

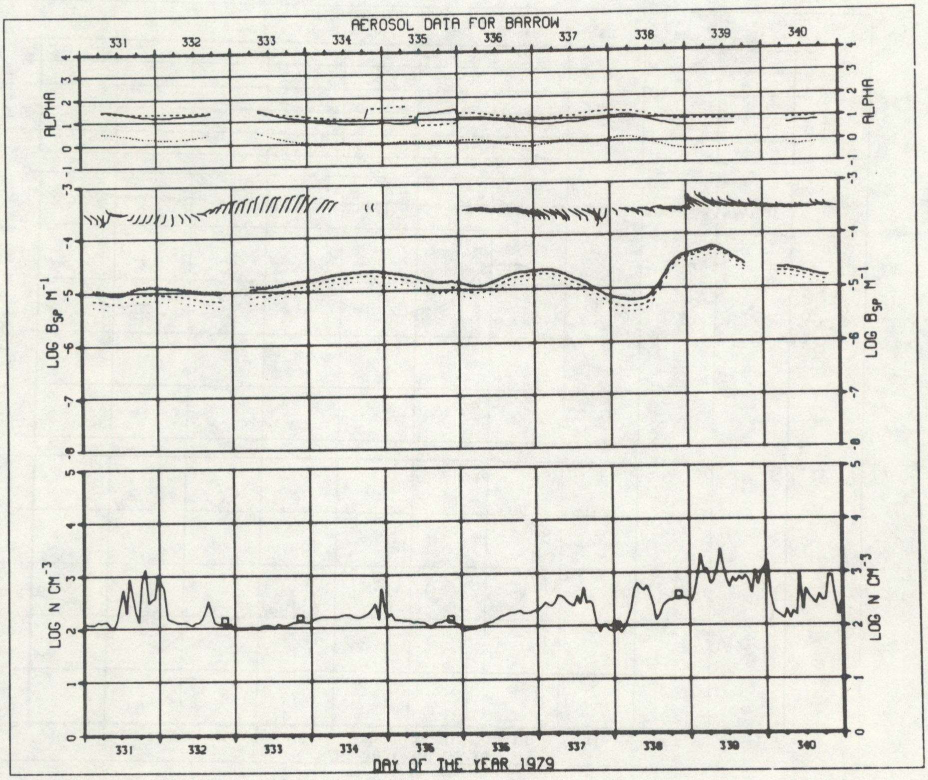
AEROSOL DATA FOR BARROW
ALPHA
LOG B_SP M^-1
LOG N CM^-3
DAY OF THE YEAR 1979

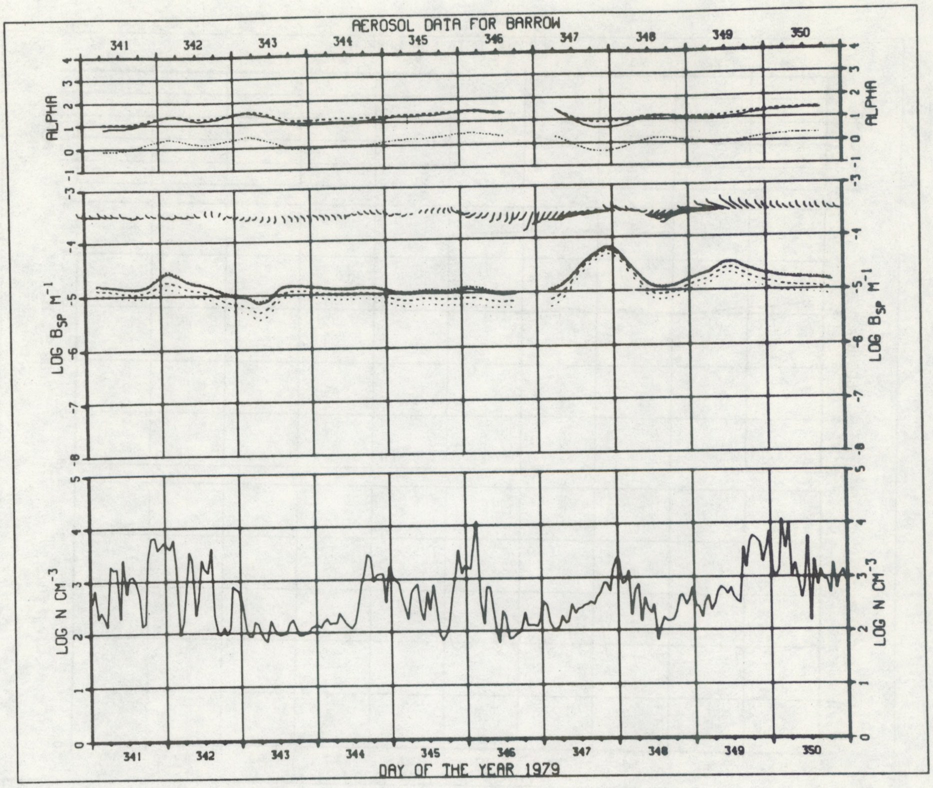
AEROSOL DATA FOR BARROW
ALPHA
LOG B_{SP} M^{-1}
LOG N CM^{-3}
DAY OF THE YEAR 1979

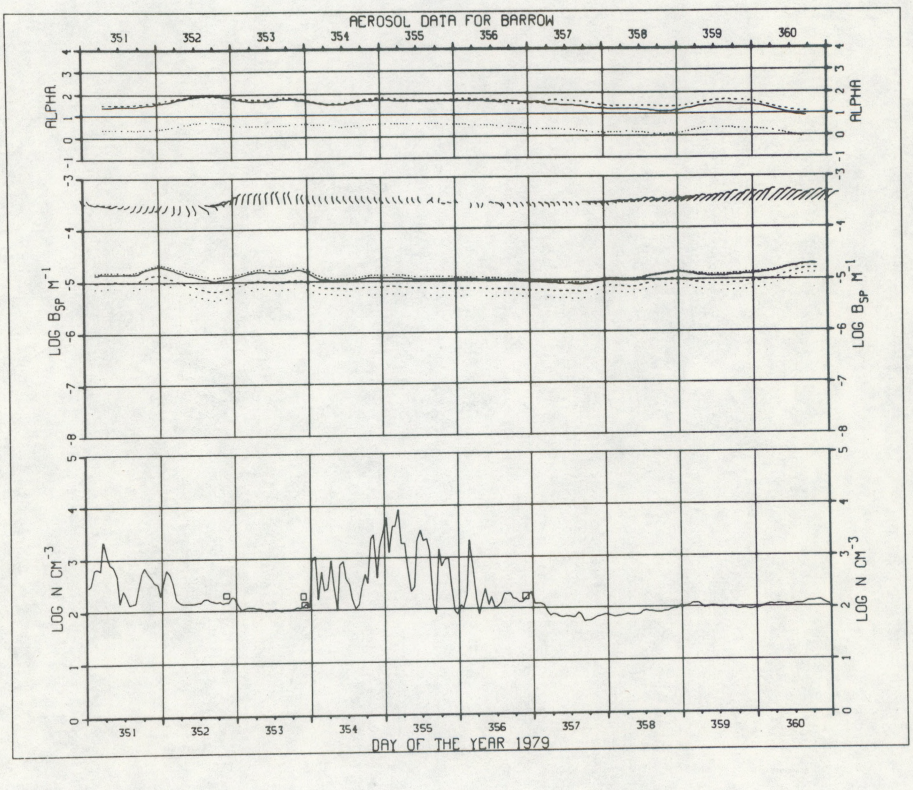
AEROSOL DATA FOR BARROW
ALPHA
LOG B_{SP} M^{-1}
LOG N CM^{-3}
DAY OF THE YEAR 1979

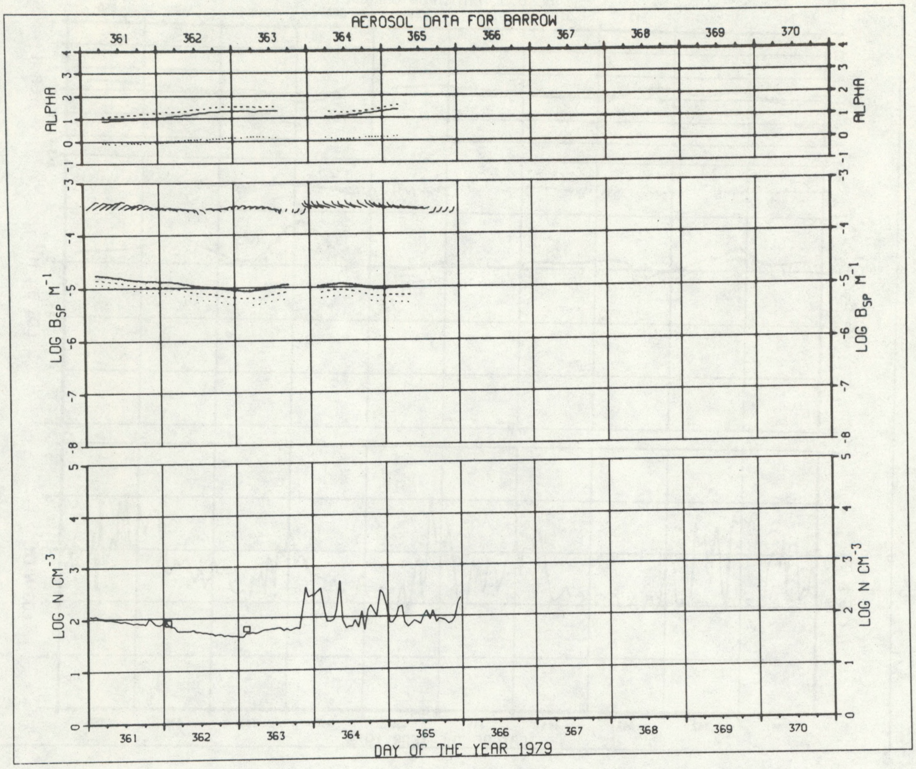
AEROSOL DATA FOR BARROW
ALPHA
LOG B_{SP} M^{-1}
LOG N CM^{-3}
361
362
363
364
365
366
367
368
369
370
DAY OF THE YEAR 1979

APPENDIX E

Appendix E contains the plots of daily mean nuclei concentrations, Pollak counter observations, light scattering data, and Angstrom exponents of each complete year on a single graph plotted on a logarithmic scale for 1976 through 1979.

----

for each plot:

the top graph contains: Alpha (2-3) Angstrom exponent

the center graph contains: light scattering data

wavelength 450 nm: dashed line
wavelength 550 nm: solid line
wavelength 700 nm: long dashed line
wavelength 850 nm: short dashed line

the lower graph contains: nuclei concentrations

G.E. counter: solid line
Pollak counter: squares

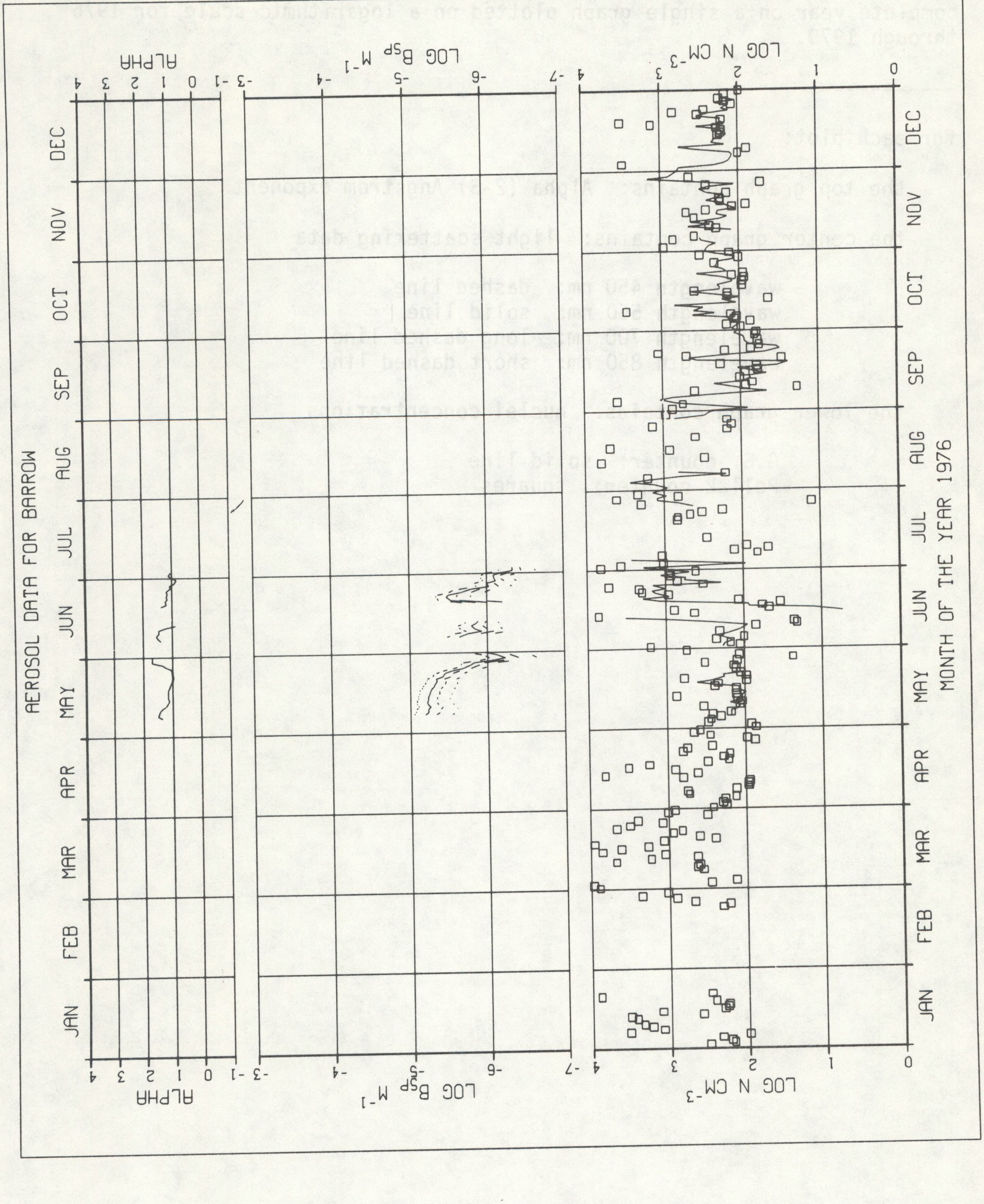

AEROSOL DATA FOR BARROW
MONTH OF THE YEAR 1976
JAN FEB MAR APR MAY JUN JUL AUG SEP OCT NOV DEC
ALPHA
4 3 2 1 0 -1
LOG B SP M -1
-3 -4 -5 -6 -7
LOG N CM -3
4 3 2 1 0

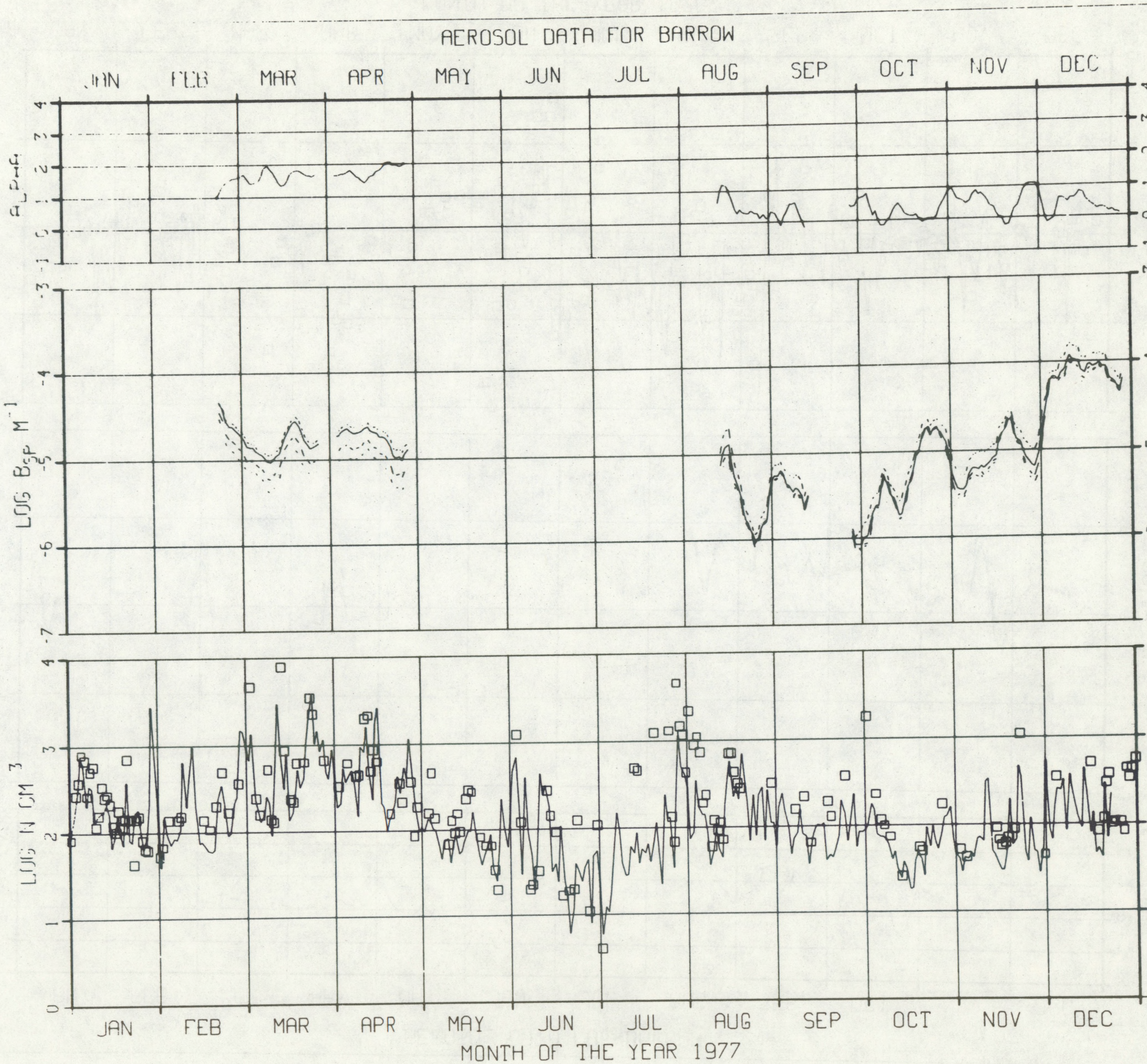
AEROSOL DATA FOR BARROW
JAN FEB MAR APR MAY JUN JUL AUG SEP OCT NOV DEC
ALPHA
LOG B_{SP} M^{-1}
LOG N CM^{-3}
MONTH OF THE YEAR 1977

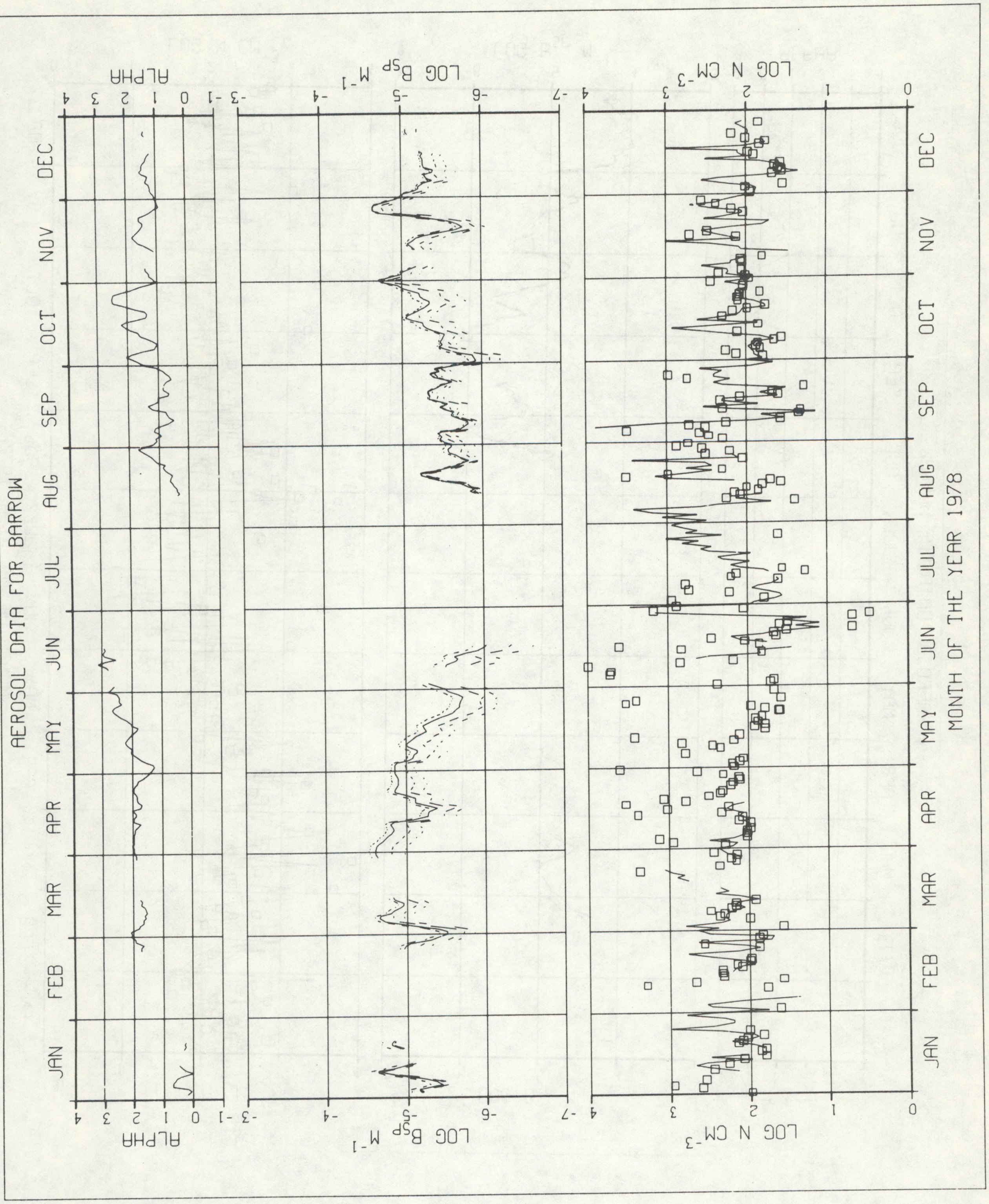
AEROSOL DATA FOR BARROW
ALPHA
LOG B SP M -1
LOG N CM -3
JAN FEB MAR APR MAY JUN JUL AUG SEP OCT NOV DEC
MONTH OF THE YEAR 1978

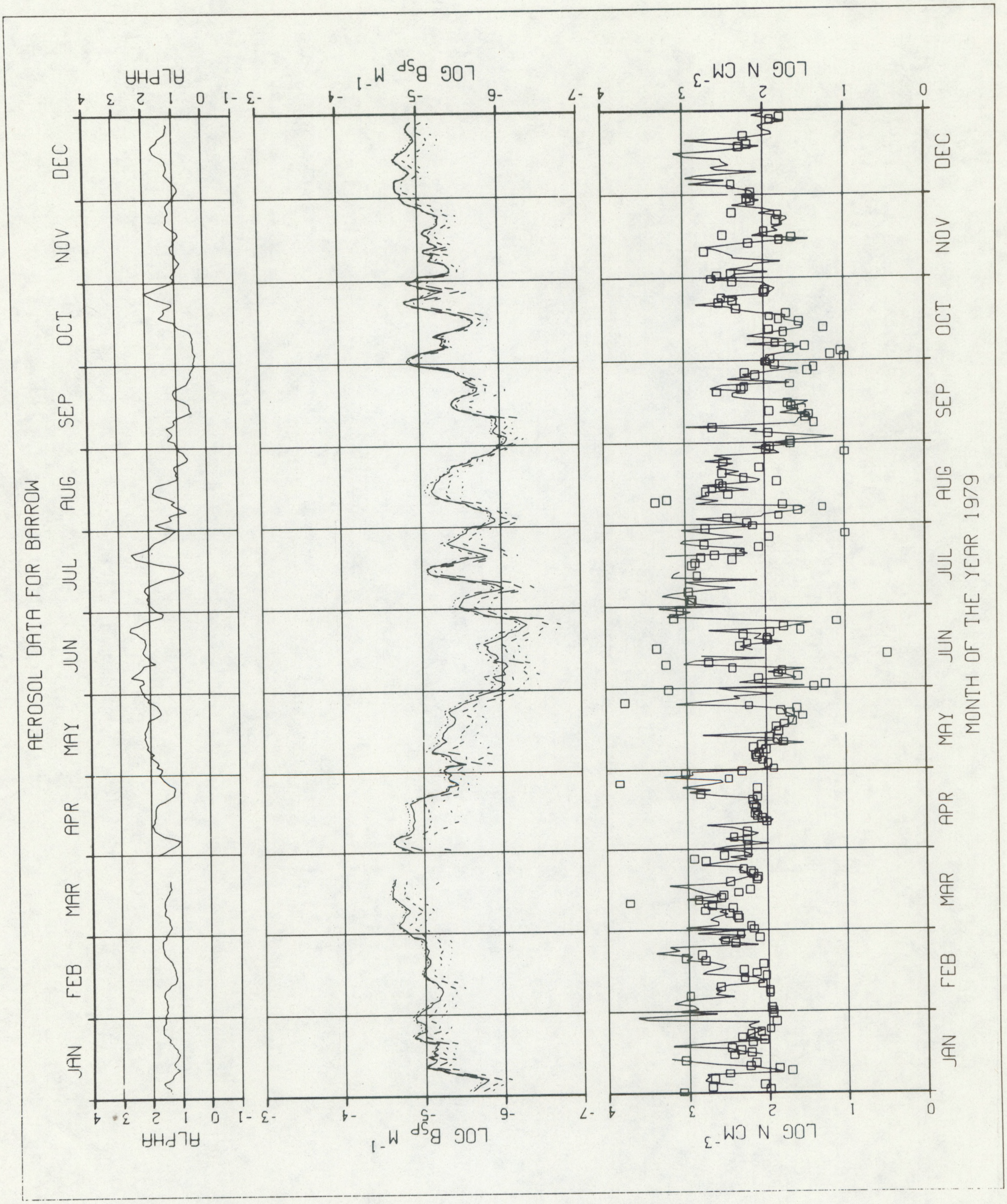
AEROSOL DATA FOR BARROW
ALPHA
LOG B SP M -1
LOG N CM -3
JAN
FEB
MAR
APR
MAY
JUN
JUL
AUG
SEP
OCT
NOV
DEC
MONTH OF THE YEAR 1979